ABSTRACT

Title of Dissertation:	LINKING ALLOMETRIC SCALING THEORY WITH LIDAR REMOTE SENSING FOR IMPROVED BIOMASS ESTIMATION AND ECOSYSTEM CHARACTERIZATION
	Laura Duncanson, Doctor of Philosophy, 2015
Dissertation Directed By:	Dr. Ralph Dubayah, Department of Geographical Sciences

Accurate quantification of forest carbon stocks and fluxes is critical for the successful modeling and mitigation of climate change. This research focuses on forest carbon stock quantification, both in terms of testing emerging remote sensing approaches to forest carbon modeling, and examining allometric equations used to estimate biomass stocks in field plots. First, we test controversial theoretical predictions of forest allometry through the mapping of the allometric variability using field plots across the U.S. we find that there is considerable variability in forest allometry across space, largely driven by local environment and life history. However, in tall forests, allometries tend to converge toward theoretical predictions, suggesting that theory may be a useful constraint on allometry in certain forests. Second, we shift to an analysis of empirical allometries by developing an algorithm to extract individual crown information from forest systems and using it for biomass mapping and allometric equation testing. Third, we test whether individual tree structure bolsters biomass modeling capabilities in comparison to

tradition, plot-aggregated LiDAR metrics. As part of this analysis we also test an allometric scaling-based approach to biomass mapping. We find that individual tree-level structure only improves biomass models when there is considerable spatial heterogeneity in the forest. Also, allometric scaling-based only worked in one study site, and failed in the other two sites because there was little or no relationship between basal area and maximum canopy height. Finally, we applied LiDAR datasets to an analysis of the effects of sample size on empirical allometry development. We found that small samples sizes tend to result in an under sampling of large stems, which yields a more linear fit than the true allometry. An assessment of the potential carbon implications of this problem yielded site-level biomass predictions with biases of 10-178%. We suggest that empirical allometric equations developed on small sample sizes, as applied in the U.S., yield potentially large errors in biomass and therefore require careful reassessment. In combination with our findings regarding the spatial variability of forest allometry, we believe that the limiting factor to forest carbon estimation is the use of allometric equations.

LINKING ALLOMETRIC SCALING THEORY WITH LIDAR REMOTE SENSING FOR IMPROVED BIOMASS ESTIMATION AND ECOSYSTEM CHARACTERIZATION

By

Laura Duncanson

Dissertation submitted to the Faculty of the Graduate School of the
University of Maryland, College Park, in partial fulfillment
of the requirements for the degree of
Doctor of Philosphy, 2015

Advisory Committee:
Professor Ralph Dubayah, Chair
Dr. George Hurtt
Dr. Matt Hansen
Dr. Bruce Cook
Dean's Representative:
Dr. Joe Sullivan

Preface

This dissertation includes four research papers of which Laura I Duncanson is the primary author. Laura Duncanson designed the research and conducted all of the analysis in this dissertation, but each research chapter also represents the comments and edits of several coauthors. Chapter 2 is coauthored by Ralph Dubayah and Brian Enquist, both of whom contributed greatly to the scope and writing of the chapter. This chapter is still in preparation for submission. Chapter 3 was coauthored by Ralph Dubayah, Bruce Cook, and George Hurtt. Bruce provided the data, helped with technical aspects of the work, and contributed to the writing of the manuscript. Ralph provided many edits and comments, particularly with respect to algorithm validation. This paper is published in Remote Sensing of Environment. Chapter 4 is coauthored by Bruce Cook, Ralph Dubayah, Jackie Rosette, and Jess Parker. Field data was provided at Parker Tract by Jackie Rosette, SERC by Jess Parker, and members of the VCL lab at Sierra Nevada. This dissertation did not involve the direct collection of any field data. All coauthors contributed to the final draft of this chapter, currently in its second round of review at Remote Sensing of Environment. Chapter 5 is still in preparation for submission, and the enclosed manuscript has been edited by Joe Mascaro, and helpful comments have been provided by Ralph Dubayah and Oliver Rourke.

Dedication

Dedicated to my parents, Caroline and Bob, who taught me to love nature.

Acknowledgements

This research would not have been possible without funding from the Natural Sciences and Engineering Research Council of Canada (NSERC)'s Postgraduate Scholarship Program and NASA's Earth and Space Science Fellowship Program (NESSF). These graduate fellowships allowed me to focus almost exclusively on research through the course of my dissertation and I am very grateful. I would also like to thank the NASA Earth Exchange (NEX) program for allowing me to participate in a two week short course on supercomputing, and process my LiDAR datasets on the Pleiades supercomputer at NASA Ames. The technical knowledge I gained through NEX, as well as access to their computing facilities, greatly increase the scope and impact of this research.

I would also like to thank many individuals who contributed directly to this research. First, my committee members, George Hurtt, Bruce Cook, and Matt Hansen who have generously donated their time to meetings and many of whom have acted as coauthors for various chapters of this dissertation. I greatly appreciate the guidance and feedback you have given me. Bruce Cook, in particular, has been tremendously helpful with various technical elements of this dissertation and provided the LiDAR data that is at the core of this research. George Hurtt has also given me considerable guidance over the years, and has fostered a positive and social working atmosphere in the research lab. Other coauthors on my manuscripts are Brian Enquist, Jackie Rosette, Joe Mascaro, and Jess Parker who have both directly contributed to this research and improved my writing by example. Additional thanks go to Justin Fisk for technical support throughout my PhD, Anu Swatantran for many useful

discussions, Ron Luna for giving me the opportunity to teach, and Alyssa Whitcraft, Kusuma Prabhakara, Steve Flanagan, Rachel Moore, Leeann King and Katelyn Dolan for significant moral support.

I also have tremendous gratitude for the friendships I have gained while in Maryland and Washington, D.C. These individuals have made my PhD years incredibly enjoyable. I love you all and am so grateful to have you in my life. I have been blessed with so many fantastic friendships here, but particularly want to acknowledge Colin Robertson, Kusuma Prabhakara, Matt Brolly, Becki Brolly, Linsay Deming, Landon Letzkus, Adam Prim, Ted Jones, Ash Enrici and Ben Stewart.

I also want to thank my family for their endless support, particularly my Grandfather, John Duncanson, my parents Caroline & Bob, and my siblings, Heather and Sander. Heather, in particular, has been endlessly supportive throughout this process.

Finally, I want to thank my supervisor and mentor Ralph Dubayah. I have learned an incredible amount from you over these few years and look forward to working closely with you in the future. You have taught me the importance of doing things right rather than doing them fast. Thank you for your support, mentorship, guidance, and friendship. It has been an absolute pleasure being your student.

Table of Contents

List of Tables

List of Figures

Chapter 1: Introduction

Overview

Forest ecosystems play a critical role in global biogeochemical cycling, particularly with respect to carbon, and represent the largest terrestrial carbon stock on the planet. Indeed, the flux of carbon into forests through photosynthesis and out of forests through respiration and degradation largely controls annual fluxes of atmospheric carbon (Keeling et al., 1976). Understanding changes to plant growth and disturbance is therefore of the utmost importance for improving carbon cycle models and mitigating climate change.

One approach to mitigation is the U.N.'s Reduced Emissions from Deforestation and Degradation (Gibbs et al., 2007), which involves a market-based strategy designed to decrease forest carbon loss. Theoretically, REDD+ works by providing financial incentives to land owners who commit to leave forested land undisturbed. The magnitudes of incentives are based on the estimated carbon content of the forests in question. This program has spurred the development of carbon monitoring efforts, particularly with respect to monitoring reporting and verification systems, which are critical to the ultimate success of REDD+ (Goetz & Dubayah, 2011). Many international research agendas have focused on improving our abilities to map forest carbon stocks. These efforts include airborne and spaceborne data acquisitions as well as field campaigns to increase the number and range of validation plots. NASA has been an active agency in these projects, both collaboratively through initiatives such

as Silvacarbon, and directly through the funding of Carbon Monitoring System projects, and more recently the selection of the Global Ecosystem Dynamics Investigation (GEDI) mission. Additional missions have been selected elsewhere, including the BIOMASS mission by the European Space Agency (Le Toan et al., 2011). Clearly great attention has been focused on the development of technologies and methods for mapping forest carbon stock.

Additional attention has been paid to forest carbon flux, either using repeat measurements over two time periods (Dubayah et al., 2010, Hopkinson et al., 2008, Hudak et al., 2012), or through ecosystem models such as the Ecosystem Demography model, that predicts changes in carbon stock based on existing forest demographics, environment, and disturbance (Moorcroft et al., 2001, Hurtt et al., 2002). Both approaches provide rough but meaningful estimates of expected changes to future carbon stocks in forests, and as such are integral to carbon management initiatives.

Underlying all of these carbon stock and flux activities is the problem of forest allometry. Remote sensing and modeling-based maps of forest carbon stock and flux are validated and/or locally calibrated with field data. Field datasets are generally accepted as the most accurate information available on forest structure, and forest carbon maps typically report errors with respect to field estimates. The error of field estimates themselves tends to be overlooked in these models, and although researchers accept that field estimates are imperfect, data have not been available to

quantify field-based errors. Field estimates of carbon are typically based on the application of an allometric equation, which relates measurable properties of a tree to its aboveground biomass (e.g. Jenkins et al., 2003). Allometric equations are developed with limited samples of destructively sampled trees, and often applied irrespective of environment. The sensitivity of these equations to sample size, sampling strategy, and environment are largely unknown.

Research Goals and Objectives

This dissertation research addresses forest allometry from both theoretical and empirical perspectives. The goals of this research are twofold: first, to determine the generality of forest allometric scaling relationships across the United States, and second, to apply novel datasets to increase our understanding of the limitations of past empirical allometric approaches for biomass modeling. To achieve these goals we have addressed the following seven objectives:

First, Objective 1, **to determine the spatial variability in forest allometry using Forest Inventory Analysis (FIA) data across the United States**. This analysis allows an understanding of the spatial variability of forest scaling, and the degree to which allometric relationships are universal.

Secondly, Objective 2 is **to determine the effects of forest age, height, location, topography, climate, and forest class on the observed allometric variability**. This

research expands on the spatial mapping performed under Objective 1 by explaining variability as a function of environment and life history.

Third, Objective 3 is **to determine the conditions under which Metabolic Scaling Theory predictions apply in the United States**. If theoretical predictions are valid they could provide useful constraints on empirically derived allometries.

Contrasting this theoretical work, the latter chapters of this dissertation address questions of empirical allometry. To accomplish this, individual tree information is required at greater sample sizes than are available through field datasets. Objective 4, therefore, is **to develop an algorithm capable of extracting individual tree structure from LiDAR datasets across disparate forest environments**.

Using LiDAR-based individual tree structure, Objective 5 is **to evaluate whether LiDAR-based biomass models can be improved through the inclusion of individual trees and scaling-based approaches**. This objective addresses the importance of spatially detailed data for biomass mapping, determining whether individual tree-based information bolsters modeling initiatives or if allometric scaling can be used to reduce information requirements.

The second application of the individual tree LiDAR dataset is Objective 6**, to determine the effects of sample size on allometric equation parameterization**. This research tests the effects of developing tree height to crown radius allometries

with small sample sizes in comparison to developing allometries with a full 'population' level dataset.

Objective 7 expands on Objective 6 by using MST predictions to estimate individual tree biomass as a function of crown radius, allowing me **to assess the biomass implications of applying allometric equations based on small sample sizes.**

Background

Forest allometry refers to mathematical equations developed to describe how various tree and forest structural and functional measurements relate to one another (Huxley, 1932). The most common allometric equations used in forestry relate the Diameter at Breast Height (DBH) of a tree to its aboveground biomass (AGB). However, allometric equations also exist relating DBH to height, growth rate, volume, etc. Scores of allometric equations exist for different tree species, species groups, or geographic areas (Henry et al., 2013). Allometric equations for biomass are arguably the most difficult to develop, as they require the destructive sampling of trees. Destructive sampling refers to measurement that requires the felling of trees rather than measurements that can be taken directly in the field. These measurements are logistically difficult, and require the ability to transport felled trees to laboratory facilities. As such, sampling tends to be biased towards small, accessible trees, which do not represent the size and structure distribution for which the allometries will be applied. Additionally, sample sizes tend to be small, ranging from as few as five trees to perhaps a few thousand per species. Many attempts have been made to provide

more reasonable allometric equations for practical forest management. These include the pooling of datasets to increase sample sizes (Ung et al., 2008), the grouping of existing allometric equations for generalized application (Jenkins et al., 2003, Chojnacky et al., 2014), or the development of allometric equations for specific geographic ranges rather than species (Chave et al., 2005). Regardless of these attempts, the accuracies of existing allometric equations for biomass estimation outside of model calibration areas remain unknown.

In contrast to empirical work, ecologists have attempted to explain forest structural and functional allometries based on theory. The most basic example of this is perhaps the pipe model's prediction that a tree's leaf mass will scale linearly with the mass of non-photosynthetic material (bole mass), as leaves are serviced by a network of vascular tubes (Shinozaki, 1964). Similar work predicts the community-level allometries of tree size distribution through 'laws' of self-thinning, in that the number of trees in a size class will scale with that size class to the power of -3/2 (Yoda et al., 1963). More recently, West, Brown & Enquist (1999) have presented a more complete set of theoretical allometric equations based on some explicit, simplifying assumptions. Namely, they assume that trees and forests are structured as space-filling fractals that have evolved to minimize the amount of energy required for the distribution of resources. Additionally, they assume that the smallest functional unit of plants (the leaves or petioles) of a given species will not vary with the size of the plant, and that systems have even distributions of resources, and use all resources available to them. Using these assumptions, and fractal geometry, Enquist et al.

(2009) present a set of idealized allometric equations relating tree properties such as DBH, Height, Volume, Biomass, and growth rate, as well as community level properties such as tree size distribution. Coined Metabolic Scaling Theory (MST), because the fundamental prediction relates individual metabolism to mass, their predictions take the form of precise power law equations. They have predicted that MST allometric predictions should apply universally, irrespective of species or environment (Enquist & Niklas, 2001). Perhaps because of these bold assertions, or because these predictions are relatively easy to test with new datasets, many researchers have attempted to prove or disprove metabolic scaling theory's predictions in forest systems (Coomes et al., 2003, Muller-Landau et al., 2006, Lai et al., 2013 Price et al., 2007). Although many of these studies have concluded that MST is invalid based on local findings, few studies have provided a systematic test of MST across environmental gradients. Some ecosystems appear to follow MST scaling, while others do not. Although most studies speculate as to why MST predictions appear invalid in their sites, data have been generally unavailable to test these predictions across wide environmental gradients (Lines et al., 2012). If MST is valid in some areas, and discrepancies can be explained by environment, predictions may provide much needed theoretical constraints on empirically developed allometries.

Dissertation Organization

The seven objectives outlined above are presented in four original research chapters, which are structured as stand alone papers. First, in Chapter 2, we address Objectives

1, 2 and 3 through mapping of two forest allometric exponents across the United States, in an attempt to better understand the degree and drivers of allometric variability.

In chapter 3 we redirect our attention to empirical allometry. Analyses of empirical allometries have been limited by small, often destructively sampled datasets. The LiDAR remote sensing community has recently developed techniques to extract individual tree information. This appeared to be an ideal opportunity to use much larger individual tree-level datasets for allometric analyses across multiple forest ecosystems. Upon inspection, however, existing algorithms for individual tree-level extraction appeared inappropriate for many forest ecosystems in the U.S., particularly in closed canopy Eastern forests. In order to produce large area individual tree-level datasets, a new individual crown extraction algorithm was required. Therefore, as part of this dissertation, we developed a novel three-dimensional crown delineation algorithm (Objective 4) the details of which are presented in Chapter 3, which is published in Remote Sensing of Environment.

Given the findings from chapters 2, and with the data available from Chapter 3, we return to biomass mapping in Chapter 4, addressing Objective 5. This chapter focuses on a general assessment of new methods for biomass mapping, both through the incorporation of individual tree information, and the testing of universal application scaling-based approaches that attempt to incorporate theories such as MST. This chapter also addresses the importance of allometric equation selection for field-based

biomass estimates, and is under review at Remote Sensing of Environment after two rounds of mixed reviews that yielded a recommendation accept after major revision.

Extending on the allometric findings from Chapter 4, we focus on empirical allometric analyses in Chapter 5 by using the individual crown information to address the effect of sample size on empirical allometric equation parameterization (Objective 6). Chapter 5 takes data from six LiDAR study areas across the U.S. and develops allometric equations relating tree height to crown radius, as these variables are readily available from crown delineation algorithm. This chapter quantifies, for the first time, the effects of developing allometric equations with excessively small sample sizes, and uses MST equations to translate their results with respect to biomass (Objective 7). This chapter will be submitted to PNAS.

Chapter 2: Assessing the Generality of Forest Allometric Scaling Relationships in the United States

Abstract

Allometric equations relating various forest structural and functional properties, such as used for biomass estimation, are applied in North America irrespective of location. This application assumes that the allocation of biomass both within trees and across forests is invariant with respect to environment or life history. Similarly, a set of theoretical allometric scaling predictions from metabolic scaling theory, MST, are hypothesized to be environmentally invariant. We test these assumptions of invariant scaling by mapping forest allometry across broad environmental gradients in the U.S. using 223,492 forest plots. We find considerable spatial variability in forest allometric relationships, which is partially explained as a function of environment, forest species composition, and forest height. Forest height, a proxy for successional status, is the primary factor controlling allometry, suggesting that different equations are needed in forests across gradients of system maturity. Although the majority of forest plots deviate from theoretically predicted scaling, MST is generally supported in plots exhibiting resource and demographic steady state. Deviations from MST are partially explained as a function of environmentally driven recruitment limitations and successional status. Future development of MST will therefore need to incorporate variation in demographic dynamics in younger successional forests, and factors influencing recruitment limitations, to better predict observed variation. Greater attention to environment and life history is needed both in the future

development of MST and in the application of empirical allometries in order to improve carbon mapping initiatives and guide global change models.

Introduction

Understanding the drivers of forest structure, function and change is a fundamental problem both in theoretical ecology (Brown et al., 1999) and in applied forestry for carbon mapping and monitoring (Chave et al., 2005, Chojnacky et al., 2014, Van Breugel et al., 2011). Estimates of forest aboveground carbon content or biomass, are typically based on the application of empirically derived allometric equations. These equations are generated with small samples of felled trees, and errors associated with their use are largely unknown, particularly in environments outside the range of conditions found at model development sites (Chave et al., 2004, Jenkins et al., 2003).

Currently, in temperate systems, empirically derived allometric equations are applied in a widespread fashion, often ignoring environment or forest maturity (Jenkins et al., 2003). This is due primarily to a lack of available data with which to build more complete allometries that consider environment. Often, a single allometric equation relating Diameter at Breast Height (D) and Aboveground Biomass (M) is developed either for a species or group of species, and applied irrespective of environment. This inherently assumes that a single tree species will have a consistent structural form regardless of environment, that is they are spatially invariant. While the theoretical basis for relaxing this assumption is not clear, allometries have been created which

also include tree height in an attempt to account for observed variability in scaling relationships caused by factors such as elevation.

The assumption of spatial invariance independent of environment is both ubiquitous and firmly established, as evidenced by methods such as Jenkins. This view is supported by theoretical predictions presented by West, Brown, and Enquist, who proposed a general theory for the origin of allometric scaling in biology (Brown et al., 1999). Broadly known as metabolic scaling theory (MST), it is based on first principles of the physical distribution of resources through branching vascular networks. MST predicts that allometric relationships, how physiological and anatomical attributes of organisms change with changes in their size, should cluster around unique mathematical functions regardless of species composition or environment (Enquist & Niklas, 2001). If valid, these theoretical predictions could serve as constraints on empirically-derived allometries, which are highly limited by the small sample sizes used to create them. Thus, theory in one sense could serve as a substitute for the enormous difficulty in creating empirically derived equations supported by sufficient destructive sampling. However, the general applicability of these predictions is the subject of considerable controversy (Coomes et al., 2003, Coomes et al., 2007, Kerkhoff & Enquist, 2007, Lai et al., 2013, Lines et al., 2012, Muller-Landau et al., 2006, Price et al., 2007). Furthermore, MST also assumes spatial invariance (Enquist & Niklas, 2001) and their reconciliation with the limited empirical evidence of variability caused by environment and forest maturity is still under examination.

Applied to plants, MST predicts specific values for the exponents of numerous scaling laws relating various structural and functional attributes of individual trees. The theory has also been extended to predict scaling at the community level in forest systems (Brown et al., 1999, Enquist et al., 2009). MST deliberately makes several simplifying assumptions, including that: (i) forests are in approximate resource and demographic steady state; (ii) trees grow and fill up all available space so that the forest is space filling, and; (iii) natural selection has shaped the allometry of resource use and canopy branching so as to minimize vascular transport resistance but yet maximize the scaling of photosynthetic surface areas. The first assumption implicitly assumes that there is no recruitment limitation, all tree mortality is from competitive thinning, and that there is no external disturbance. In a forest that adheres to these assumptions, several forest- and ecosystem- level scaling relations are predicted (Brown et al., 1999, Enquist et al., 2009). Clearly, not all forests will follow these assumptions, and therefore we expect some forests to deviate from theoretically predicted scaling. The environmental conditions under which MST predictions are valid, however, remain unknown.

The overall goal of this research is to provide a continental scale analysis of allometric variability, with the goals of determining: (a) whether observed allometric relationships are spatially invariant; (b) whether environment can be used to explain observed allometric variability and (c) the conditions under which MST predictions match observations. Answering these questions requires a comprehensive

examination of forest scaling behaviour that spans large variability in species, demographic stages, and environmental gradients. One source of such data are the U.S. Forest Inventory and Analysis (FIA) program which provides individual tree measurements over hundreds of thousands of plots in the U.S.

We use two allometric relationships to address these goals. First, we assess the allometric scaling relationship between the basal stem diameter of a tree, D, and its height, H, predicted by MST as:

$$H \propto D^{2/3} \quad (1)$$

Second, we test the forest scaling prediction for the scaling of the number or frequency of trees (N) as a function of tree size, D,

$$N \propto D^{-2} \quad (2)$$

These particular allometric relationships were selected because tree diameter and height can be directly measured in the field, while attributed such as tree volume or biomass are estimated through allometry. Although we do not directly test allometries for biomass in this study due to data limitations, the general conclusions drawn from variability in these other two allometries should apply to allometries for biomass. The first predicts scaling at an individual tree level, which should relate to individual tree *D:M* relationships, while the second predicts system level scaling, at the approximate aggregate spatial scale (~1ha) that many remote sensing-based biomass maps are generated (Asner & Mascaro, 2014). Theoretical constraints on either individual tree-

level or plot-level allometries would dampen sensitivity to outliers, sampling strategies, and localized environmental conditions.

Methods

Data

Our research is based on the U.S. Forest Service's Forest Inventory Analysis (FIA, Reams et al., 2005) data for individual tree structural information. The FIA program routinely measures key biophysical parameters of individuals across thousands of spatially extensive plots in the U.S. FIA plots span gradients of climate and land use history and differ dramatically in species composition (Reams et al., 2005). In addition, forests sampled by FIA encompass various demographic stages, from secondary early succession to older growth forests.

We relate allometries derived from FIA date to environmental attributes from both the FIA data and the North American Regional Reanalysis (NARR) dataset (Li et al., 2005). The primary data taken from FIA are individual tree diameters (D) and heights (H). Diameter is measured for every tree in every plot, although different states adopt different forest sampling practices. We filter the data at each plot to D >=10 cm to ensure consistency among FIA plots. Topographic information, stand age, forest species class, and disturbance type are also obtained from the FIA dataset.

The North American Regional Reanalysis dataset is a 32 km gridded set of environmental data, including monthly precipitation, incident Photosynthetically Active Radiation (PAR), and temperature (Li et al., 2005). We use a thirty-year

monthly average from 1979-2010 for these three environmental variables, producing 12 monthly average values for each variable. We additionally calculate the annual averages, maximums, totals, and standard deviations. For each environmental attribute (e.g. precipitation), there are 16 associated inputs to our environmental-based models of allometric exponents.

Allometric Curve Fitting

For the relationship between *D* and *H*, equation (1), we fit the scaling exponent as the slope of a log-log linear relationship using OLS in model 2 regression analysis (Fig. 2-1a). OLS was selected because the error in *H* measurement is much greater then three times the error in *D* (Legendre, 1998). For the forest size-frequency distribution, equation (2), we used the maximum likelihood estimator (Clauset et al., 2009) to fit a pareto distribution over a range of *D* values (Fig. 2-1b).

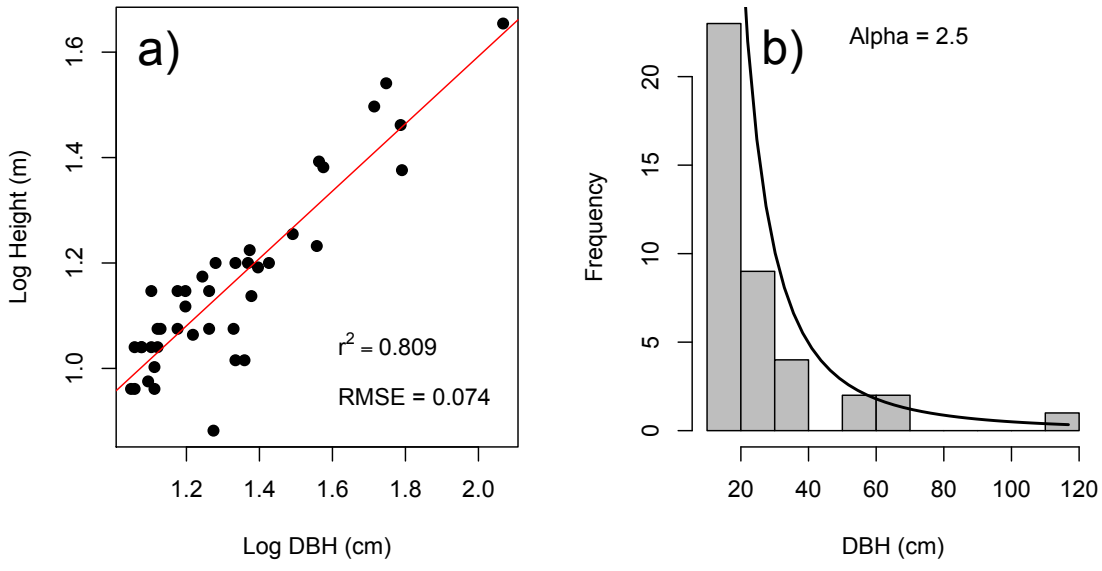

Figure 2-1. Visualization of two methods for allometric equation fitting. For a log-log linear relationship is fit (a) while for tree size distribution a maximum likelihood power law is fit using KS statistics.

When applying power law fits to tree size distributions in FIA plots, often there were fewer small individuals in the smaller size classes (close to 10 cm *D*) than expected. In these plots, it would be inappropriate to fit a Pareto distribution over the full range of *D* size classes measured. Thus theoretical predictions do not apply to smallest size classes in these forests, as the smaller size classes do not fit a power law. Our analyses do show, however, that scaling relationships do apply to forest size distributions above a certain size class. We followed the Clauset method (Clauset et al., 2009) to fit power law exponents with an assigned minimum *D* value. Allowing full flexibility to the assignment of *D,* the x_{min} value is set to the value of *D* that maximizes the KS statistic comparing observed data to a power law distribution. However, this value of *D* was often large enough to reduce the sample size above *D* to an inappropriately low number for power law fitting (n<25). To balance the trade off between maximizing sample size and ensuring statistically significant power law fits, we iteratively calculated the KS statistic for increasing values of *D* and selected the smallest *D* that yielded a KS statistic with a 95th percentile probability that the data fit a power law. These values of x_{min} were used to classify plots as having apparent recruitment limitation (x_{min} >=20 cm) or without apparent recruitment limitation (x_{min}<20 cm). Additionally, these x_{min} values were used to develop random forest models of recruitment limitation (Table 2-1).

For every FIA plot across the U.S. an exponent was fit for equation (1) if there were more than 10 *H* measurements taken, and equation (2) if there were more than 25 *D* measurements taken. The discrepancy between minimum number of trees sample is due to the different fitting techniques used for each equation. When a plot was sampled over multiple years, the most recent year was taken. Although the total number of FIA plots across the US is over a million, the total number of FIA plots that met our analysis criteria was only 223,492.

Random Forest Modeling

Random forest regression is a nonparametric statistical technique based on combining many classification or regression trees, each generated with a different bootstrapped subset of the original data (Breiman, 2001). We developed random forest models of the two scaling exponents as well as our proxy for recruitment limitation (x_{min}) to understand variability as a function of environmental. Here, we filter FIA plots again to include only those with statistically significant scaling fits ($p>0.05$ for equation (1)) or errors expected to be <20% (more than 25 trees above the fitted x_{min} value for equation (2)) (Clauset et al., 2009). Predictor variables are latitude, longitude, stand age, slope, aspect, elevation, forest type, maximum tree height, monthly averages and annual total, mean, and standard deviation of monthly PAR, temperature, and precipitation.

We use random forest variable importance to determine the relative impact of environmental attributes. Variable importance is calculated as the change in model accuracy (mean squared error) when a given variable is randomly permuted in the

out-of-bag samples (Genuer et al., 2010). Variable importance is normalized by the maximum variable importance for each random forest model (Table 2-1).

Results

We observe spatial variability in both scaling relationships across the U.S. Mapping these exponents shows spatial patterns in the allometries for *D* to *H* (equation (1), Fig. 2-3) and tree size distribution (equation (2), Fig. 2-4). These patterns suggest that the structural allometry of forests varies strongly as a function of location. The median scaling exponents for equation (1) and equation (2) were 0.55 and -2.77 (Fig. 2-2), and deviate from the theoretical predictions of 2/3 and -2.0 (Enquist et al., 2009), respectively.

Our random forest models explain 35% and 40% of the variability in the allometric diameter-height scaling exponent, equation (1), and forest size distribution scaling exponent, equation (2), respectively. These results imply that at least some of the observed variability in allometry is a function of environmental conditions. For equation (1), forest species composition, temperature variability, longitude, maximum forest height and elevation were the most important variables used by the random forest model (Table 2-1). *D* to *H* scaling exponents in young forests between 5-35 meters become steeper (in log-log space) with increasing *H*. For forests taller than about 35 m, the exponents asymptotically converge to a single value, though this value is different for broadleaf forests than for conifer forests (Fig. 2-5). Broadleaf

forests asymptotically converge approximately to the MST prediction of 2/3, while conifer forests asymptote at ~0.7.

For equation (2), forest maximum height is the most important driver of tree size distribution, while forest species composition and location were also important variables (Table 2-1). Size distribution scaling exponents become shallower with increases in maximum forest height but then asymptote at the theoretical prediction of -2, observed across taller (about 35 m and beyond), mature forests, regardless of forest species type.

In approximately 10% of FIA plots, the tree size distribution did not take the form of a power law when considering the full range of stem sizes. This was due to a lack of small stems in these plots, where a statistically significant power law was only found when considering trees over a certain stem size (x_{min}) (see Methods). We can interpret x_{min} as a loose proxy for recruitment limitation, as it indicates the relative absence of small stems in a given forest plot. Modeling x_{min} as a function of our environmental and forest attributes (r^2=0.45) we found that elevation, the standard deviation of temperature, and the standard deviation of precipitation were the largest drivers of variability in x_{min}. In plots with an x_{min} >=20 cm D, we see that scaling exponents for equation (2) are considerably steeper, or more negative, than plots without an apparent dearth of small stems.

Testing the conditions under which MST predictions match observations is one goal of this study. However, how does one classify whether a forest plot follows MST?

Other researchers (Muller-Landau et al., 2006a) have focused on calculating a 95% confidence interval of tree size distributions through the bootstrapping of many spatially correlated plots. This approach violates the bootstrapping assumption of uncorrelated samples, and therefore likely estimates overly narrow confidence intervals. Regardless, we do not have data available over large contiguous areas with which to develop confidence intervals in this way. From our curve fitting procedures we calculate confidence intervals on fitted exponents, but the widths of these intervals are related to the number of trees included in each fit. Because FIA plots typically sample less than 50 trees, the confidence intervals around fitted exponents are wide, and consequently we would likely over report the number of plots that follow MST if we were to follow such an approach. We therefore refrain from confirming or refuting MST predictions at a plot level, and instead focus our study on trends in exponents as a function of environment.

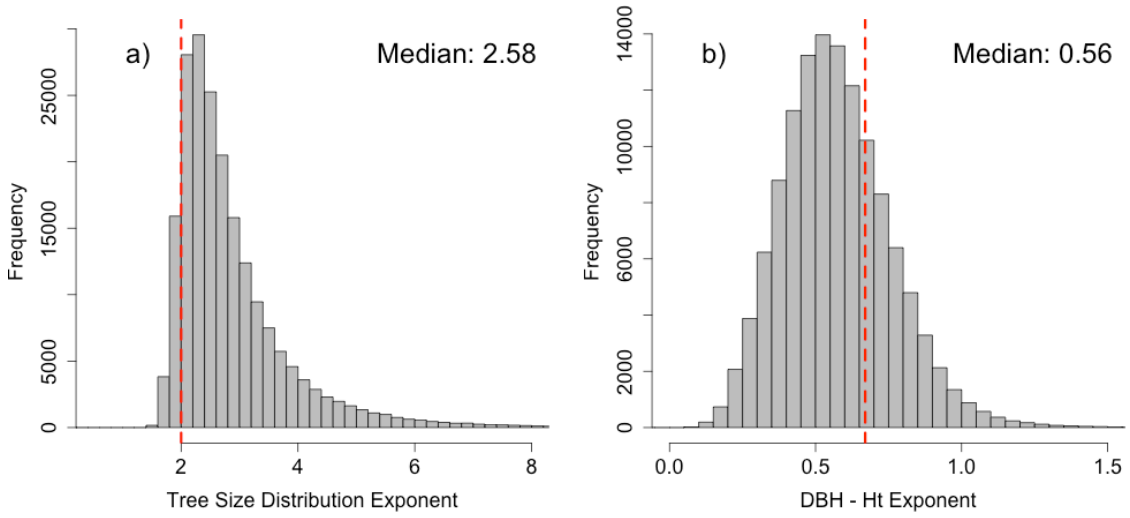

Figure 2-2. Distribution of fitted scaling exponents for Equation 1 (a) and Equation 2 (b). Red dotted lines represent the MST predictions for the two allometries.

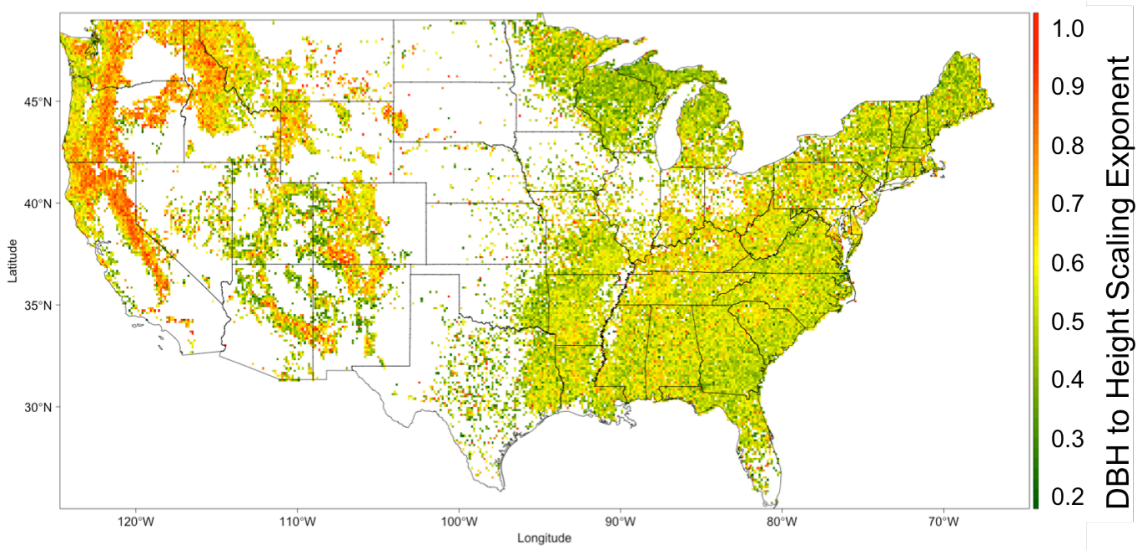

Figure 2-3. *D* to height scaling exponents mapped across the US. The greener regions of the map are shallower (smaller) exponents, indicating shorter trees for a given *D*. The redder regions of the map are steeper (larger) exponents, indicating taller trees for a given *D*.

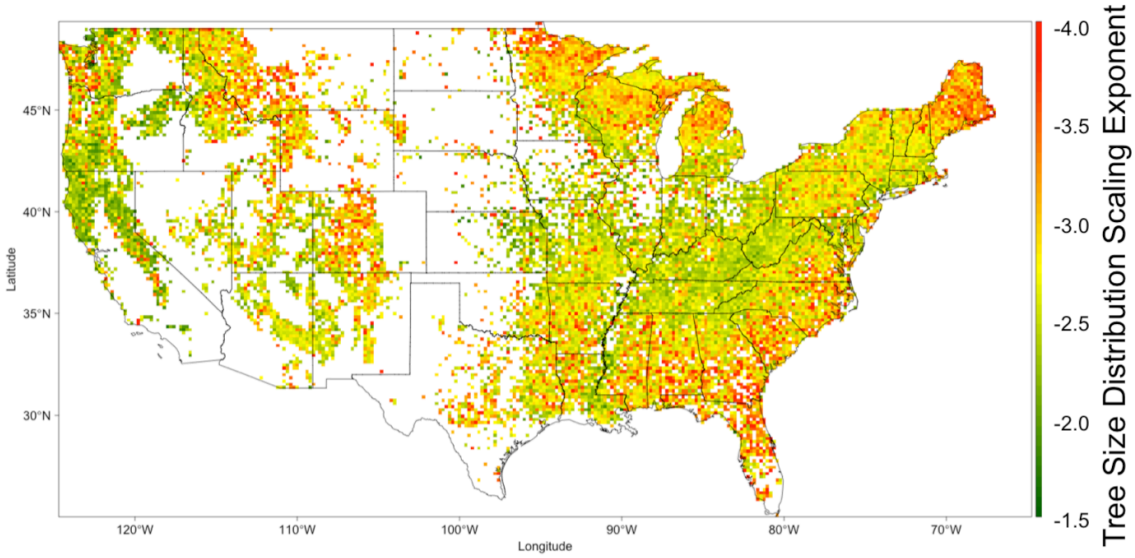

Figure 2-4. Plot-level tree size distribution scaling exponents mapped across the US. Steeper exponents (yellow and red) are forests where there are proportionally more small trees with respect to big trees. Shallower exponents (green) are forests with proportionally less small tree with respect to large trees.

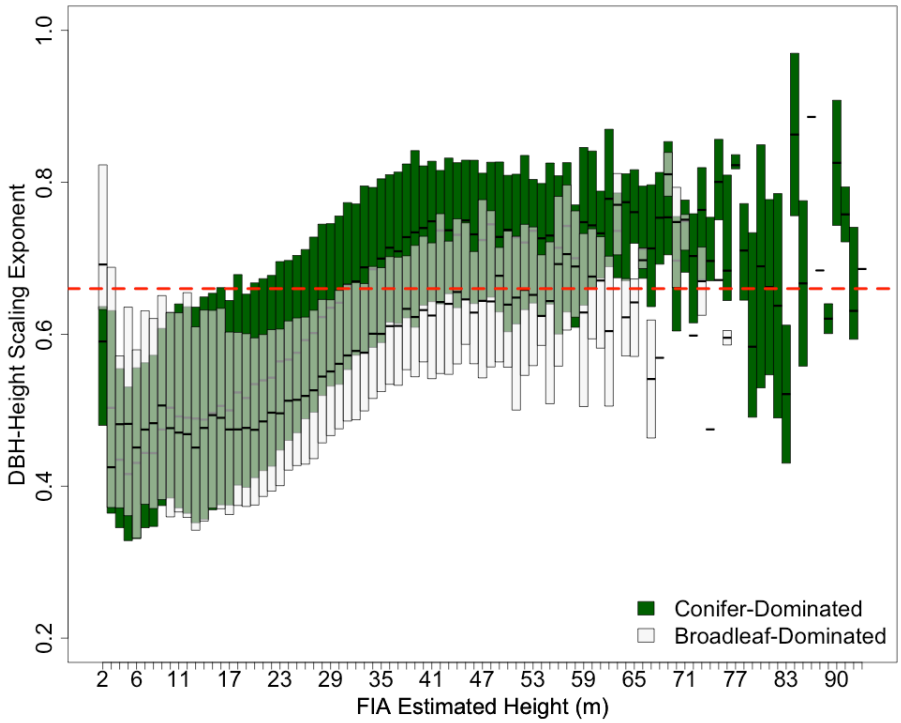

Figure 2-5. . *D* to *H* scaling exponents as a function of forest maximum height and tree species class. The bars on this plot represent the 10th to the 90th percentiles of scaling exponents in each height bin. Conifer-dominated forests

have a higher stabilization, generally growing taller for a given *D*.

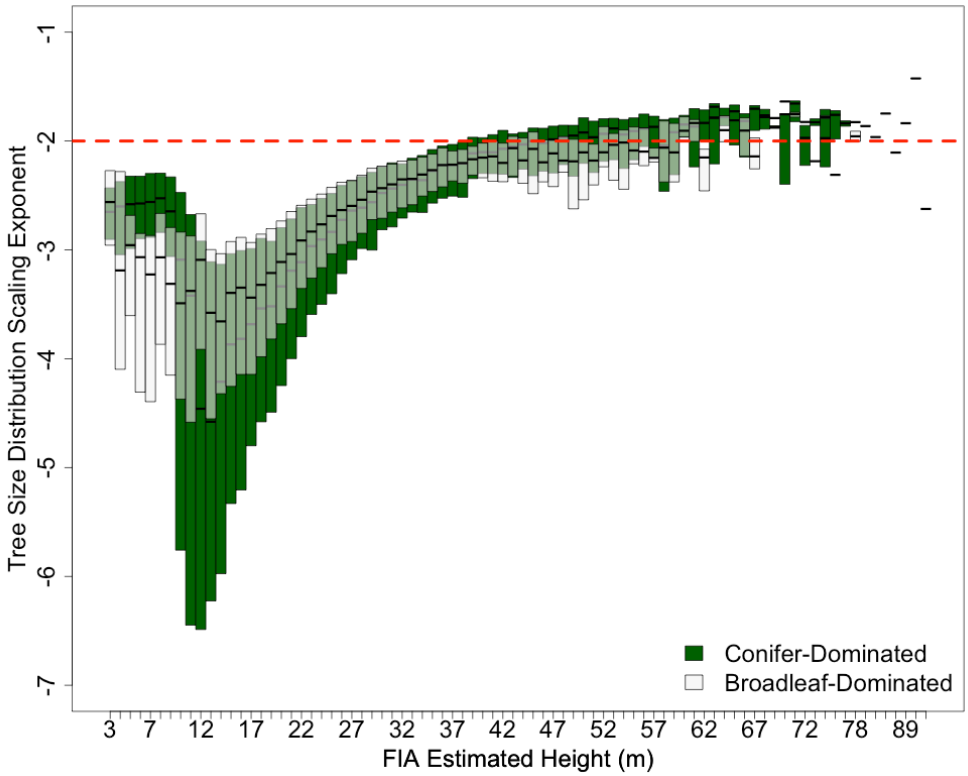

Figure 2-6. Forest tree size distribution scaling shown as a function of forest height and tree species class. The bars on this plot represent the 10th to the 90th percentiles in each height bin. This figure does not include the 10% of the forests plots exhibit apparent recruitment limitations (Fig. 2-7).

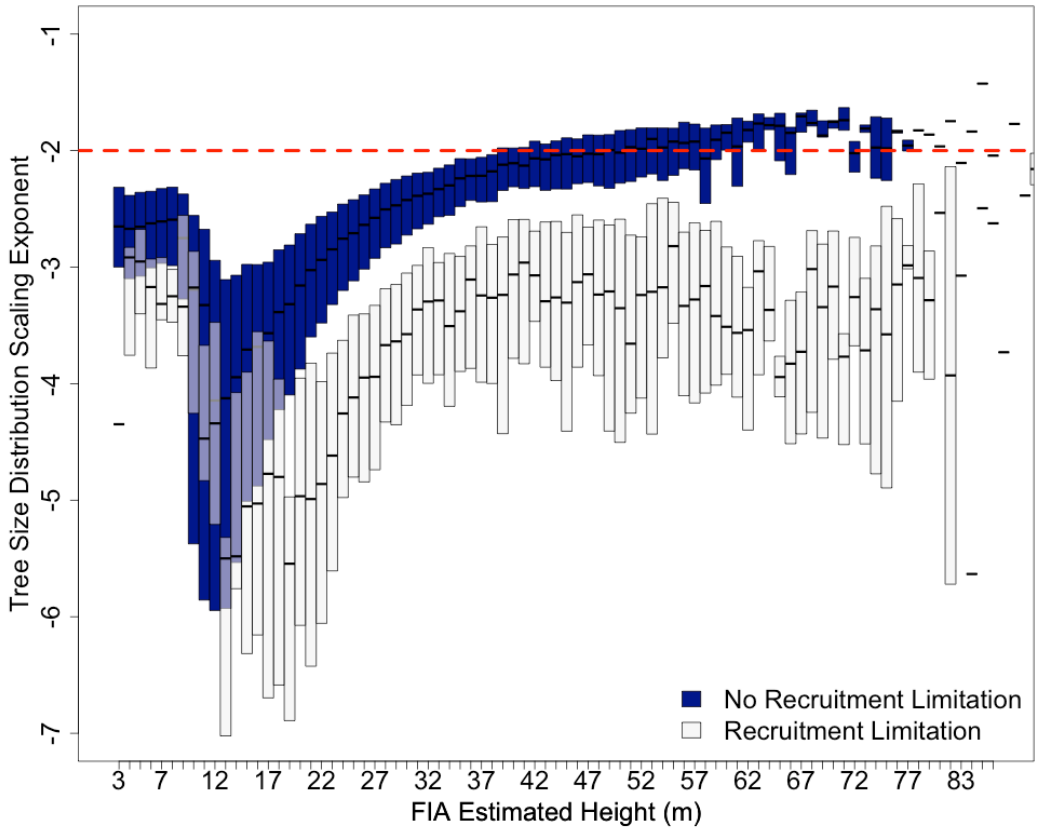

Figure 2-7. Forest tree size distribution scaling exponents in plots with and without apparent recruitment limitation, as a function of forest height. Apparent recruitment limitation is based on the x_{min} value of Pareto fits (see Methods). We assume that low values of x_{min} (10-20 cm) correspond to systems with no recruitment limitation, while values of x_{min} > 20 cm indicate forests within which the success of small trees is limited.

Table 2-1. Standardized relative importance of predictor variables in the random forest models of scaling exponents and recruitment limitation proxy (x_{min}). Each importance value from the random forest models has been divided by the maximum importance observed, therefore the variable with the highest importance has a value of 1.00. More important variables (>0.5) are presented in bold. Note that some input variables are correlated, which may affect their relative importance rankings (Gregorutti et al., 2014).

Environmental Variable	*H:D*	Tree Size Distribution	Recruitment Limitation Proxy (x_{min})
Latitude	0.43	**0.63**	**0.72**
Longitude	**0.87**	**0.53**	**0.81**

Age	0.12	0.2	**0.59**
Slope	0.07	0.07	0.07
Aspect	0.03	0.04	0.03
Elevation	**0.55**	0.41	**0.68**
Annual Total Temp	0.40	0.46	0.29
Mean Annual Temp	0.43	0.44	0.29
SD Monthly Temp	**0.65**	0.45	**0.54**
Total Annual Precip	0.24	0.29	0.27
Mean Annual Precip	0.26	0.29	0.29
SD Monthly Precip	0.18	0.23	**0.62**
FIA Forest Type Code	**1.0**	**0.72**	0.44
Total Annual PAR	0.27	0.46	0.45
Mean Annual PAR	0.29	0.46	0.43
SD Monthly PAR	0.44	0.32	0.37
Max Forest Height	**0.60**	**1.0**	**1.0**

Discussion

The goals of this research are to determine whether forest scaling is spatially invariant, whether any observed variation is a function of environment, and the conditions under which MST predictions appear to be consistent with observations. We find considerable spatial variability in both individual tree-level scaling (equation 1) and plot level scaling (equation 2). Variables associated with environmental conditions account for about 35%-40% of this variability. Both scaling relationships appear to asymptote with increasing forest height. This suggests that while shorter, younger forests may take on a variety of scaling exponents, mature forests (i.e. tall forests) exhibit consistent scaling exponents.

Height to Diameter Scaling

We find no evidence of a universal scaling relationship for equation (1). Indeed, *H:D* scaling exponents in young forests between 5-35 meters become steeper (in log-log space) with increasing forest maximum height. However, for forests taller than about 35 m, the exponents asymptotically converge to a single value, although this value is different for broadleaf forests than for conifer forests (Fig. 2-5). Broadleaf forests asymptotically converge around the theoretical prediction of 2/3, while conifer forests converge around 0.7 (differing from MST).

This discrepancy between conifer and broadleaf forests is observed consistently, and may be attributable to differences in wood density (Dietze et al., 2008). Lower wood density in conifer trees may allow for increased vertical biomass allocation without approaching critical buckling height while greater wood density may promote horizontal branching in broadleaf angiosperm trees (Iida et al., 2012). If we consider forest height as a proxy for light availability, then trees in taller, light-limited forests are expected to allocate biomass preferentially to height to compete for light (Koch et al., 2004), although this competition is likely to vary with environment (Lines et al., 2012). In contrast, trees in shorter, more open forests are not expected to allocate biomass to height expansion and instead allocate a larger proportion of their biomass to lateral expansion (Iida et al., 2012).

Our findings with respect to *H:D* allometries are similar to other studies, both in tropical and Mediterranean systems. Our median scaling exponent, 0.56, is close to

the value of 0.593 found at BCI in Panama (Muller-Landau et al. 2006a), 0.609 for aggregated species from the Spanish Forest Inventory (Lines et al., 2012), and within the range of 0.485-0.617 found for continental aggregates in a pantropical study (Feldpausch et al., 2011). Additionally, our finding that large conifer trees have higher *H:D* scaling exponents than their broadleaf counterparts is consistent with Spanish forests (Lines et al., 2012).

Thus, to summarize, there is considerable spatial variability in *H:D* scaling exponents, some of this variability appears to be related to environmental variables, and there is some support that mature forests follow MST scaling predictions, but even here there is deviation from theory based on broadleaf vs. conifer forests.

Tree Size Distribution Scaling

Regarding the second allometric relationship we consider, tree size distribution, we again find no evidence of a universal allometry; forest allometry in the U.S. varies considerably across the landscape as a function of local environment and life history. We find the tree size distribution scaling exponent to be sensitive to changes in forest height (Table 2-1) in young, maturing forests, while size distributions appear more stable in tall forests that have may have reached resource and demographic steady state (Fig. 2-6). This corroborates findings from other studies that show shallower slopes as forests mature (Enquist et al., 2009). Other studies have rejected MST's prediction for tree size distribution because they did not find an exponent of precisely -2.0 in their field sites (Coomes et al., 2003, Muller-Landau et al., 2006b, Coomes et

al., 2007, Lai et al., 2013). In our study, deviations from MST are observed in forests that presumably do not follow the inherent assumptions of MST. For example, MST assumes that a system has met resource and demographic steady state, and that there is no recruitment limitation. Young, shorter forests are unlikely to meet these criteria because they have not had time to occupy all available physical and resource space. Additionally, forests with a dearth of small stems likely exhibit recruitment limitations. Therefore the highly idealized conditions requisite for MST to hold are rarely exhibited in the U.S.

Our findings regarding apparent recruitment limitation are of particular ecological interest. In differing environments, the establishment and growth of seedlings and saplings can be limited by cold temperatures, light limitations (Muller-Landau et al., 2006b), ground fires, or herbivory. Our proxy for recruitment limitation appears ecologically reasonable, as about 45% of the variability in x_{min} is explained by environment in our random forest model, with elevation, forest height, and temperature and precipitation variability yielding the highest importance values. Small trees and saplings are known to be less successful at high elevation, in tall, dense forests, and in areas with highly variable climates.

In forests with size distributions consistent with apparent recruitment limitation (about 10% of our plots) we find forest tree size-frequency exponents steeper than predicted by MST (Fig. 2-8). Studies in tropical forests have also found steeper than expected scaling exponents when considering only trees >20 cm (Muller-Landau et al., 2006b). This may seem counter intuitive, as steeper exponents indicate a larger

relative proportion of small stems. However, we only fit scaling exponents above the smallest size class that yields power law scaling, and therefore small stems in these cases are stems close in size to the selected x_{min}. In these 'recruitment-limited' plots, steep scaling exponents could indicate (a) more medium sized trees than expected, or (b) fewer large trees than expected. We believe these plots are being affected by size dependent mortality, with disturbance preferentially affecting larger trees (Coomes et al., 2003, Lai et al., 2013, Fellows & Goulden, 2008, Lines et al., 2010). It has been demonstrated that there is a U-shaped relationship between mortality rate and tree size in the Eastern U.S. (Lines et al., 2010) with both small and large stems exhibiting higher mortality rates. Differential disturbances from external forces are not currently included in MST (Enquist et al, 2009, Price et al., 2007).

In summary, with respect to tree size distribution, there is spatial variability in exponents that can be partially explained by environmental variables, particularly forest maximum height. In tall, presumably mature forests, exponents asymptote to approximately the MST prediction of -2. In plots exhibiting apparent recruitment limitation, however, exponents are steeper than MST predictions. Although MST may be theoretically valid, most forests in the U.S. do not follow predicted scaling, potentially due to the violation of MST assumptions that forests are in resource and demographic steady state with no recruitment limitation or size dependent mortality.

Conclusions

For both of the relationships we tested, we see that forest allometries are not invariant with respect to environment or life history. Rather, in short, presumably maturing forests, there is considerable spatial variability in allometric relationships that can be partially explained as a function of environment and forest structure. Therefore, neither empirically nor theoretically derived allometric equations should be applied without a careful consideration of environment. With respect to theoretical allometries, from MST, we find that the vast majority of U.S. forest plots do not follow predicted scaling. This does not, however, mean that MST is theoretically invalid. The *D:H* allometric exponents asymptote in tall forests at approximately the MST prediction of 2/3 for broadleaf forests, but asymptote at a higher value in conifer systems. For the plot-level tree size distribution exponents, both broadleaf and conifer forests asymptote at approximately the MST prediction of -2 in tall forests.

This study does not negate the findings of other researchers who rejected MST, but rather contextualizes them as samples from a relatively tight range of environments that may not follow MST scaling. Forests should naturally shift toward MST predictions with time, provided there is no persistent perturbation consistently preventing the system from entering steady state, e.g. a recruitment limitation. However, most forests across the U.S. are still recovering from disturbance and have not yet reached the demographic steady state necessary for theoretical predictions to apply. Indeed, some forests may never follow MST scaling if they are perpetually disturbed.

Our main conclusions are two-fold. First, empirically derived allometries should be developed across ranges of environmental gradients, and caution should be taken when applying an allometry outside the range of conditions under which it was developed. Second, MST appears theoretically valid, but requires updating to apply to the ranges of environmental conditions and successional states found in U.S. forests. There is great potential for linking theoretical and empirical allometry, but applying MST to problems such as carbon stock and flux mapping will require its expansion to include considerations of system maturity, recruitment limitations, and size-dependent disturbance.

Chapter 3: An Efficient, Multi-layered Crown Delineation Algorithm for Mapping Individual Tree Structure Across Multiple Ecosystems

Abstract

Deriving individual tree information from discrete return, small footprint LiDAR data may improve forest aboveground biomass estimates, and provide tree-level information that is important in many ecological studies. Several crown delineation algorithms have been developed to extract individual tree information from LiDAR point clouds or rasterized Canopy Height Models (CHM), but many of these algorithms have difficulty discriminating between overlapping crowns, and also may fail to detect understory trees. This approach uses a watershed-based delineation of a CHM, which is subsequently refined using the LiDAR point cloud. Individual tree detection was validated with stem mapped field data from the Smithsonian Environmental Research Center (SERC), Maryland, and on a plot and stand level through comparisons of stem density and basal area to delineated metrics at both SERC and a study area in the Sierra Nevada, California. For individual tree detection, the algorithm correctly identified 70% of dominant trees, 58% of codominant trees, 35% of intermediate trees and 21% of suppressed trees at SERC. The algorithm had difficulty distinguishing between crowns of small, dense understory trees of approximately the same height. Delineated crown volume alone explained 53% and

84% of the variability in basal area at the SERC and Sierra Nevada sites, respectively. The algorithm produced crown area distributions comparable to diameter at breast height (DBH) size class distributions observed in the field in both study sites. The algorithm detected understory crowns better in the conifer-dominated Sierra Nevada site than in the closed-canopy deciduous site in Maryland. The ability for the algorithm to reproduce both accurate tree size distributions and individual crown geometries in two dissimilar and complex forests suggests great promise for applicability to a wide range of forest systems.

Introduction

LiDAR has become the dominant technology for mapping 3D forest structure (Wulder et al., 2012, Zoltros et al., 2013). Discrete return and waveform LiDAR have been widely applied for forest height, crown volume and biomass estimation. While medium or large footprint (20-70 m) LiDAR data are useful for characterizing the vertical distribution of canopies at the resolution of the footprint, small footprint (10's of cm) LiDAR provides both vertical and horizontal information at the scale of individual trees (Wulder et al., 2012). Estimates of forest biomass have largely ignored the highly detailed spatial information from discrete return LiDAR and focused on metrics such as canopy height and cumulative vertical distributions at plot level. Providing more spatially detailed information such as the number, location, spacing, and size distribution of individual trees may improve biomass estimation at varying spatial resolutions, and should provide a more ecologically meaningful structural description of a forest.

Various methods for extracting individual tree information from high resolution LiDAR datasets have been developed. These techniques generally fall into three categories: local maxima detection and expansion (Maltamo et al., 2004, Persson et al., 2002, Popescu and Wynne, 2004, Kaartinen et al., 2012, Vastaranta, 2011, Leckie et al., 2003), watershed-based delineation (Koch et al., 2003, Chen et al., 2006, Kwak et al., 2007, Breidenbach et al., 2012), and point-cloud clustering (Ferrez et al., 2012, Rahman et al., 2012). Local maxima algorithms typically involve the selection of a search radius and detection of local maxima from a CHM. Popescu and Wynne (2004) used both circular and square windows with site-specific window sizes to increase local accuracy of maxima detection. Leckie et al. (2003) applied a valley-following approach to isolate crowns based on CHM topography that yielded both tree locations and crown geometries with 80% accuracy. However, the trees in this study were well spaced and easily visible in the CHM. Vastaranta et al. (2011), used a minimum curvature approach with local maxima detection for a boreal forest and although they did not present an individual tree accuracy, they used delineated crowns to predict basal area (R^2=0.48) and volume (R^2=0.71). Maltamo et al. (2004), also worked in a boreal forest with a local maxima detection algorithm and reported that while as much as 80% of dominant crowns were correctly detected, the total accuracy was 40% due to issues identifying understory crowns. Although local maxima techniques are computationally the fastest and simplest algorithms, these algorithms often fail to detect understory and overlapping trees in structurally

complex forests, and have difficulty detecting crown edges, typically oversimplifying crown geometry (Kaartinen et al., 2012).

Watershed-based delineations offer an improvement for crown geometries, and function on inverted CHMs by segmenting neighboring crowns along lines of local minima (Chen et al., 2006). Watershed approaches can be combined with local maxima detection to limit the number of local maxima within a segment to one. Koch et al. (2003) used a modified watershed approach, allowing for merging and refinement of delineations with *apriori* knowledge of forest structure. They found that for conifer trees, approximately 87% of trees were correctly identified using this technique but for deciduous species only 50% were correctly delineated, with errors arising from understory and overlapping crowns. Breidenbach et al. (2012) also found that their watershed approach could not detect understory or overlapping crowns when local maxima were undetected.

Point cloud based techniques are the newest and most computationally demanding of the three delineation approaches. Point cloud-based techniques use the full information content from discrete return LiDAR datasets and therefore offer great promise for future advancement in this field. However, current point cloud-based techniques have focused on small areas within a single study site and may not be applicable across a range of forest types. Rahman et al. (2012) use the density of LiDAR returns for crown detection, while Ferraz et al. (2012) use an iterative clustering approach based on a mean shift algorithm to detect trees in 3D space.

Ferraz et al (2012) reported that although 99% of overstory trees were detected by their algorithm, only 12.8% of suppressed trees were, suggesting that even detailed site-specific point cloud methods have difficulty detecting understory trees.

Most algorithms for crown delineation have remained focused on conifer dominated, boreal forests, with plot level validation. Kaartinen et al. (2012) conducted an analysis of several delineation algorithms in boreal systems and reported accuracies range from 40-95% accuracy for open conifer trees, 5-45% for trees neighboring a larger tree, and less than 20% for intermediate or suppressed canopies. Boreal forests are less structurally complex than temperate or tropical broadleaf forests, and therefore algorithms developed in boreal areas may be less effective in more complex forests. Current crown delineation algorithms inadequately identify understory and overlapping trees, and have rarely been tested across different biomes. There is consequently a need for an understory-sensitive algorithm that can be efficiently applied to LiDAR datasets with a range of point densities in a variety of ecosystems. The goal of this paper is to present the development and testing of a novel crown delineation algorithm that offers both applicability over varying forest types and improvement for understory and overlapping tree detection.

Methods

Study Areas

This delineation algorithm is tested in the eastern and western USA. The first study site is a broadleaf dominated experimental forest in Maryland managed by the Smithsonian Environmental Research Center (SERC). SERC is located near

Edgewater, Maryland, adjacent to a sub-estuary of the Chesapeake Bay. The area is generally comprised of two forest types; mature secondary upland forest and floodplain forests. Dominant species in the upland forest include tulip poplar, several species of oak, beech, and several species of hickory, with mid canopy red maple and sour gum and understory American hornbeam, spicebush and paw-paw. Dominant species in the flood plain area are ash, sycamore, and American elm. Both the upland and the floodplain forests have been relatively undisturbed for approximately 120 years.

The second study site is the Teakettle Experimental Forest in the western Sierra Nevada mountain range, California. Dominant species include California black oak, white fir, ponderosa pine and red fir (Hunsaker et al., 2002). The elevation ranges from approximately 1000 m to 2500 m, with aboveground biomass values averaging ~ 200 Mg/ha with individual trees up to 20.0 Mg. The forest is mature, featuring clusters of trees in flatter areas of the land with thicker soils, and rocky outcrops in steeper areas (Swatantran et al., 2011).

Field Data

In the SERC study area, field data were taken from the SIGEO field acquisition, in which a 16.0 ha plot was laid out and every tree greater than 1 cm DBH was sampled and stem mapped between 2008-2011 (http://www.sigeo.si.edu/). Tree location, species, DBH, crown class (dominant, codominant, intermediate or suppressed) and crown condition were recorded. Dead and damaged trees were eliminated from the dataset prior to comparison with delineation results due to a lack of description of the

type of damage. For validation, the 16 ha stem map was subset into 16, 90 meter square subplots. The stem map at SERC is based on georegistered based on a series of monumented posts that were located every 200 m on a true N-S geographic grid. The location of these posts had an accuracy of less than 1-2 meters. Additional posts were located at 10 by 10 meter spacing within the SIGEO area, and trees were stem mapped using measuring tapes. The additional posts were laid out using a combination of laser rangefinders and compasses, as well as a total station (Parker, G., Pers. Comm.).

In the Teakettle forest area, 90 m square sample plots were collected in the summer of 2008 (n=12). The DBH, species and condition of all trees were recorded. Dead trees were removed from the analysis. Within each central sub plot the location and height of trees were also recorded. However, given issues with georegistering tree locations to LiDAR data, stem mapped data were not used to pursue an individual-based tree validation for the Sierra Nevada site.

LiDAR Data

LiDAR data for SERC were collected with NASA Goddard's LiDAR, Hyperspectral and Thermal Imager (Cook et al., *in press*) instrument. G-LiHT uses a 300 kHz multi-stop scanning LiDAR with a 60° field of view and 10 cm diameter footprint, and the site was flown with 50% overlap in north-south and east-west directions to achieve a mean return density of up to 50 laser pulses/m^2. Leaf-off and leaf-on data were acquired during March, 2012 and June, 2012, respectively.

LiDAR data for the Sierra Nevada site were flown in the summer of 2008 with the University of Florida's OPTECH GEMINI ALSM unit, operating at 100-125 kHz with a maximum 25° scanning angle. Data were flown ~600-750 m above ground, with 50%-75% swath overlap yielding an average return density of approximately 18 pts/m^2.

Algorithm Development

Figure 3-1 shows the processing framework applied by this algorithm. The only inputs to the algorithm are raw LiDAR point cloud files. These LiDAR point clouds are preprocessed adding a 20 m buffer to LiDAR tiles to ensure that tile edges do not affect the outputs. The algorithm generates a series of rasters with a 0.5 m pixel size. The first raster, a Digital Terrain Model (DTM), is generated using all returns with a moving window and local minima detection and smoothing. The second raster, a Canopy Height Model (CHM), is generated by finding the maximum Z value (from all returns) in each pixel and subtracting the corresponding DTM value (Figure 3-1.1). This raw CHM is then smoothed using a customized moving window average filter (Figure 3-1.2). The window size can be varied, but a 5 by 5 window was used here.

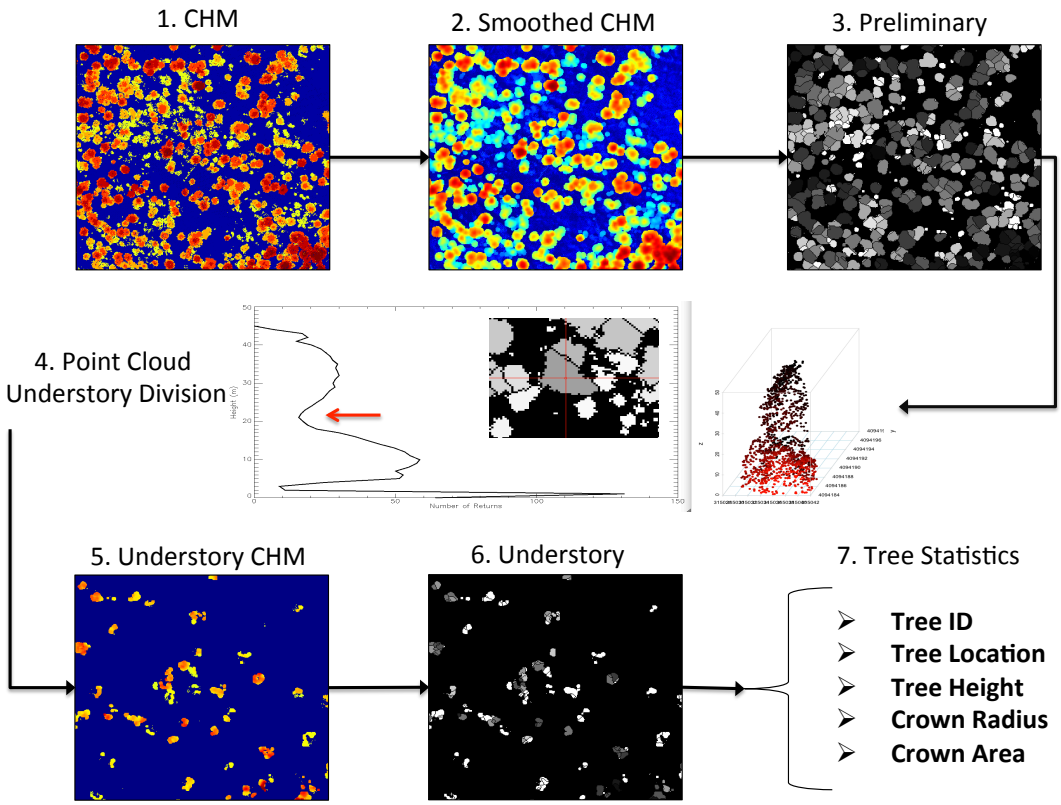

Figure 3-1. Processing flow of algorithm. First a CHM is generated. Second, the CHM is smoothed and internal crown gaps are filled. Third, a preliminary watershed delineation is applied. Fourth, the raw LiDAR returns from each segmented area are extracted and binned vertically, a trough finding algorithm is applied, and returns are classified as either overstory or understory. Fifth, overstory and understory CHMs are generated. Sixth, the overstory and understory CHMs are segmented. Steps 4-6 are applied iteratively. Finally, tree statistics are generated.

The customized smoothing algorithm is described as follows. First, pixels are classified as canopy or ground pixels using 2 m as a separation between canopy and potential ground hits. Ground pixels are not included in averaging to avoid underestimating tree heights. For each 'ground' pixel, the algorithm searches neighboring pixels to determine whether the pixel is within a crown or outside of a crown. If four or more neighboring pixels are canopy pixels, the central pixel will be classified as a within crown low return. These pixels are assigned the average value

of their neighboring crown pixels to reduce over segmentation of crowns due to either high return density LiDAR or sparse canopies. It should be noted that the 2 m height filter means that this algorithm does not detect understory vegetation at less than 2 m of height.

After smoothing, a preliminary delineation is conducted using an inverted CHM and a watershed function (Figure 3-1.3). Every pixel in the image is assigned the ID number of the associated watershed. Pixels with an elevation less than 2 m are assigned as ground pixels, and set to a value of zero.

The preliminary watershed segments may represent a single tree or a cluster of trees. To separate returns from understory trees, the raw point cloud data are extracted for the area overlapping each preliminary segment (Figure 3-1.4). These raw points are binned with a vertical resolution of 10 cm, generating a LiDAR height histogram for each preliminary segment. A trough finding algorithm smoothes the height histogram and detects troughs by determining when there is a continuous decrease and subsequent continuous increase in bin magnitude for a moving window of 9 bins (Figure 3-2). When multiple troughs are detected the highest trough is selected as the point of return separation. It is assumed that there will be no significant troughs found in height histograms returned from a single tree, and that there will be a trough found before the peak return from lower trees in the case of tree clusters. Figure 3-2 shows four examples of this point cloud refinement.

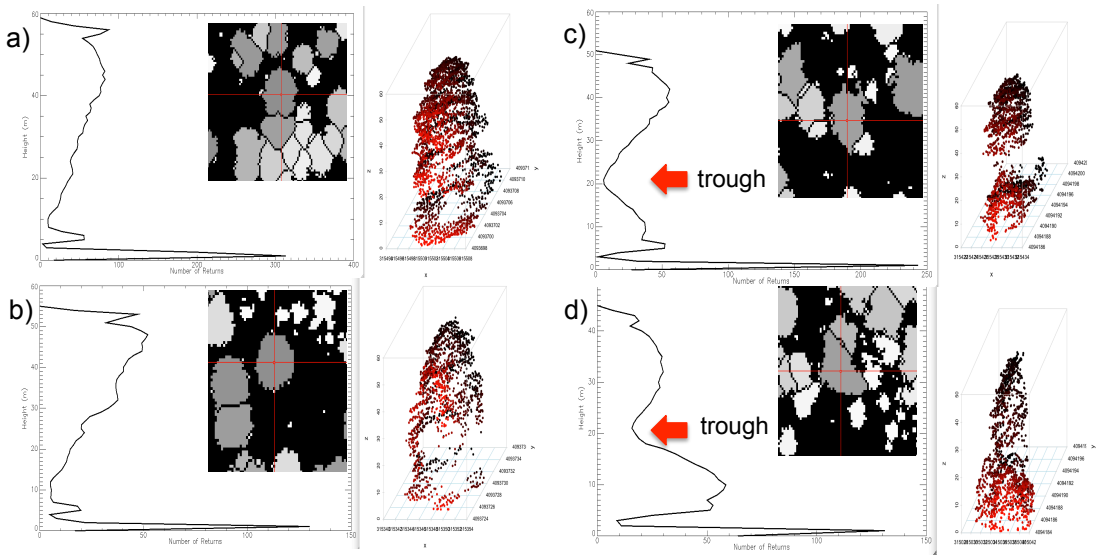

Figure 3-2. Four examples of point cloud extraction and binning showing the preliminary segment location under the red crosshairs, the extracted LiDAR returns with red indicating distance in Y, and the corresponding vertically binned pseudo waveforms. a) and b) were determined to be individual trees while c) and d) were flagged as multiple trees. The returns below the indicated troughs were separated for generation of an understory CHM.

The LiDAR returns below each detected trough are separated from the higher LiDAR returns. Each set of returns is then used to generate two new CHMs for the entire area, one of higher canopies, and one of lower canopies (Figure 3-1.5). These secondary canopy height models are then segmented with another watershed delineation, resulting in the separation of tree clusters and the delineation two layers of tree crowns (Figure 3-1.6). If there are only two layers in a system, an overstory and an understory set of tree crowns will be detected. In the case of multilayered forests, the process of generating height histograms, separating vertical returns, and generating understory canopy height models, is iterated until no further understory trees are detected. Therefore this algorithm is capable of detecting infinite layers of tree crowns, however in both of the systems in this study, three layers were detected.

Therefore the first layer is referred to as an ‘overstory’ layer, the second as a ‘midstory’ layer, and the third as an ‘understory’ layer.

The location, height, area, and radius of trees are generated from the algorithm (Figure 3-1.7). Crown area is calculated as the number of pixels in the crown multiplied by the area per pixel (0.25 m^2). Crown radius was computed as the mean crown radius along the north-south and east-west directions. Tree heights were extracted from the unsmoothed CHM corresponding to the canopy layer. For example, if the algorithm is run for three layers, tree segments from the highest layer are assigned heights from the overstory CHM, tree segments from the middle layer are assigned heights from the mid layer CHM, and tree segments from the lowest layer are assigned heights from the lowest, or understory, CHM.

Figure 3-3 illustrates the potential power of multilayered crown delineation. A few tall trees in the original CHM resulted in preliminary segments representing clusters of trees rather than individuals. Separating the tall trees for processing as overstory crowns allowed for shorter crowns to be correctly detected and delineated.

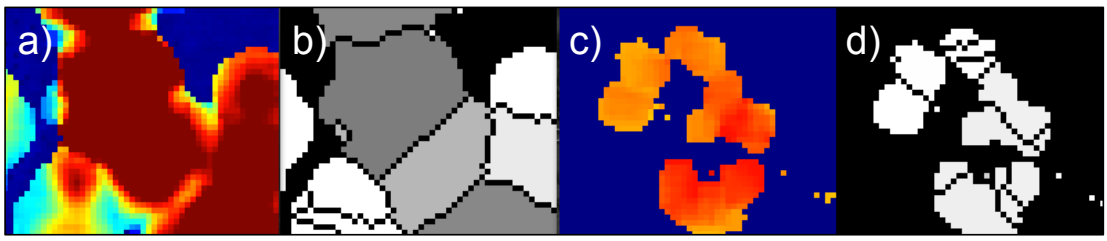

Figure 3-3. a) Smoothed CHM b) preliminary segmentation c) understory CHM and d) understory segmentation. The shorter trees seen in the c) and d) were not apparent in the original CHM because of taller overstory trees.

Although this algorithm is computationally demanding, it has been optimized for use in parallel computing systems resulting in computational efficiency. 32 cores (CPUs), each with 2GB RAM processed the SERC dataset in 1.5 hours and the Sierra Nevada dataset in 30 minutes. The algorithm is written in IDL and GDL, and could be run in serial however it would take at least 32 times longer to run (~32 hours) for these relatively small areas. This algorithm was run on NASA's Pleiades supercomputing system through affiliations with the NASA Earth Exchange (https://c3.nasa.gov/nex/).

Results

Individual Tree-level Validation

At SERC, the number of trees correctly detected in each crown class in June, as a percentage of number of stems in the field dataset, is 70% dominant trees, 58% codominant trees, 35% intermediate trees and 21% of suppressed trees (Table 3-1, Figure 3-4).

To test the algorithm's sensitivity to leaf-off versus leaf-on LiDAR data collection, two data collection periods were compared. Figure 3-5 shows the accuracy of individual tree detection in SERC during the leaf-off period. Overall, the algorithm performs similarly in both leaf-on and leaf-off condition (Table 3-1). However, 14% fewer dominant trees are correctly detected during leaf off, while 8% more suppressed trees are correctly identified.

Table 3-1. Individual tree level reported accuracies at the SERC study site. The % correct is the number of corrected identified stems divided by the total

number of stems from the field dataset. The % Estimated is the number of total identified stems (correct and errors of commission) divided by the total number of stems in the field.

		March	June
% Correct	Dominant	56%	70%
	Codominant	52%	58%
	Intermediate	32%	35%
	Suppressed	29%	21%
% Estimated	Dominant	56%	70%
	Codominant	98%	103%
	Intermediate	199%	201%
	Suppressed	58%	50%

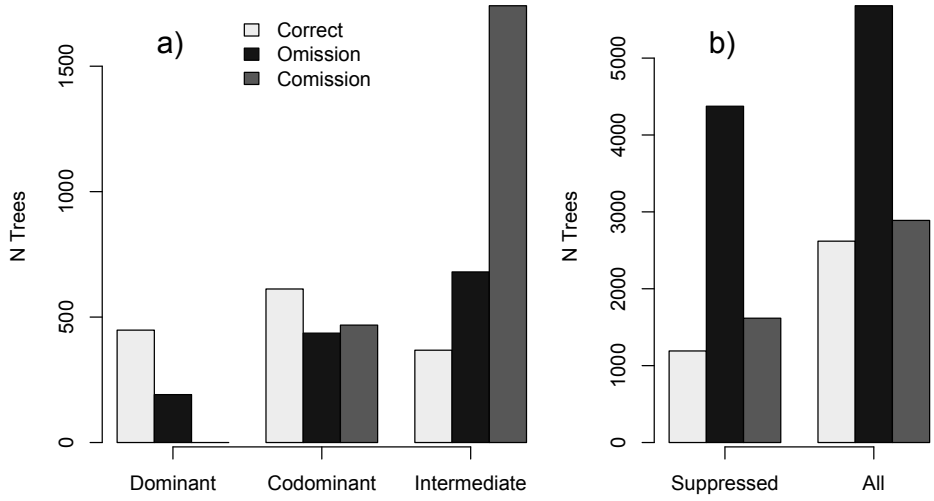

Figure 3-4. The individual tree-based accuracy assessment at SERC during the leaf-on period showing the number of trees correctly classified as well as errors of omission and commission. a) comparisons for dominant, co-dominant and intermediate classes and b) suppressed and total errors.

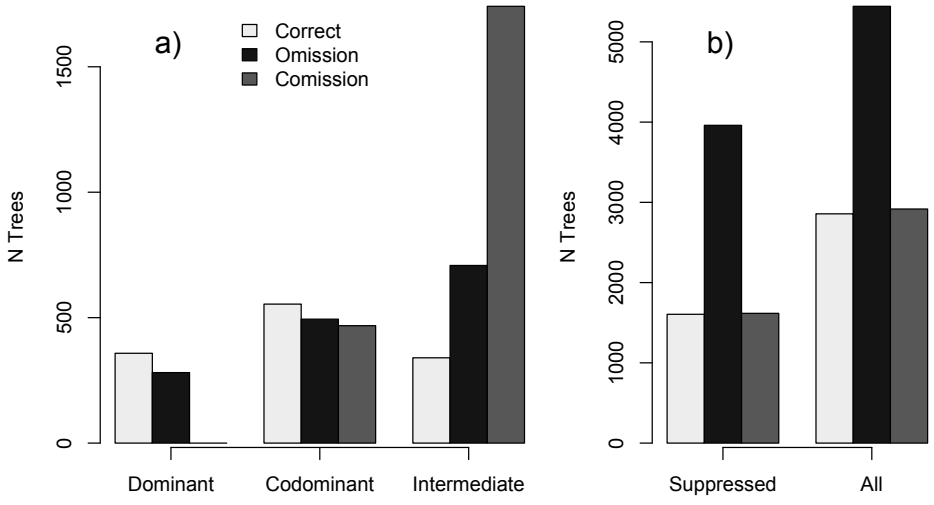

Figure 3-5. Individual tree-based accuracy assessment during leaf-off period at SERC. a) shows comparisons for dominant, co-dominant and intermediate classes and b) shows suppressed and total errors.

Plot-level Validation

The utility of the algorithm for plot-level ecological properties such as stand density and basal area is demonstrated in Figures 3-6 and 3-7. Stem density was underestimated at both the SERC and Sierra Nevada sites. On average stem density is underestimated by 20% at the SERC site (Figure 3-6a) and 32% at the Sierra Nevada site (Figure 3-6b), the majority of this estimation being from undetected small trees.

There is a stronger relationship between plot level cumulative delineation metrics and basal area at Teakettle than at SERC (Figure 3-7). R^2 values between basal area and crown area were 0.36 and 0.81 at SERC and Teakettle, respectively. R^2 values were higher for crown volume: 0.53 and 0.84, at SERC and Teakettle, respectively.

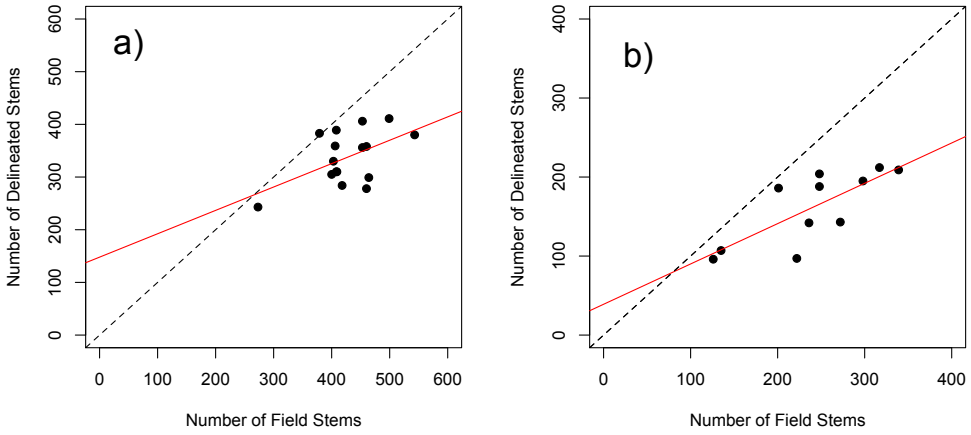

Figure 3-6. Number of stems in the field compared to number of stems estimated by the algorithm at the 90 meter plot level in a) the SERC site and b) the Sierra Nevada site. The dotted line shows the 1:1 line, illustrating an underestimation of stem density at both sites. This is attributed to the algorithm failing to detect some small stems.

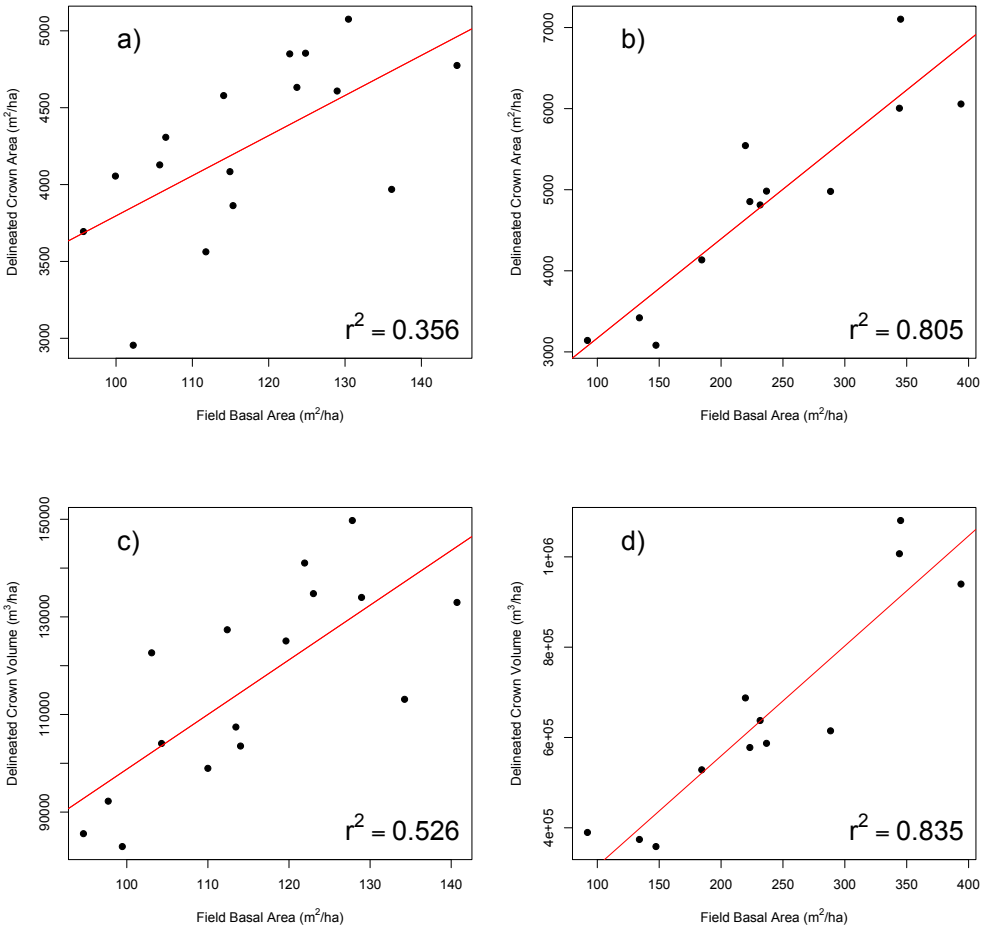

Figure 3-7. Field estimates of basal area compared to cumulative crown area at a) SERC site, b) Teakettle and cumulative crown volume (area*height) at c) SERC and d) Teakettle.

Stand-level Validation

The shape of the tree size distributions is well captured at both study sites, as seen in the histograms of crown area and DBH (Figures 3-8,3-9). To make a more direct comparison between field and delineated datasets, two species independent DBH-crown diameter models were applied. The relationship between DBH and crown diameter at SERC was diameter=(0.39*DBH)*(1-exp(-DBH*0.44)). The relationship developed between crown diameter and DBH at Teakettle was diameter=2.5+1.8*DBH^0.65 (R^2=0.72, RMSE=0.69, n=281). Each model was applied to the respective field dataset to produce field estimates of crown radius and area. Figure 3-10 shows quantile-quantile plots of delineated crown areas against field-estimated areas at a) SERC and b) Teakettle.

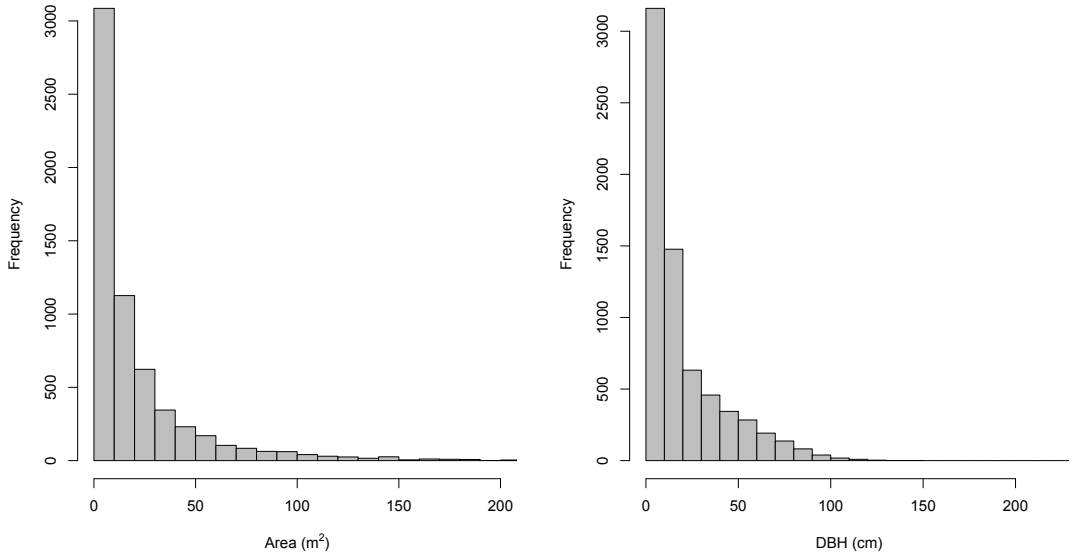

Figure 3-8. Histograms of delineated crown area (left) and DBH (right) for SERC site showing that the shape of the histograms matches closely although there is an underestimation in the smallest trees by the algorithm.

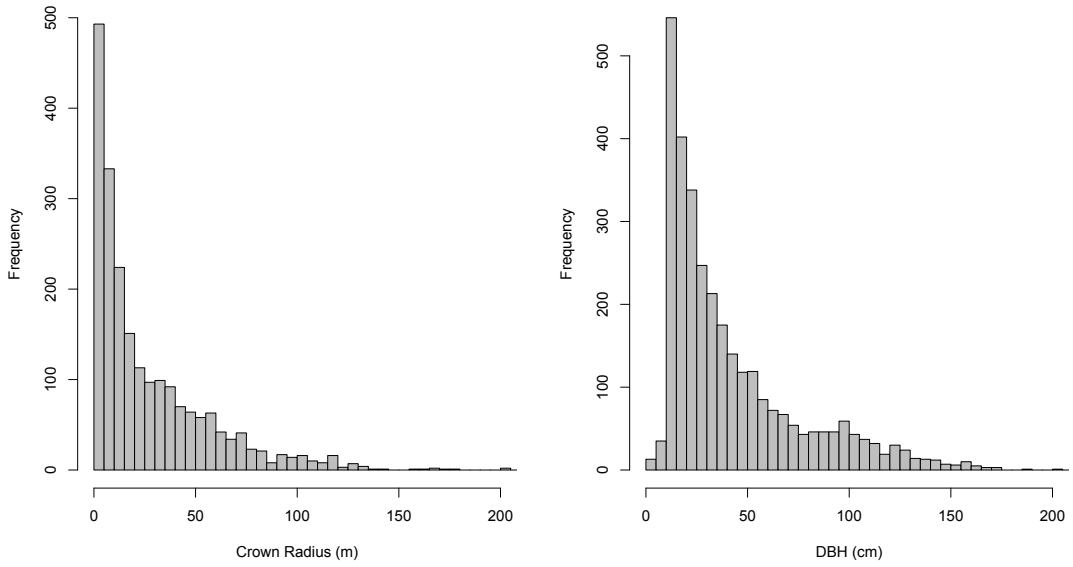

Figure 3-9. The histograms of delineated crown area (left) and DBH (right) for the Sierra Nevada site, showing that the shape matches well and DBH in cm is approximately comparable to area in m^2.

At SERC the algorithm tends to underestimate crown area while at Teakettle there is a slight overestimation. However it is noteworthy that the near linear relationships shown in Figure 3-10 indicate that stand level distributions were well captured at both sites. Only at very large (~150-200 m^2) crown sizes do the relationships between field and delineated distributions begin to falter. These results indicate that tree size distributions over large areas can be accurately estimated with the algorithm.

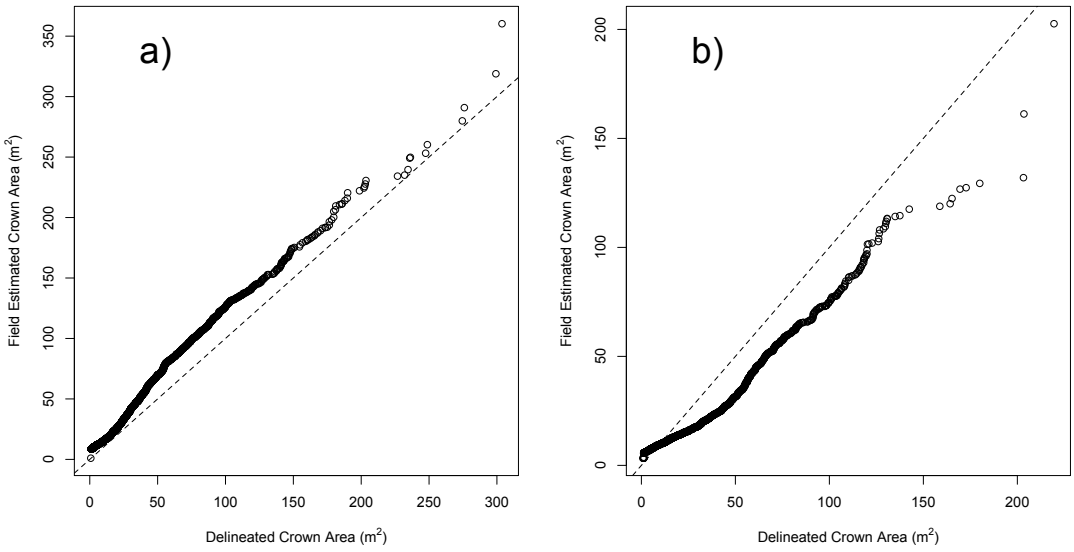

Figure 3-10. Quantile-quantile plots of delineated crown areas against field estimated crown areas at a) SERC and b) Teakettle. The linear patterns observed in these figures suggest that the algorithm produces crown area distributions with the same shape as field derived distributions, with a slight underestimate in crown are at SERC and overestimate in crown area at Teakettle.

Discussion

Individual Tree Validation

The individual tree accuracies (Figure 3-4, 3-5) compare favorably with other crown delineation results in deciduous systems that report ~50% accuracy for deciduous crowns (Koch et al., 2003). Intermediate and understory results are comparable to results from conifer-dominated systems that report less than 20% accuracy (Kaartinen et al. 2012). The algorithm therefore performs best for dominant and codominant trees, while intermediate trees are over predicted (commission) and understory trees are often undetected (omission).

Errors of commission are likely caused by the complex canopy structures found at SERC. In a closed deciduous forest, such as SERC, a single tree may be delineated into multiple crowns due to isolated branching units being falsely identified. This will be less common in conifer-dominated forests with conical crowns for which trees typically yield only one local maxima. Conversely, errors of omission at SERC are likely caused either by overlapping crowns of neighboring trees, or small understory trees from which few or no LiDAR hits are returned. In the first case, this algorithm may identify a cluster of trees as a preliminary segment (Figure 3-3b) and the point cloud refinement may fail to subsequently separate these crowns. The utility of the point cloud refinement is strongly dependent on individual crowns yielding separate signals in vertical profile. Neighboring trees of a similar height with overlapping crowns will be merged by the algorithm because they will neither be separated by watershed segmentation (due to overlapping crowns) nor point cloud refinement (due to similar heights). This is one explanation for the overestimation of intermediate crowns: multiple neighboring suppressed trees in dense understory may be detected as an intermediate-sized crown rather than several smaller crowns. In the second case, the detection of small trees under dense canopies is limited for all airborne-based LiDAR delineations, without further improvements in technology and algorithms.

Understory tree detection is slightly improved when using leaf-off LiDAR data, but at the cost of decreasing the delineation accuracy of large crowns. This improvement is likely caused by the greater penetration of LiDAR hits both to the understory and the ground in leaf-off conditions. However, the increased penetration also causes more

gaps within larger crowns, yielding more errors involving the detection of multiple crowns for a single large tree. Essentially, branching units are more likely to be detected as individual crowns when leaves are not present to fill in gaps between branches. This tradeoff should be considered when designing data collection campaigns focused on individual tree level information.

Despite difficulties detecting small crowns, 21% of all suppressed trees greater than 5 cm DBH are correctly identified at SERC. Given that SERC represents a challenging, closed-canopy forest these results suggest that this algorithm has utility across varies forest systems. If stem mapped data were available at Teakettle, accuracies at the individual level would likely be much higher, as suggested by numerous studies in conifer forests.

Plot Level Validation

Basal area is a structural attribute that has been widely studied due to both its commercial importance in forestry and high correlation to aboveground biomass for carbon mapping initiatives. The cross sectional area of a tree trunk should scale linearly with crown area, while basal area should scale with crown volume in the form of a power law with an exponent of 3/4 (Enquist, 2002). Therefore comparing crown areas and volumes to basal area is not only a reasonable approach for plot-level algorithm validation, but also allows for an assessment of how useful crown delineation might be for forestry and carbon mapping applications.

The relationship between basal area and crown area will depend largely on light environment. In an open system, tree crowns are not spatially limited and basal area increases will be reflected by corresponding increases in crown area and volume. In a closed-canopy environment, however, crown growth is often limited to light availability, and increases in biomass may be allocated disproportionally to stem vertical growth. Additionally, plot level cumulative canopy area will likely remain constant as basal area continues to increase, because crowns are limited in terms of lateral growth by their neighbors. Therefore discrepancies between plot level basal and crown area at SERC (Figure 3-7a) are not solely explained by algorithm error. The stronger relationship at Teakettle can be explained either by higher algorithm accuracy in an open conifer site, or by a tighter link between crown and basal area in an open light environment.

Crown volume accounts for both increases in tree height and crown area as trees accumulate biomass. Therefore crown volume to basal area were also compared with improved results (Figure 3-7c, 3-7d). There is a stronger relationship at both sites between basal area and crown volume than with crown area. Again, the Sierra Nevada site shows a stronger relationship with crown volume than the SERC site, indicating that this algorithm performs better in the open conifer site. However, 53% of the basal area can be explained solely with delineated crown volume at the SERC site, suggesting that this approach may be useful for forestry and carbon applications even in closed canopy deciduous forests that present some of the most problematic conditions for crown delineation. In contrast, Lefsky et al. (1999) explained 69% of

variability in basal area in a lower biomass area of SERC using stepwise regression of LiDAR-derived height and density metrics while 53% were explained with a single metric. This result, along with the strong relationship shown in Figure 3-7d, suggests that this approach may be useful for biomass estimation and should be further explored for detailed carbon mapping initiatives.

Stand Level Validation

The algorithm reproduced the shape of the distribution of crown sizes observed in the field datasets at both sites. However, there was an apparent underestimation in crown area at SERC and overestimation at Teakettle. This was caused either by algorithm error, or error in the DBH-crown area equations developed from limited field data acquisitions at both sites. At Teakettle, for example, the DBH-crown area relationship was derived using 281 individual crowns, which did not capture the entire distribution of crown sizes across the stand. Additionally, the relationship was tighter for smaller crowns with great variability at larger stem sizes. Therefore the apparent overestimation in crown area from the algorithm may have been caused by an underestimation from the field dataset.

However, it is logical that there would be an underestimation in crown area at SERC. Closed canopy crowns often extend into neighboring crowns, potentially causing truncations in crown segmentation. This issue would not occur in open conditions such as found at Teakettle, explaining the discrepancy between the two systems.

Regardless of slight over or underestimations of crown areas, the linear relationships observed in the quantile-quantile plots demonstrate that stand level tree size distributions can be accurately produced from the crown delineation algorithm for both ecosystems.

This algorithm was developed with collaboration with NASA Ames and the NASA Earth Exchange (NEX). NEX is a program that allows scientists to take advantage of the large datasets and computing facilities available at NASA through remotely accessing their system. Although the goal of this paper was on algorithm development and validation rather than operationalization, large datasets could be processed using this algorithm, providing data to ecologists or forest managers interested in expanding the spatial scope of field data collections, adding crown-specific information that can be difficult to assess from the ground, or allowing consistent analysis of forest change through repeat pass LiDAR.

Conclusions

Airborne LiDAR remote sensing systems are increasingly being used to map large forested areas at high point density. The point clouds from these data result from the interaction of laser energy with trees, that are well-defined, discrete objects. It is therefore not surprising that so much effort has gone into the inverse problem of organizing these clouds back into trees. For a variety of applications, from habitat structure, to fire modeling, to biomass estimation, there are sound ecological reasons for doing so. However, the problem is a difficult one, and finding an algorithm with

general efficacy across ecosystem structures has been challenging. The algorithm presented here is one further step in this direction.

Closed canopy broadleaf forests, such as SERC, and needle-leaf conifer forests, such as Teakettle, span a wide range of species functional types that result in markedly different spatial and vertical canopy structures, and as a result provided a reasonable test of accuracy and applicability. Considering there was no change in parameterization between the two sites, the algorithm shows promise for wide applicability, with the potential to accurately extract crown information across systems. As computing capabilities and data storage facilities continue to improve, and high-resolution LiDAR datasets are increasingly available, trade-offs between spatial detail and area of coverage may no longer be necessary. The algorithm, in tandem with high end computing, could be used to extract individual tree information at regional or even national levels given data availability. This algorithm therefore represents a shift toward detailed mapping over large areas, with the potential to provide unprecedented volumes of highly detailed structural information of great value for forest management, carbon and habitat mapping.

Chapter 4: The Importance of Spatial Detail: Assessing the Utility of Individual Crown Information and Scaling Approaches for LiDAR-Based Biomass Density Estimation

Abstract

LiDAR remote sensing has emerged as one of the best technologies for mapping aboveground biomass in forest systems. Recent developments in LiDAR instruments, computer processing power, and algorithm development have enabled the mapping of individual tree structure from LiDAR remote sensing, yet the utility of individual tree metrics has not been fully explored for aboveground biomass mapping. Conversely, scaling-based approaches using minimal data inputs have been presented as an alternative method for mapping regional biomass. These two emerging avenues of LiDAR-based biomass mapping are compared to traditional, plot-aggregated biomass modeling techniques. Three forested ecosystems were assessed: a mature, closed-canopy deciduous broadleaf forest; a mature evergreen needleleaf forest; and a Loblolly pine plantation with a range of even-aged stands. For individual tree based approaches, individual tree metrics improve explanatory power from R^2=0.77 to R^2=0.84 and R^2=0.82 to R^2=0.97 in the deciduous and open conifer sites, respectively. With large field sample sites in areas of open canopy cover, individual tree metrics can significantly improve aboveground biomass (AGB) estimation as they directly take into account stand density. Regarding scaling-based approaches, proposed methods are currently unsuitable in forests without a tight relationship

between canopy top height and basal area, as seen in two of the study areas. Individual tree information shows more promise for improving AGB modeling capabilities, and may also facilitate scaling-based approaches, but further research regarding the application of allometric equations and the spatial scale of models is also necessary to continue advancing the field of forest biomass accounting.

Introduction

Earth's forests represent one of the largest carbon sinks on the planet, yet the magnitude and location of the sink is largely unknown, and likely shifts with changing land use (Pan et al., 2011). Monitoring carbon stocks is therefore critical for modeling climate change, and providing important information to mitigation strategies such as Reduced Emissions from Deforestation and Degradation (REDD+, Corbera and Schroeder, 2011). However, there remain considerable uncertainties in current AGB maps (Houghton et al., 2001, Baccini et al., 2012). There is an increasingly large and variable suite of AGB estimation methods involving a wide range of remote sensing technologies, statistical techniques, and spatial scopes. Large area AGB maps have been generated using a combination of spaceborne LiDAR, radar and passive optical data (Baccini et al., 2008, Boudreau et al., 2008, Goetz et al., 2009, Saatchi et al., 2011); however, there are discrepancies between these products and they require reliable local maps for validation. Airborne LiDAR has emerged as the premier technology for producing accurate local to regional AGB maps (Wulder et al., 2012, Lefsky et al., 2005, Pflugmacher et al., 2008, Ni-Meister et al., 2010). Airborne LiDAR can serve to provide either detailed contiguous maps

for local carbon accounting (Goetz and Dubayah, 2011; Swatantran et al., 2011) or be used in a sampling scheme for wider area mapping (Asner, 2009, 2011).

LiDAR-based AGB maps are traditionally generated through statistical modeling of field estimated AGB using LiDAR metrics derived from either discrete return or full waveform systems (Wulder et al., 2008, Næsset, 2004, Lim et al., 2003, Dubayah and Drake, 2000, Næsset et al. 1997). Both discrete return and waveform datasets are typically processed in similar fashions: plot-level height and density metrics are derived from point clouds or waveforms and regressed against plot-scale field AGB estimates (Drake et al., 2002). Other studies have adopted variations to height and density metrics by using voxel-based LiDAR density metrics (Lefsky et al., 1999a, Lefsky et al., 1999b, Coops et al., 2007), using landscape segments as modeling areas (van Aardt et al., 2006), or using individual tree based metrics (Suárez, 2013, Bortolot and Wynne, 2005, Popescu et al., 2003, Popescu & Zhao, 2008, Zhao et al., 2012). Few studies, however, have directly compared different estimation techniques or developed models for multiple forest types.

Individual tree-based AGB approaches theoretically overcome many of the scale-related issues seen in wide area AGB mapping. This is because individual tree approaches are theoretically scale invariant (Zhao et al., 2009) as plot or regional AGB is a simple sum of the individual tree biomass found within the plot or region. Individual tree-based biomass mapping has been conducted in a few studies using Canopy Height Model (CHM)-based delineated crowns (Bortolot and Wynne, 2005,

Popescu et al., 2003). These studies showed that individual tree-based AGB maps in pine plantations yield comparable results to other LiDAR-based AGB modeling techniques. However, few comparisons have been made between individual tree-based LiDAR metrics and point cloud or waveform-based AGB metrics. Ferster et al. (2009), conducted a comparison between delineated metrics from the software TreeVaw (Popescu et al., 2002) and LiDAR percentile height and density metrics in complex coastal conifer forests on the east coast of Vancouver Island. They found that individual tree metrics from TreeVaw were less useful than traditional metrics. However, TreeVaw detects crowns based on a CHM, and in high biomass complex forests fails to detect most mid and understory crowns (Ferster et al., 2009). Further, only TreeVaw height and density metrics were used in this study, ignoring the potential predictive power of crown diameter, area or volume. Finally, Zhao et al. (2012), found that individual tree-based metrics were more useful than plot-aggregate metrics for AGB model development in the Sierra Nevada, California. Considering the increasing availability of high resolution LiDAR data and improvement of crown delineation algorithms (Breidenbach et al., 2010, Kaartinen et al., 2012, Vastaranta, 2011, Duncanson et al., 2014, Reitberger et al., 2009), individual tree-based AGB models should be more thoroughly explored as they present a theoretically more robust and transferable, scale-invariant approach to AGB mapping (Zhao et al., 2009).

Other approaches to AGB modeling are emerging at the opposite end of the spatial detail spectrum. Recently, Asner and Mascaro (2014) developed a single equation for

plot-level AGB estimation based on allometric scaling and regionally calibrated coefficients. This method provides an alternative to traditional empirically driven biomass mapping by fusing empiricism and scaling theory. Based on the dependency of biomass on tree height, basal area, and wood density, Asner and Mascaro use LiDAR canopy top height, a regional equation to relate basal area to LiDAR canopy height, and a regional wood specific density (Asner and Mascaro, 2014) to estimate AGB. This approach facilitates computationally consistent and simple wide area mapping, and could be of great use to the biomass mapping community. However, this technique remains untested across a range of ecosystem types. Specifically, the assumption that basal area can be accurately modeled as a function of canopy top height requires verification in temperate forests.

As demonstrated by these two emerging approaches (individual tree-based biomass modeling and scaling-based approaches), there remains a tension in the LiDAR community between detailed localized techniques and wider area mapping of AGB. Collecting higher point density, contiguous data is costly, and storing and processing this data can be problematic. Conversely, collecting lower point density LiDAR over larger areas (often as transects) facilitates large area mapping but at the potential risk of losing accuracy. This study has three goals: (1) test individual tree-based methods for aboveground biomass density estimation, (2) explore the applicability of scaling-based approaches and (3) explain the utility of the two approaches as a function of forest structure and allometry in three structurally distinct forest ecosystems.

Methods

Study Areas and Field Data

In this paper AGB density is modeled from individual tree metrics and a scaling equation, and compare these models to traditional LiDAR-based models, in three structurally and ecologically different forests in the United States. The first study site is a high biomass conifer dominated forest in the Sierra Nevada, California. The second is a closed canopy broadleaf dominated forest on the east coast of Maryland. The third is an area in North Carolina comprised of both mature, high biomass broadleaf stands and heavily managed conifer plantations. Field and LiDAR data information for the three study areas is provided in Table 4-1.

Table 4-1. Description of traditional and delineated LiDAR metrics

	Teakettle, California	**Parker Tract, North Carolina**	**SERC, Maryland**
Field Date	2008	2011	2008-2011
Number of Plots	12	33	16
Plot Size	90 m square	Variable Radius	90 m square
Forest Type	High biomass conifer	Mature broadleaf stands and conifer plantations	Closed-canopy broadleaf/mixed
LiDAR Date	2008	2011	2012
LiDAR instrument	Optech Gemini ALS	G-LiHT	G-LiHT
LiDAR pt density	18 returns/ m^2	~40 returns/ m^2	~50 returns/ m^2

The Teakettle study site is located in the Western Sierra Nevada Mountain range in California. Dominant species include *Abies Concolor (*white fir), *Pinus Ponderos* (ponderosa pine), *Abies Magnifica* (red fir) and *Quercus Kelloggii* (California black oak) (Honaker et al., 2002). The elevation range of the site is approximately 1000 m to 2500 m above sea level, with AGB values averaging 200 Mg ha^{-1} with individual

tree values up to 20 Mg tree^{-1}. The forest is mature, with rocky outcrops intermixed between clusters of trees. AGB density values have been observed as high as 1000 Mg ha^{-1} in Giant Sequoia stands (Swatantran et al., 2011).

At Teakettle, 90 m (~1 ha) square sample plots were established during summer of 2008 (n=12). The DBH, species and condition (live, dead, broken) of all trees were recorded. Dead trees were removed from the analysis. Generalized allometric equations were applied to estimate total aboveground dry biomass as a function of Diameter at Breast Height (DBH) (Jenkins et al., 2003).

The Smithsonian Environmental Research Center (SERC) study site is located near Edgewater, Maryland, adjacent to a sub-estuary of the Chesapeake Bay. The area is generally comprised of two forest types: mature secondary upland forest, and lowland forests. Dominant species in the upland forest include *Liriodendron Tulipifera* (tulip poplar), *Fagus* (beech), several species of oak, and hickory, with mid canopy *Acer Rubrum* (red maple) and *Nyssa Sylvatica* (black tupelo) and understory *Carpinus Caroliniana* (American hornbeam), *Lindera Benzoin* (spicebush) and *Asimina Triloba* (paw-paw). Dominant species in the lowland areas are *Fraxinus* (ash), *Platanus Occidentalis* (sycamore), and *Ulmus Americana* (American elm). Both the upland and the floodplain forests have been relatively undisturbed for approximately 120 years.

In the SERC study area, a 16.0 ha plot was laid out and every tree greater than 1 cm DBH was measured and stem mapped between 2008-2011. This forms part of the

Smithsonian Institution Global Earth Observatories (SIGEO, 2013). Tree location, species, DBH, crown class (dominant, codominant, intermediate or suppressed) and crown condition were recorded. Dead and damaged trees were eliminated from the dataset prior to comparison with delineation results due to a lack of description of the type of damage. The 16 ha plot is split into 16, 90 m subplots in order to compare results to Teakettle. It is assumed that minimal change occurred between the field acquisition and the LiDAR acquisition date the following summer.

Aboveground biomass was calculated with the SERC field dataset using a combination of the so-called "Jenkins equations" (Jenkins et al., 2003) and region appropriate species-specific allometric equations. Species-specific equations were applied for Red Maple (Fatemi et al., 2011), Northern Red oak (Pastor et al., 1984), Dogwood and Black Gum (Phillips 1981), Hickory species, Chestnut Oak and White Oak (Martin et al., 1998), Beech (Siccama et al., 1994), White Ash (Monteith et al., 1979), Green Ash and Sweetgum (Clark et al., 1985), American Elm and Sycamore (Clark et al., 1986), Loblolly pine (Naidu et al., 1998), Cherry species and Sassafras (Williams and McClenanhan, 1984), Black Locust (Clark and Schroader, 1986), and Tulip Poplar (local SERC study). Two sets of AGB estimates were calculated, the first comprised of the combined generalized and regional allometries, and the second using only the Jenkins generalized allometries. This allowed an examination of the sensitivity of AGB estimation to allometry at ~1 ha.

The Parker Tract study site is located near Plymouth in North Carolina, USA. It is largely a commercially managed Loblolly Pine plantation (*Pinus taeda)* although some stands have a mixed composition, containing native broadleaf species. One segment of the site is retained as natural forest. Being at an elevation of approximately 8 m a.s.l., the site suffers from poor drainage and a network of drainage channels assist this within the clearly defined stands.

Field data were collected at Parker Tract by the Weyerhauser Company during July 2011. Species and DBH were recorded for all trees above 2.54 cm DBH in 33 plots of 7.3m radius within the range of stand ages. General biomass equations (Jenkins *et al.*, 2003) were then used to calculate biomass using DBH for each plot.

AGB density was calculated for each plot by summing individual tree biomass per plot, and dividing by the plot area. Basal area was calculated by translating DBH to cross sectional area for each tree, summing these tree basal areas and dividing by the plot area.

LiDAR Data

LiDAR data at Teakettle were flown in the summer of 2008 with the University of Florida's OPTECH GEMINI ALTM unit, operating at 100-125 kHz with a maximum 25° scanning angle. Data were flown ~600-750 m above ground, with 50%-75% swath overlap yielding an average return density of approximately 18 returns/m^2.

LiDAR data for SERC and Parker Tract were collected with NASA Goddard's LiDAR, Hyperspectral and Thermal Imager (G-LiHT; Cook et al., 2013) instrument. G-LiHT uses a 300 kHz multi-stop scanning LiDAR operating at 1550 nm with a 60° field of view and 10 cm diameter footprint. The site was flown from an altitude of 335 m AGL with 50% overlap in north-south and east-west directions to achieve a mean return density of up to 50 returns m^{-2}. Leaf-off and leaf-on data at SERC were acquired during March 2012 and June 2012, respectively. G-LiHT data were collected for Parker Tract in August 2011.

Plot Aggregate LiDAR metrics

The plot-aggregated LiDAR metrics are Relative Height (RH) and Density Decile (DD) metrics (Table 4-2). Relative height metrics were calculated as the heights above ground below which a certain percentage of LiDAR points are returned. Conversely, relative density decile metrics were calculated as the number of returns in a height bin as a given percentage of maximum canopy height, divided by the total number of LiDAR returns (Figure 4-1). Mean elevation and maximum relief were also included based on a DEM generated from the LiDAR data.

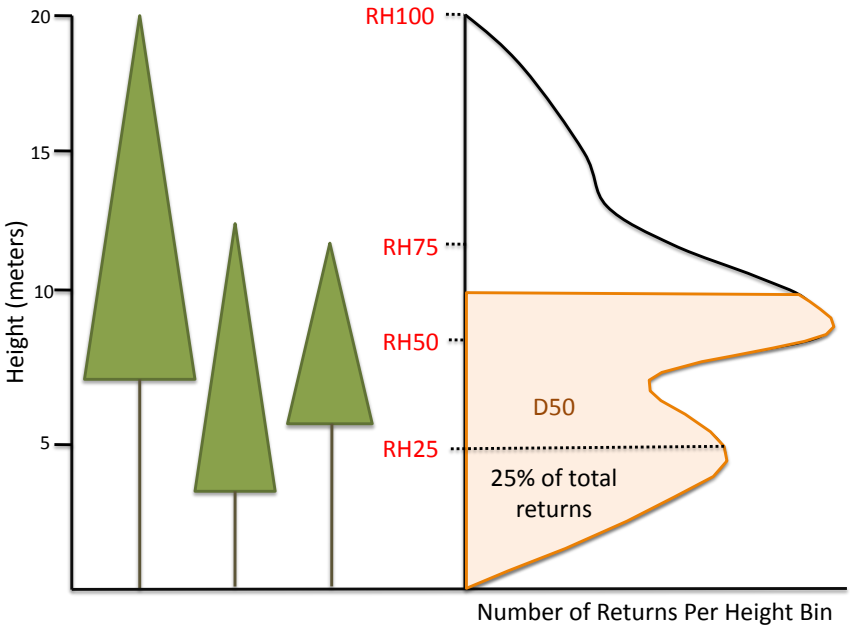

Fig 4-1. Traditional metrics used in this research were Relative Height (RH) metrics and density decile (D) metrics. These metrics are calculated at the plot level, so all LiDAR hits are aggregated and for ease of visualization represented as a waveform here.

For each study area, the LiDAR point cloud was extracted to match the area of field plots. At Teakettle, LiDAR data were extracted to match the 12, 90 m square plots. At SERC, data were extracted for each of 16, 90 m square plots subset from the 16.0 ha area of coverage. Finally, at Parker Tract, LiDAR points were extracted to match 7.3 m diameter circles centered on the field plot centroid.

Individual Tree-Based LiDAR Metrics

Individual tree metrics were derived from the LiDAR point cloud through a multilayered canopy delineation algorithm (Duncanson et al., 2014). The algorithm performs a preliminary delineation on a smoothed Canopy Height Model (CHM) using a watershed delineation (0.25 m^2 pixels). Preliminary segments are then refined using the LiDAR point cloud to search for understory returns within each preliminary segment. Through this process the entire LiDAR point cloud is separated into overstory and understory returns. Each of these datasets is used to produce a new CHM. Both the understory and overstory CHM are then segmented, yielding a multi-layered crown delineation product. This process is iterated until no further understory trees are detected. The outputs of this algorithm are individual crown locations, heights, radii, crown areas, and volumes. Crown area is the 2D area calculated by summing the pixels in each delineated crown. Crown volume is calculated by multiplying the crown area and height. Note that this is a simplification, and ignores crown shape, providing a near conical proxy of crown volume.

The canopy delineation algorithm was validated at both the SERC and Teakettle in a previous study (Duncanson et al., 2014). Parker Tract data were not available at the time this study was conducted. At SERC, validation was performed at an individual crown level using 16.0 ha of stem mapped tree data > 5cm DBH from the SIGEO program for both leaf-off and leaf-on LiDAR data acquisition. At both SERC and Teakettle, validations were also performed at the plot and stand level, comparing basal area, stem density and tree size distribution from field datasets to algorithm

output. At SERC, 70%, 58%, 35%, and 21% of dominant, codominant, intermediate, and suppressed trees, respectively, were correctly identified by the algorithm. Cumulative crown volume from the algorithm explained 53% and 84% of the variability in field observed basal area at SERC and Teakettle, respectively. There was no difference in algorithm parameterization between the two sites, suggesting that this algorithm holds promise for wide scale applicability across many different forested ecosystems. This does not mean, however, that it will perform comparably in all systems, as some systems are more structurally amenable to crown delineation. Indeed, the algorithm performed better in open conifer systems than closed-canopy deciduous systems, and this will likely impact the utility of individual tree metrics for AGB estimation. Errors of commission and omission were comparable, and therefore at a 1 ha plot scale these errors will balance and should not greatly impact AGB modeling results. Errors would have a greater impact, however, on the smaller plots at Parker Tract. For further details on algorithm development and validation refer to Duncanson et al. (2014).

Individual Tree-based and Plot Aggregate AGB Modeling

AGB models were produced by fitting both traditional and delineated sets of metrics to field observed AGB (Table 4-2). Topographic metrics of mean elevation and relief were also used for the analysis. Several of the 20 relative height metrics and 20 density decile metrics were highly correlated. In order to maximize predictive capability of the models without producing errors from multicollinearity, Partial Least Squares (PLS) regression was employed. PLS regression recombines input metrics using principal components, producing new, non-correlated metrics that are linear

combinations of the original metrics. These new metrics are then used in multiple linear regressions to develop models of field-observed AGB. PLS regression can over fit data if too many components (new metrics) are used for prediction (Abdi, 2010). To minimize the likelihood of over fitting the model, Leave-One-Out cross-validation (LOOCV) was performed, and a predicted Root Mean Squared Error (RMSE) was calculated from using one to ten components for modeling fitting. The number of components that minimizes the LOOCV RMSE was selected for each model. LOOCV is a method used to estimate the error of a model if test data independent from the model training data are not available. Here, it was used not only to select the most useful number of components in PLS, but also as a statistic for comparing traditional and delineated models, and model robustness between sites.

Table 4-2. Description of traditional and delineated LiDAR metrics

	Metric	Description
Traditional	RH05, RH10, RH15, …. RH100	Relative height metrics calculated as the height below which some percentage of LiDAR returns fall
	D05, D10, D15…. D100	Density decile metrics are the number of returns that fall within a given percentile height bin
Delineated	Cumulative Volume (Cvol)	The sum of the product of individual tree area and individual tree height
	Cumulative Area (Carea)	The sum of all individual crown areas in a plot
	Max Height (T_max_ht)	The maximum LiDAR height observed in the plot
	Max Area	The maximum crown area observed in a plot
	Max Radius	The maximum crown radius observed in a plot
	Max Volume	The maximum individual crown volume (area multiplied by radius)
	Pseudo Lorey's Height	The average crown height divided by crown area
	Number of Trees	The number of delineated crowns in a plot
Topography	Elevation	The average DEM elevation
	Relief	The maximum minus minimum DEM elevation in a plot

To determine whether differences between the traditional and delineated LiDAR metrics models are statistically significant, PLS was used to predict plot level AGB, and these predictions were fit to field estimated AGB using a normal linear regression. This model fitting was bootstrapped using 100 iterations to calculate the 90% confidence interval for the R^2 values using the R package 'boot'.

Scaling Approaches

To evaluate the potential efficacy of the AGB modeling approach presented by Asner and Mascaro (2014), their method was followed to estimate AGB as a function of canopy top height, basal area, and a regional wood specific density:

$$AGB=a+bTCH^c + dBA^e + fp_{BA}^g \quad (1)$$

Where BA is basal area estimated from TCH, and p_{BA} is basal area weighted wood specific gravity, and TCH is the mean height of pixels in a 1 m Canopy Height Model. BA was estimated from RH100 using OLS regression, and estimated average wood specific gravity per plot from field datasets. Exponents were fit in equation 1 using multiple linear regression of log transformed data, as follows:

$$ln(AGB)=b(lnTCH) + d(lnBA) + f(lnp_{BA}) \quad (2)$$

AGB estimates were back transformed and multiplied by MSE/2, following Asner and Mascaro (2014). Finally, scalars were fit for each variable with a second multiple linear regression. One such scaling model was produced for each of the three study sites.

This scaling approach makes the assumptions that (a) basal area scales predictably with canopy top height and (b) regional wood specific density is sufficient for model calibration. To test the first assumption, models of basal area were examined as a function of TCH. Additionally, basal area was modeled as a function of a single individual tree-based metric, cumulative volume, in an attempt to address whether individual tree information may help facilitate the application of LiDAR-based wide area scaling approaches. For wood specific gravity, two of the study sites had wood density values that did not vary across the site (in the case of a single wood density for all trees at Teakettle, and the same species distribution in contiguous plots at SERC). At Parker Tract, however, wood specific gravity varied between pine plantation plots and mature deciduous plots. Consequently the median tree-based wood specific gravity per plot was assigned for testing scaling approaches at Parker Tract. These scaling-based biomass models will be optimistic, as wood specific gravity directly is directly extracted from the field datasets.

Results

This section summarizes individual tree-based and the scaling-based models at each site, and compares them to traditional LiDAR models. Table 4-3 lists the metrics used in the AGB models along with the associated model accuracies.

Table 4-3. Model performance summaries for AGB models. The metrics used in each PLS model are listed, in order of importance for the tree metrics. All traditional models used all 20 of the relative height metrics. The number of PLS components, the corresponding leave one out cross validation coefficient, and the 90% confidence intervals for r^2 are provided. PLS components and LOOCV are not reported for scaling models, which were generated using multiple linear regression.

Model	Metrics	r^2	Std. Error (Mg/ha)	n PLS Comps	r^2 90% CI	LOO CV
Teakettle: Traditional	RH05:RH100	0.824	59.2	3	0.54-0.92	100.45
Teakettle: Delineation	Cumulative volume, maximum volume, cumulative area, elevation, releaf, maximum area, cumulative radiusm, number of trees	0.975	22.1	5	0.94-0.99	55.2
Teakettle: Scaling-Based	TCH	0.08	174.4	NA	0.003-0.43	NA
Parker Tract: Traditional	RH05:RH100, DD65:DD85	0.873	32.1	5	0.8-0.93	43.68
Parker Tract: Delineation	Cumulative volume, maximum volume	0.802	40.1	5	0.6-0.86	51.09
Parker Tract: Scaling-Based	TCH	0.63	55.82	NA	0.39-0.75	NA
SERC: Traditional	RH05:RH100	0.773	14.5	4	0.48-0.89	33.98
SERC: Delineation	Cumulative volume, maximum volume, cumulative area	0.838	12.2	4	0.67-0.93	16.39
SERC: Scaling-Based	TCH	0.31	20.4	NA	0.14-0.62	NA

Individual Tree-Based Models

Teakettle

At the California site, there was a greater difference between the individual tree-based and plot-aggregate models (r^2=0.975, 0.824, respectively, Figure 4-2), and this difference was statistically significant despite the small sample size (Table 4-3). All 20 of the relative height metrics were recombined into three principal components for modeling. The associated LOOCV RMSE was the highest out of any of the models, indicating that the plot-aggregate model at Teakettle was sensitive to individual observations. Therefore the plot aggregate metrics may be over fitting the model, which is unsurprising given the small sample size of only 12 plots. The individual tree metrics, conversely, showed a LOOCV RMSE reduction of almost 50% against the plot-aggregate metrics, indicating that this model was more robust. Therefore at Teakettle the individual tree-based LiDAR metrics outperformed the plot aggregate LiDAR metrics for AGB modeling.

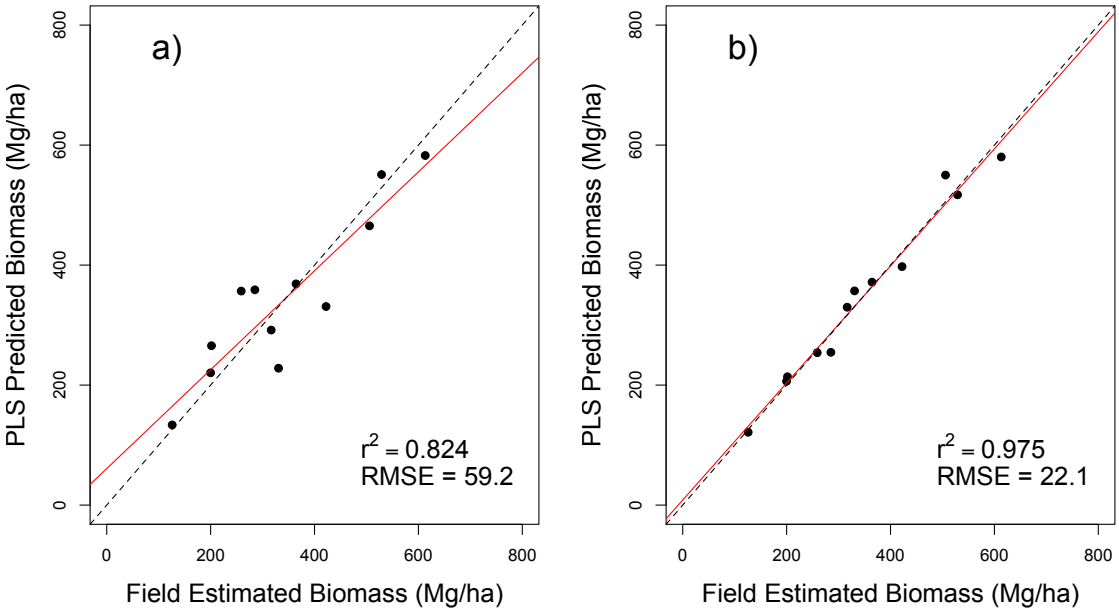

Figure 4-2. Teakettle PLS biomass models using traditional metrics (a) and delineation metrics (b). Delineation metrics were able to capture within plot spatial distributions of biomass, as well as the vertical distribution. This suggests that delineation metrics perform well in open canopies.

SERC

At SERC, the individual tree metrics explained a larger percentage of the variance in AGB than the plot-aggregated metrics (r^2=0.838, 0.773, respectively, Figure 4-3). However, this increase in r^2 was not statistically significant, as indicated by the 90% confidence intervals in Table 4-3. There was little variation in AGB across this site, likely due to the subsetting of a relatively spatially contiguous 16.0 ha area. As at Teakettle, all 20 of the relative height metrics were recombined into three principal components for modeling. None of the relative density decile metrics were useful at this site. While 20 metrics were used from the plot-aggregated dataset, only 3 metrics were used in the individual tree dataset: cumulative volume, maximum tree volume, and cumulative crown area. Although the improvement in model performance seen by

the individual tree metrics was not statistically significant due to the small sample size used in this study, the higher range in r^2 values and lower LOOCV RMSE show promise for delineation metrics in closed canopies.

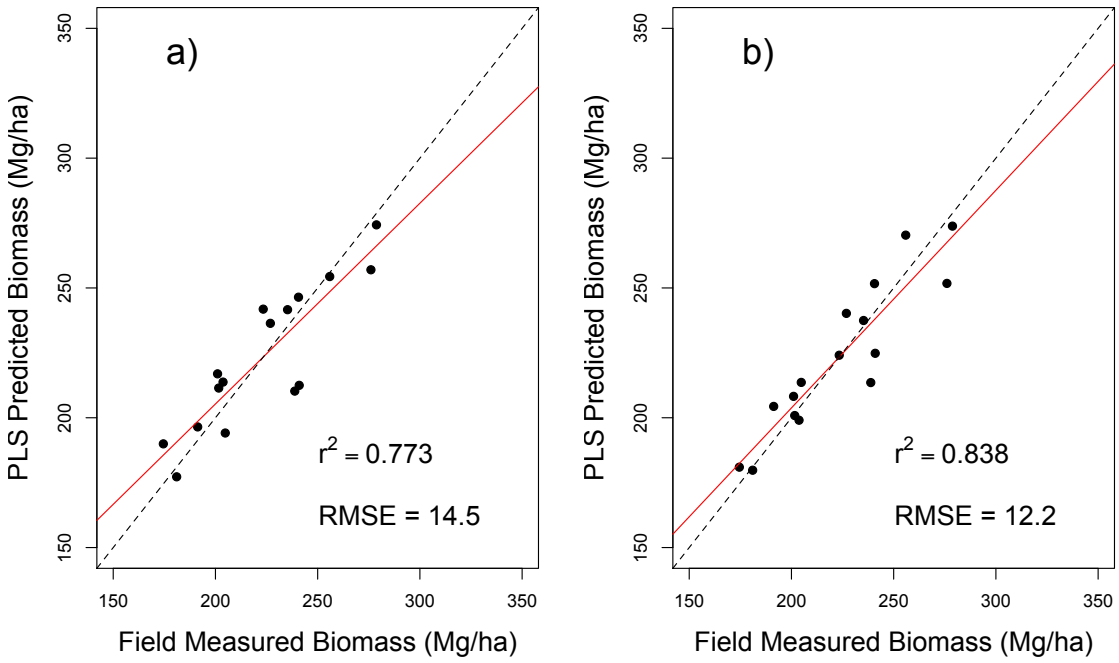

Figure 4-3. SERC PLS biomass models using traditional metrics (a) and delineation metrics (b). Traditional metrics (a) explained less variability in AGB than delineation-based metrics (b) at SERC. However, this difference is not statistically significant.

Parker Tract

At Parker Tract, the results from Teakettle are reversed. The plot-aggregate LiDAR metrics performed better than the individual tree-based LiDAR metrics (r^2=0.873, 0.802, respectively, Figure 4-4). However, as at SERC, this difference was not statistically significant based on the 90% confidence intervals (Table 4-3). As at SERC and Teakettle, all 20 RH metrics were used for the plot-aggregate AGB model at Parker Tract. Additionally, the Density Decile (DD) metrics DD65, DD70, DD75

and DD85 were used in the model. Estimating AGB with five non-autocorrelated principal components yielded an R^2 of 0.87 with an associated RMSE of 32.1 Mg/ha. Only two individual tree-based metrics were used at Parker Tract – cumulative volume and tree maximum volume. The individual tree-based model yielded an R^2 of 0.80 with an associated RMSE of 40.1. There was a 7.3% reduction in LOOCV RMSE for the plot-aggregate dataset, indicating that at Parker Tract the plot-aggregate metrics yield higher accuracies and more robust models.

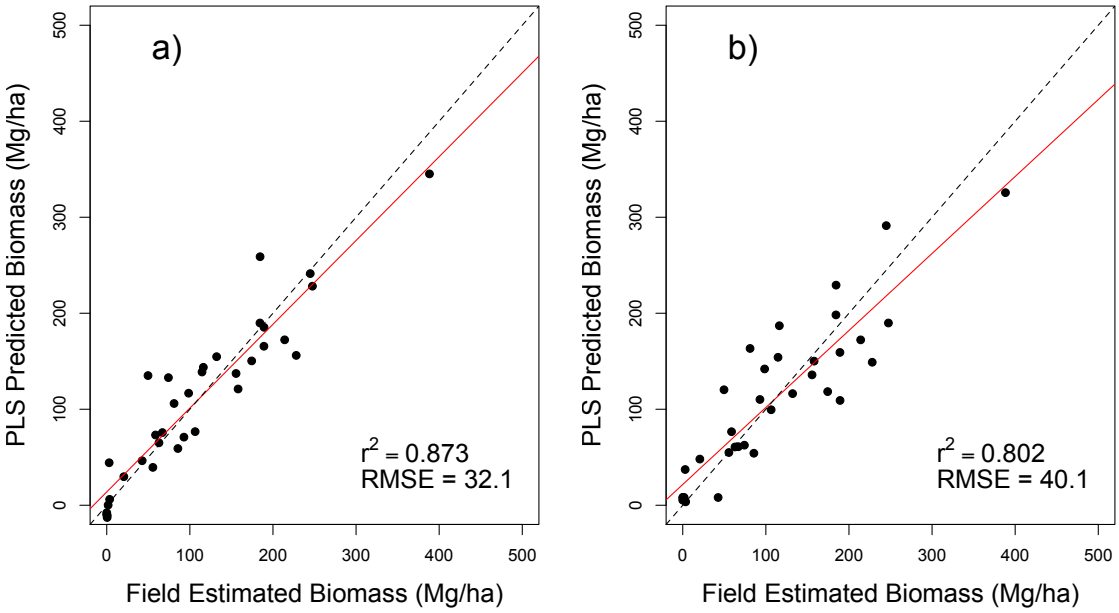

Figure 4-4. Parker Tract PLS biomass models using traditional metrics (a) and delineation metrics (b). At this site the traditional metrics performed better for biomass estimation, likely because of edge effects related to the small field data collection sites.

Scaling-based AGB Modeling

At Teakettle and SERC the scaling based approach was unsuccessful, only explaining 8% and 31%, of the variability in field AGB, respectively. At Parker Tract, however, the scaling approach seemed more successful, explaining 63% of the variability in

field AGB. These results are explained by the relationship between canopy top height and basal area at each study cite. There was no statistically significant correlation between TCH and basal area at Teakettle or SERC (Figure 4-5a, 4-5e). However, at Parker Tract, there was a good fit between TCH and basal area (Figure 4-5c). Scaling-based approaches will not be successful unless LiDAR can be used to successfully predict basal area. An individual tree-based metric was used to predict basal area instead of canopy top height, and we found a good fit between cumulative volume and basal area at Teakettle (Figure 4-5b), a reasonable fit at Parker Tract (Figure 5-5d), and a poor but statistically significant relationship at SERC (Figure 4-5f). Therefore scaling could be used to successfully predict biomass at Parker Tract, and could be used with inclusion of more detailed LiDAR at Teakettle. However scaling approaches could not be used at SERC where there is a decoupling of LiDAR derived structure and basal area.

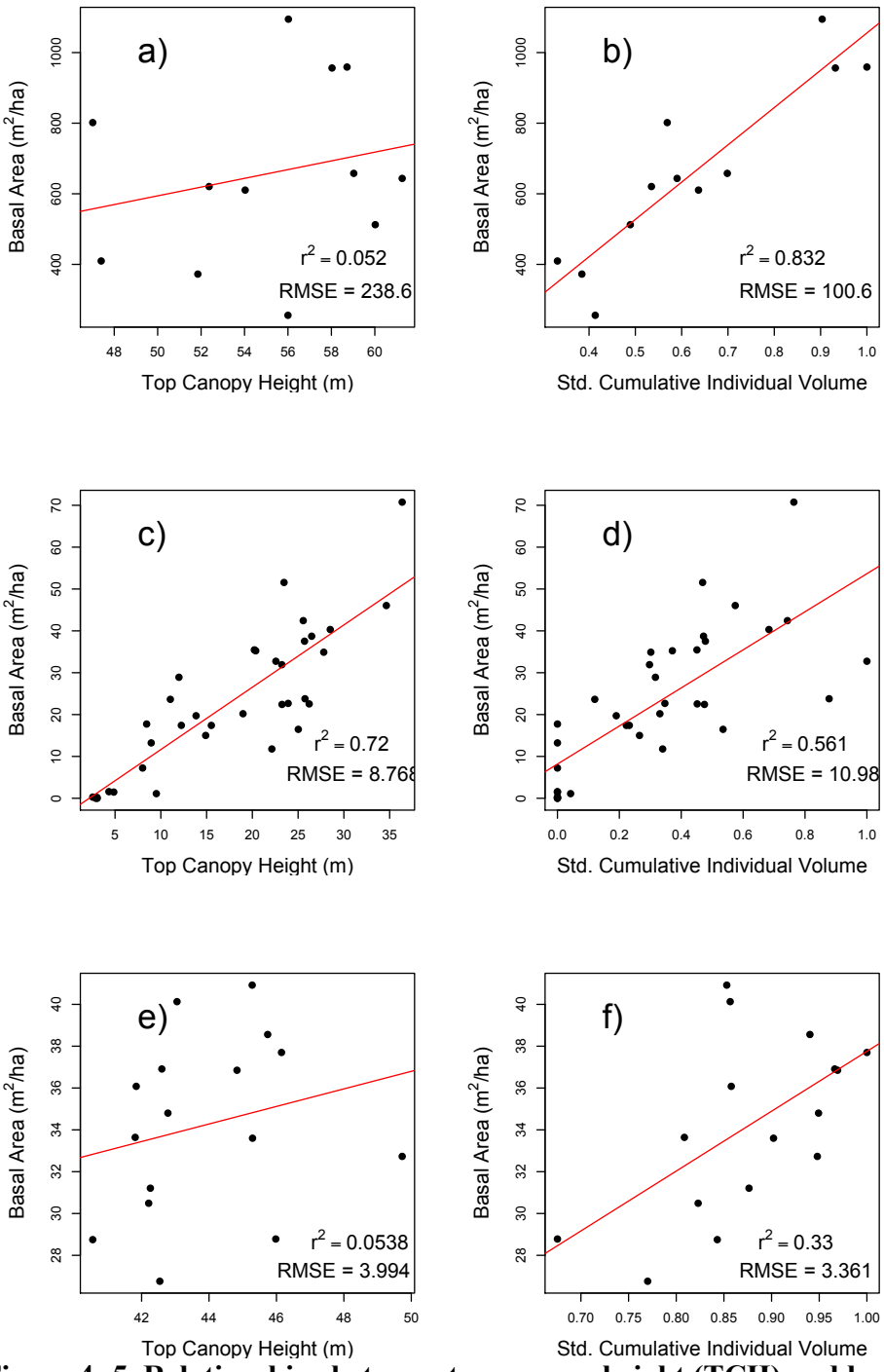

Figure 4- 5. Relationships between top canopy height (TCH) and basal area at Teakettle (a), Parker Tract (c) and SERC (e) compared to individual tree volume and basal area at Teakettle (b), Parker Tract (d) and SERC (f) show that individual tree information is more useful for basal area modeling than maximum canopy height alone.

The Impact of Allometry

In order to help understand observed differences between individual tree-based and plot-aggregate LiDAR methods for AGB estimation, and applicability of scaling-based approaches, it is necessary to consider drivers of model error. Of the three study areas both the AGB and basal area modeling attempts were least successful at SERC. The relationship between field measured basal area and field estimated AGB, at SERC, was weaker than at both Teakettle and Parker Tract (Figure 4-6). At SERC, AGB was estimated using regional equations (Figure 4-7b), which had a larger range of exponents than the Jenkins equations because they are often species-specific (Figure 4-7c). This is demonstrated by a comparison between the allometric equations used at Teakettle, where the field sites only included softwood trees and all but two trees used a single generalized allometric equation (Figure 4-7a). A comparison between regional-based allometries, Jenkins generalized allometries, and basal area (Figure 4-7c,d) further suggests that allometry may explain the disconnect between basal area and AGB at SERC. The generalized allometries, overall, estimated lower AGB quantities, reducing the estimated AGB from 275.8 Mg/ha to 215.2 Mg/ha (~20% reduction).

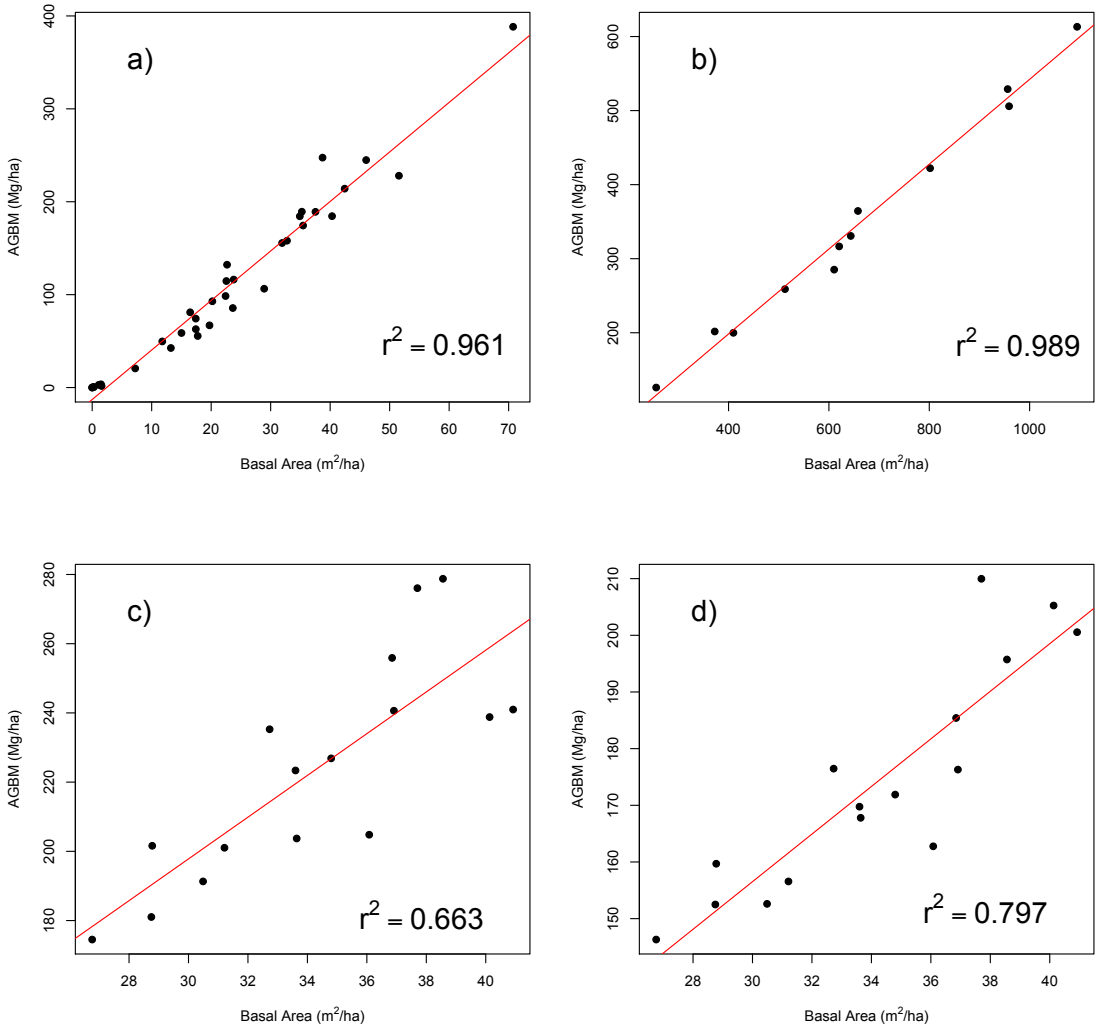

Figure 4-6. The relationship between field-estimated biomass and basal area is nearly 1:1 at Parker Tract (a) and Teakettle (b), while there is discrepancy at SERC (c, d). The relationship is weaker using regional equations (c) than Jenkins generalized equations (d) suggesting that using a wider range of allometric equations yields a larger discrepancy between field estimates of AGB and basal area at a 1 ha level.

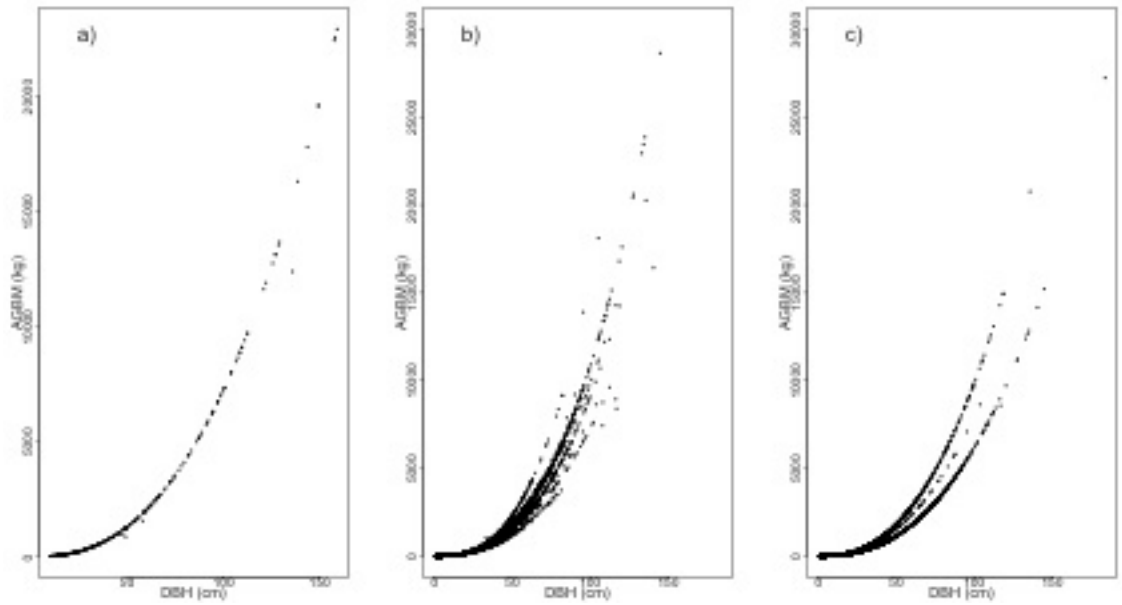

Figure 4-7. At Teakettle, a single allometric equation was used to predict individual tree biomass in the field for the majority of trees (a). At SERC, regional allometries (b) and generalized allometries from Jenkins et al. (2003) (c) were both used to estimate biomass in the field. For a given DBH there is a larger range of possible AGB values in the mixed forests at SERC, and this range is dependent on the set of allometric equations selected.

Aboveground biomass density models at SERC were also run using the Jenkins generalized allometric equations. Models fitting the generalized AGB estimates to the two sets of LiDAR metrics explained less variability (Figure 4-8) than the models of AGB density estimated from regional allometries.

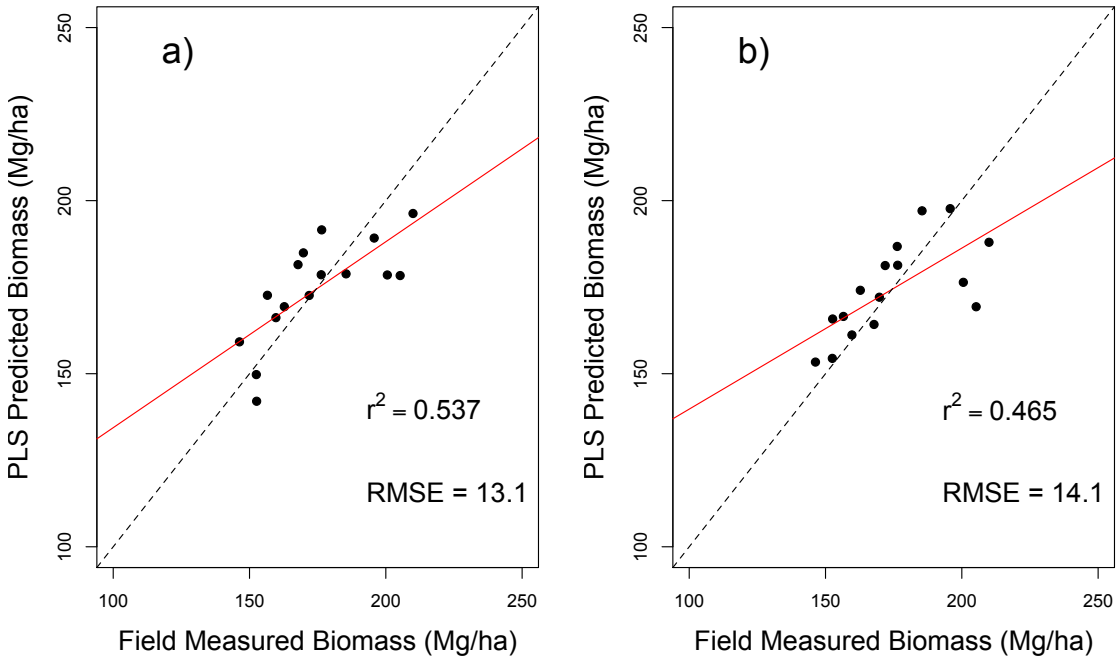

Figure 4-8. Modeling AGB at SERC using Jenkins generalized allometric equations reduced the percentage of explained variation from ~80% to ~50%. Traditional LiDAR metrics (a) perfomed slightly better than delineation metrics (b) when predicting Jenkins-based field AGB estimates, but the difference is not statistically significant.

Discussion

Individual Tree-based Mapping

Individual tree-level biomass mapping at regional scales is increasingly possible. However, the question remains whether such methods show demonstrative improvements over plot-based estimates using summary LiDAR statistics, and if so under what conditions. Conversely, scaling-based approaches have emerged from increased interest in allometric scaling by the theoretical ecology community. The work here has in a limited fashion tested whether these technological and theoretical advancements have potential to improve AGB modeling capabilities.

The results varied considerably across the three study areas in question. At Teakettle, the results suggest that individual tree-based LiDAR metrics have a higher predictive power in open conifer canopies than plot-aggregated LiDAR metrics. The spatial distribution of trees in a high AGB, open forest is not fully captured by the plot-aggregated metrics. This suggests that crown delineation, when available, should bolster AGB estimates in conifer systems. Swatantran et al. (2011) explored LVIS LiDAR data for AGB mapping in a structurally similar area of the Sierra Nevada. LVIS data should provide comparable information to the traditional, plot-aggregated metrics. They found that 77% of variability in AGB was explained by LVIS metrics, and models improved to explain 84% of variability after species based stratification. The traditional metric AGB model shows comparable results with these LVIS-based results. Therefore, these models are performing as expected and that the improvement observed with the delineation metrics is significant. Additionally, the field sites at Teakettle were populated primarily by fir and hemlock species with little difference in wood specific density, yielding the use of a single generalized allometric equation for almost all trees. Therefore, from an AGB estimation standpoint, these were homogeneous plots, which may be an additional factor in the utility of crown delineation for AGB modeling at Teakettle.

At Parker Tract, the delineation metrics did not perform as well as the plot-aggregated metrics, although this result is not statistically significant. That the delineation metrics did not perform better at Parker Tract may be explained in part by the small

plot size and field geolocation issues. The much smaller plot size (7.3 m radius) encompasses far less trees than the larger plots (~1 ha) at the other sites. When extracting delineated crowns for inclusion in AGB modeling, the crown centroid was used. Due to both crown geometries and geolocation errors in the field, it is likely that some trees near the edge of plots were falsely included in the analysis, and others were excluded. This added a source of error at Parker Tract that was minimal at SERC and Teakettle given the larger plot size at those sites.

At SERC, the AGB models explained less variability than at the other sites, and the delineation-based metrics had more explanatory power than the traditional metrics but the difference between the two models was not statistically significant at 90% confidence. Both sets of metrics yielded a lower percentage of explained variability than the models at the other two sites, although results were comparable to a previous study conducted in the same study area (Lefsky et al., 2003).

There are several factors that explain why individual tree-based metrics do not perform better than traditional metrics at SERC. In theory, if every tree was delineated correctly, and there was a perfect relationship between crown dimensions and tree biomass, individual tree-based methods would be indisputably superior to plot-aggregated methods. However, the relationship between tree crowns and AGB is imperfect. This is demonstrated through an analysis of the field data, as the relationship between basal area and AGB should be a proxy for the relationship between crown dimensions and AGB. Additionally, a tight relationship between basal

area and AGB would bolster the applicability of the scaling-based approaches provided basal area can be modeled from RH100. At SERC the relationship between AGB and basal area was poor. This is likely due to allometry, because scaling AGB to 1 ha reduces the influence of individual trees on plot level AGB and basal area. As tree level biomass is a direct function of tree DBH, this disconnect between basal area and AGB is likely a function of the wider range of allometric equations used at SERC in comparison to the other sites.

The selection of allometric equations also appears to be important in these forests, as the generalized allometric equations produced on average a 20% decrease in plot-level AGB as compared to regional equations. Interestingly, two studies by Chojnacky et al., (2014) and Domke et al. (2012) compared Jenkins-based biomass estimates to FIA volume-based estimates and show that Jenkins estimates are approximately 16% and 20% lower than those produced from FIA approaches. The similar difference found in this research (20%) may indicate that the Jenkins equations are systematically low-biased. Indeed, the regional equations yielded much higher correlations to both traditional and individual-based LiDAR metrics, suggesting that they are more appropriate for AGB modeling at SERC. This sensitivity of modeling to allometric equations further suggests that allometric variability is high at SERC. LiDAR data alone will only provide physical structure, not wood density, and therefore will always have a somewhat limited capability for AGB modeling in forests with a large range of wood densities. Fusion of LiDAR with species-sensitive hyperspectral data may allow increased individual-tree level

biomass modeling capabilities. The results at SERC suggest that individual tree data show promise for AGB modeling, but that more research is needed regarding the applicability of field-based allometric equations, and the effects of species diversity on AGB modeling.

Another confounding issue that may explain the increased performance of delineation metrics at Teakettle is delineation algorithm performance. Duncanson et al. (2014) demonstrated that although approximately 71% of dominant crowns are correctly delineation at SERC, the overall algorithm performance was higher at Teakettle. This was explained by both crown geometry (conifers are easier to delineate using watershed functions than deciduous trees which have irregular canopy surfaces) and canopy closure (the open conditions at Teakettle are ideal for delineation). Therefore it is possible that given improved delineation algorithms for closed-canopy broadleaf systems, individual tree-based biomass models would also improve.

Overall, individual tree-based approaches for AGB estimation only improved modeling at one site. At the other two sites, the traditional methods performed comparably. This is largely due to the open canopies at teakettle, where the spatial distribution of biomass within plots is important for modeling. In closed-canopy plots, improvement was not seen. Given the high computational demands of 3D crown delineation, individual tree-based methods may not currently be a systematically feasible, nor cost-effective solution for AGB mapping across all biomes.

Scaling-based Approaches

Scaling-based approaches were ineffective in two of the three study sites due to a decoupling of top canopy height and basal area. However, there might be an opportunity to use individual tree-based information to facilitate the application of wide area mapping. As noted earlier, there is a tension between the acquisition of higher density LiDAR data and the ability to map AGB across large areas. For many applications, a spatial resolution of one hectare for AGB mapping seems appropriate as it captures fine scale heterogeneity caused by disturbance, but also reduces error that occurs when smaller plot sizes are used (Zolkos et al., 2013). Asner & Mascaro addressed this by formulating a scaling relationship between plot level AGB and canopy top heights for 1 ha plots, thereby avoiding any need for high density laser point coverage to facilitate tree-based segmentation. Their method is based, however, on the ability to derive accurate, regional relationships between canopy height and basal area. While they show strong relationships in some areas, in other areas these relationships are weak or non-existent. Our results showed that top of canopy height alone could not be used to estimate basal area at a one-hectare scale in two of the three ecosystems studied. However, delineation metrics improved basal area estimates for these. This suggests a potential pathway for marrying individual tree based methods with scaling approaches.

In such an approach, limited field data would be used with tree-based methods to derive a relationship between LiDAR-derived cumulative tree volume and basal area. This relationship would then be applied wherever tree based segmentation data were

available and thus serve as a proxy for basal area. Then relationships between canopy height and proxy-derived basal area could be developed. But instead of relying only on tens of field plots, would instead have thousands to tens of thousands of proxy basal area estimates (i.e. those derived from the spatially-limited tree-based delineations) to create height to basal area relationships and more fully define the variability in these relationships. Height metrics from lower density LiDAR data could then be used to map basal area and AGB everywhere following the method of Asner and Mascaro. This approach follows the standard procedure of matching field data to high-resolution remote sensing data, and subsequently extrapolating for wide area coverage (e.g. Duncanson et al., 2010, Wulder and Seemann, 2003, Baccini et al., 2008, Saatchi et al., 2011). It is uncertain if many more observations of proxy-derived basal area will show stronger relationships with canopy height when applied over large areas, but this is likely the case. At any rate further research is required to explore these questions across gradients of forest structure and environment.

Conclusions

Individual tree and scaling-based approaches have been presented as two contrasting methods to improve the accuracy and/or extent of AGB modeling initiatives. The utility of both approaches was tested in three structurally disparate forests across the US. Airborne LiDAR technology has advanced to the point of capturing crown level detail, but crown level information is only beginning to be used in ecological applications of LiDAR data. It was found that while individual tree metrics can improve AGB models, the amount of this improvement is dependent on the physical structure and species distribution of the forest in question. These metrics are most

useful in systems with open canopies that are dominated by conifers, and have a small range of wood densities. The results at SERC illuminated the importance of allometric equations for field-based estimates of AGB. No matter how high-quality remote sensing data and methods are, AGB models will always be limited to the quality of the field-based AGB estimates. More research is required to determine when generalized allometric equations are applicable, and what controls this applicability.

Another factor that affected the utility of individual tree methods was the spatial scale of modeling. The results at Parker Tract suggest that individual tree information may not be applicable at a 15 m plot level, likely because of edge effects related to crowns overlapping the edges of field plots. The individual tree information improved modeling at Teakettle, where models were developed at a 1 ha level. At SERC, there was a decoupling of field-based basal area and AGB, which was attributed to the wide range of species found at that site, and within species structural variability. In eastern forests, modeling at 1 ha may complicate the relationship between field and remote sensing structure, and careful attention to scale is advised.

As crown delineation algorithms become more refined and LiDAR technologies continue to develop, individual tree based-biomass mapping will become increasingly feasible, and should be considered as an option to increase accuracies in some forest systems.

Scaling-based approaches, on the other hand, were not feasible in two out of three of these study areas due a decoupling of basal area and maximum forest height. These approaches are inherently dependent on the ability to model basal area as a function of canopy top height, however to estimate basal area at SERC and Teakettle more structural detail is required than canopy top height alone. Scaling-based approaches are attractive for their simplicity and ease of utility but must include the development of local basal area equations for application in spatially heterogeneous, structurally complex forests. In the discussion section, one potential method to fuse scaling approaches with individual tree data is presented. Although this method presents an interesting and potentially useful solution to the limitations of scaling-based approaches it remains untested, and further research is required to address its applicability.

In conclusion, LiDAR applications for AGB modeling continue to improve both in terms of their theoretical basis, spatial detail, and extent. Both individual tree and scaling-based approaches show promise as emerging techniques, but further research is required to explore their limitations with larger field datasets over a greater range of environmental conditions. This is particularly relevant as more countries are now undertaking regional or national airborne LiDAR surveys.

Chapter 5: Small Sample Sizes Yield Biased Allometric Equations in Temperate Forests

Abstract

Accurate quantification of forest carbon stocks is critical for successful modeling of climate change. Many methods have been applied to model and map forest aboveground biomass across wide areas, but the accuracy of these methods is inherently dependent on the accuracy of the field biomass estimates used to calibrate models. In temperate forests, field estimates are typically based on the application of allometric equations that estimate the aboveground biomass of trees based on stem diameter and species. These allometric equations are developed by destructively sampling trees for a given species and/or environment, typically with small sample sizes. Insufficient attention has been paid to the accuracy and applicability of these allometric equations due to a dearth of appropriate data. In this study, we provide a quantitative assessment of the potential effects of sample size on allometric equations in temperate systems. We use LiDAR remote sensing from six study sites in the U.S. to isolate 10,000 - 1,000,000 tree height and crown radii measurements per site. We fit allometric equations to the full dataset at each site, and then apply two sampling strategies to estimate average allometric parameters at sample sizes from 10 to 2000. We find that fitted allometric parameters are highly sensitive to sample size. Allometric exponents are consistently overestimated, and allometric scalars are underestimated at small sample sizes. When applied to the full sample of trees at each site, heights are overestimated for a given crown radius. We extended our analysis to

biomass through the application of Metabolic Scaling Theory predictions, and show that site-level biomass bias may range from -4% to +178% given the small sample sizes used in many biomass mapping initiatives. Errors decrease with increasing sample size, and we suggest that sampling several hundred trees per site is required to produce accurate allometries.

Introduction

Global forests cover approximately 30% of the land's surface and have been estimated to store approximately 1.03 million metatons (Mt) of carbon (Nabuurs et al., 2007). These estimates are not only important inputs to global carbon cycle and climate change models, but integral to the mitigation of climate change through market based initiatives such as REDD+ (Corbera & Schroader, 2011, Gibbs et al., 2007). Mapping forest carbon stocks (Lefsky, 2010, Saatchi et al., 2011, Simard et al., 2011, Baccini et al., 2012) yield high errors and there are significant discrepancies between many global forest height and biomass products (Mitchard et al., 2011, 2013). Most work in this field has focused on the development and application of data and statistical techniques to match remote sensing products to field-based biomass estimates (Goetz et al., 2009, Asner, 2009). Considerably less attention has focused on the accuracies of the field-based estimates themselves, due primarily to data limitations (Chave et al., 2004, Van Breugel et al., 2011).

Remote sensing-based forest aboveground carbon stock estimates are typically generated through a combination of field-based carbon estimation and extrapolation

using remote sensing datasets (Goetz et al., 2009, Goetz & Dubayah, 2011). Virtually all field estimates rely on the application of allometric equations relating properties that can be measured in the field to individual tree carbon stock (Jensen et al., 2003). These allometric equations are typically derived through the destructive sampling of a relatively small number of trees that are measured and felled to assess their carbon stock. Forest allometric equations relate individual tree Diameter at Breast Height (DBH) alone or in combination with tree height, to tree carbon content. Equations are generated either for individual species (e.g. Gholz et al., 1979, Clark et al., 1986), groups of species (Jenkins et al., 2003, Chovjacky et al., 2011) or for geographic regions (Chave et al., 2005). Additionally, online tools are available that archive international allometric equations and assist in the selection of the most appropriate equation for a given species and environment (Henry et al., 2013). In a comprehensive assessment of errors in tropical biomass estimates, Chave et al. (2004) demonstrate that allometric equation selection is the primary source of error in tropical field-based biomass estimates, and that the sample size of trees used to generate allometric equations is one of the primary drivers of this error (Chave et al., 2004).

In the United States, Jenkins et al. (2003) performed a literature review and combined over 100 allometric datasets to produce generalized equations for various species groups. These so-called 'Jenkins equations' have become popular for field biomass estimation in North America due to their generality and simplicity. We revisited each of the papers used in Jenkins et al. (2003) and, where available, recorded the number

of trees felled in each study to produce the allometric equation. The mean number of trees felled to generate a species-specific allometry was 39.3. The median is lower, at only 23 trees, which is indicative of the few studies that reported larger number of trees destructively sampled (Bajrang et al., 1996, n=161, Barclay et al., 1986, n=96, Harding and Griagl, 1985, n=115, Ker and Van Raalte, 1981, n=298). Although Jenkins et al. (2003) provides generalized equations for all of North America, a more specific set of equations relevant to Canada was published through the Canadian Forestry Service (Lambert et al., 2005, Ung et al., 2008). Due to pooling individuals across large areas, the allometries generated by these studies are built on larger sample sizes, with a mean of 215.6 trees and a median of 81 trees. These two sets of allometric equations represent the most common method by which to estimate field biomass in North America. The U.S. Forest Service, conversely, has shifted to a 'component ratio method', which is based on estimating tree volume, and multiplying by estimated wood specific gravity (Woodall et al., 2010). This method is also fundamentally limited to the number of trees used to calibrate the volume models, which are highly parameterized functions of DBH, site index, and site basal area. Allometric equations for volume are typically based on higher numbers of destructively sampled trees, in the range of a few hundred, but the number varies considerably based on species and study area (Chojnacky, 1988, MacLean et al., 1976, Curtis et al., 1968).

In this research, we attempt to quantify the effect of sample size on allometric equation parameterization. We use high resolution LiDAR datasets in tandem with a

crown delineation algorithm to produce spatially contiguous individual tree structure maps across six structurally disparate forests in the United States. Our goals are to (a) determine the error on fitted parameters as a function of sample size (b) determine whether small samples produce a systematic bias and (c) assess the potential carbon implications of small sample sizes for allometric equation generation in temperate forests.

Methods

Study Areas

We use forested areas in the United States, selecting sites with a range of species compositions, ages, and management practices in order to determine how variable the effects of sample size are on allometric equations across disparate conditions. High-resolution airborne LiDAR data were acquired over each study site and processed through an individual tree detection algorithm (Duncanson et al., 2014). No field data is used in our study as the algorithm has already been tested in a variety of forests. The purpose of the study is to measure every tree within each area of LiDAR coverage to test the effects of sample size on allometric equation parameter estimation, and evaluate the resulting implications for carbon stock estimation.

Teakettle, Sierra Nevada, California

The Sierra Nevada site is located in the Western Sierra Nevada Mountain range in California. Dominant species include *Abies concolor (*white fir), *Pinus ponderos* (ponderosa pine), *Abies magnifica* (red fir) and *Quercus kelloggii* (California black

oak) (Honaker et al., 2002). The elevation range of the site is approximately 1000 m to 2500 m above sea level, with aboveground biomass values averaging 200 Mg ha^{-1} with individual tree values up to 20 Mg $tree^{-1}$. The forest is mature, with rocky outcrops intermixed between clusters of trees. Fire is the primary disturbance affecting the ecosystem.

SERC, Maryland

The Smithsonian Environmental Research Center (SERC) study site is located near Edgewater, Maryland, adjacent to a sub-estuary of the Chesapeake Bay. The area is generally comprised of two forest types: mature secondary upland forest, and lowland forests. Dominant species in the upland forest include *Liriodendron tulipifera* (tulip poplar), *Fagus* (beech), several species of oak, and hickory, with mid canopy A*acer rubrum* (red maple) and *Nyssa sylvatica* (black tupelo) and understory *Carpinus Caroliniana* (American hornbeam), *Lindera benzoin* (spicebush) and *Asimina triloba* (paw-paw). Dominant species in the lowland areas are *fraxinus* (ash), *Platanus occidentalis* (sycamore), and *Ulmus Americana* (American elm). Both the upland and the floodplain forests have been relatively undisturbed for approximately 120 years.

Parker Tract, North Carolina

The Parker Tract study site is located near Plymouth in North Carolina, USA. It is largely a commercially managed Loblolly Pine plantation (*Pinus taeda)* although some stands have a mixed composition, containing native broadleaf species. One segment of the site is retained as natural forest.

Gus Pearson, Arizona

Gus Pearson Experimental forest is a mature conifer forest located near Flagstaff, Arizona. The site is comprised primarily of ponderosa pine (*Pinus ponderosa*). The primary disturbance at this site is from thinning and burning experiments that have effectively decreased the frequency of small trees, shifting the tree size distribution toward larger individuals (Bailey & Covington, 2002).

Howland Forest, Maine

The Howland Research Forest is a conifer-dominated mixed forest located in central Maine. The site is dominated by Red Spruce, Eastern Hemlock, and White Cedar. The site is mature, with stand ages ranging from 45 to 130 years. Although it has been used for studying the effects of acid rain and carbon flux, management has not significantly altered the natural tree size distribution.

Hubbard Brook, New Hampshire

The Hubbard Brook Experimental Forest is the largest study area examined in this study. The area is a mixed forest site located near Woodstock, New Hampshire, and is primarily dominated by second-growth northern hardwoods, red spruce, and balsam fir. The site exhibits considerably ecological variation across topographic gradients (Thomas et al., 2008).

LiDAR Data

LiDAR data were acquired by NASA Goddard's LiDAR, Hyperspectral and Thermal Imager (G-LiHT, Cook et al., 2013). G-LiHT uses a 300 kHz multi-stop scanning-LiDAR operating at 1550 nm with a 60° field of view and 10 cm diameter footprint. Sites were typically flown from an altitude of 335 m AGL with 50% overlap in north-south and east-west directions to achieve a mean return density of up to 50 laser pulses m^{-2}.

Canopy Delineation

Individual tree metrics are gleaned from the LiDAR point cloud through a multilayered canopy delineation algorithm (Duncanson et al., 2014). The algorithm performs a preliminary delineation on a smoothed Canopy Height Model (CHM) using a watershed-based delineation. Preliminary segments are then refined using the LiDAR point cloud to search for understory returns within each preliminary segment. Through this process the entire LiDAR point cloud is separated into overstory and understory returns. Each of these datasets is used to produce a new CHM. Both the understory and overstory CHM are segmented, yielding a multi-layered crown delineation product. This process is iterated until no further understory trees are detected. The outputs of this algorithm are individual crown locations, heights, radii, crown areas, and volumes. Crown radius is the average of crown dimensions in north-south and east-west directions.

The algorithm is run on the Pleiades supercomputer at NASA Ames as part of the NASA Earth Exchange.

Allometric Equation Fitting

Relationships between tree structural properties such as DBH, height and biomass have been demonstrated to linearly scale in the form of power laws (Enquist et al., 2009, Feldpausch et al., 2011, Ketterings et al., 2001). Ideally, individual tree-based DBH to biomass allometries would be explicitly tested in our study. However, these variables are not directly extractable from LiDAR datasets. Instead, we use the structural allometry of individual tree height to crown radius. This can be theoretically translated to DBH to biomass allometry through the application of allometric scaling relationships (Enquist et al., 2009), as described below.

Individual tree heights and crown radii are extracted from the LiDAR point cloud at each study area. Crown radii are filtered as $CR<12$ m, the expected maximum crown radius in any of our study sites based on field data. Each of our study areas includes a very high number of delineated crowns, with a differing tree size distribution. To remove the influence of tree size distribution on our analyses, we binned our data by calculating the median tree height in 0.25 m crown radius bins. Log-log linear models have been demonstrated as the best descriptions of the relationship between DBH and Height (Feldpausch et al., 2011). Accordingly, we fit a model in the form of a power law using the full tree dataset at each study site to produce a set of site-level scaling parameters. Each power law model is fit using Model 2 regression on log transformed, binned data with ranged major axis (RMA). RMA is used because errors

exist in the estimation of both tree heights and radii (Legendre, 1998). *B* is the scaling parameter, *a* is the fitted exponent, as follows:

$$H=b*CR^{a} \quad (1)$$

Where *H* is height and *CR* is crown radius. The allometric parameters that are calculated using the full population of delineated trees at each site are assumed to be the true scaling parameters representing the allometry at each site. We then extract samples from the full dataset to assess the influence of sample size on the fitted parameters. From the literature, studies either do not report how they selected trees to fell, or report that they selected trees that appeared representative of the apparent size distribution. In this paper, we present two sampling strategies: (1) random sampling, and (2) stratified random sampling.

Random sampling

For our random sampling approach, we iteratively generate samples from our full dataset in each study area, selecting trees randomly with sample sizes increasing from 10 to 2000, with increments of 10. For each randomly sampled set of trees, we follow the model fitting procedure used for the site-level analysis, as outlined above. As random sampling produces highly variable fitted parameters, we iterate the random sampling 500 times for each sample size, and calculate the average parameter over the 500 iterations. Therefore we produce a single average estimate of *a* and *b* for each sample size.

Stratified Random Sampling

In an attempt to simulate a more realistic approach to sampling in the field, we also apply a technique that samples trees that are taken from plots. We adopt a stratified sampling scheme we believe is approximately representative of field mensuration. It should be noted, however, that sampling for biomass equation development varies considerably, often based on arbitrary decisions made in the field. In our stratified sampling approach, we simulate sampling at a pseudo plot-level. We randomly select locations within each study area, and extract all trees in a 30 m plot corresponding to each randomly selected location. We then select five trees from within each plot, taken at the 10^{th}, 30^{th}, 50^{th}, 70^{th}, and 90^{th} percentiles of crown radii. A sample size of five consequently corresponds to one pseudo plot. Sample size is increased by selecting more plot locations, and extracting five trees from each new plot. For each sample size, the data are pooled, binned, and a model is fit following the methods for the site-level and random sampling analysis.

Carbon Implications

As discussed, we test the allometry between crown radius and height rather than between DBH and biomass. In an attempt to translate our results to the relationship between DBH to biomass, we use theoretical predictions from Metabolic Scaling Theory (MST, Enquist et al., 2009). MST presents a set of power law equations relating various forest structural and functional properties, as follows:

$$H \propto DBH^{2/3} \quad (1)$$

$$DBH \propto M^{3/8} \quad (2)$$

$$H \propto M^{1/4} \quad (3)$$

$$DBH \propto CR \quad (4)$$

Where H is height, DBH is Diameter at Breast Height, M is aboveground tree biomass, and CR is crown radius. Combining these three equations allows us to translate errors in the estimation in exponents relating CR and H to the relationship between CR and M. This is a theoretical translation and only allows a general understanding of the importance of sample size on biomass estimation rather than a precise quantification.

$$H = bCR^{a} \quad (5)$$

$$M = b^{4}CR^{4a} \quad (6)$$

To estimate site-level biomass we use Equation 6 to calculate the individual tree level biomass for each 25 cm CR bin in each study site, and multiply by the number of trees within that bin. The biomass in all CR bins is summed to estimate site level biomass. First, we estimate site-level biomass with the site-level allometric parameters, followed by parameters corresponding to sample sizes of 30, 50, 80, 100, 150, 200, and 500 for each sampling strategy (random and stratified). The biomass estimates corresponding to each sample size are divided by the biomass estimate using the site-level allometry to give a percentage over or underestimate of biomass for each site as a function of sample size.

Results

Site-Level Allometries

In general, small trees follow near linear scaling but then continue to grow laterally while increases in height slow (Fig 5-1). In each study site, there is considerable variability in these relationships, represented by the blue bars in Fig. 5-1 that show the 10^{th} to 90^{th} percentiles of height for each crown radius bin. Ignoring the variability in these relationships, they can be simplified as power laws describing the average (median) height in each crown radius bin. Fig. 5-2 shows these average site-level allometries, with the red line representing the site-level allometric equation. Pooling the six site-level allometries (Fig. 5-3) we see that there is considerable variance between our study sites, as expected because we purposefully selected structurally disparate forests from across the U.S.

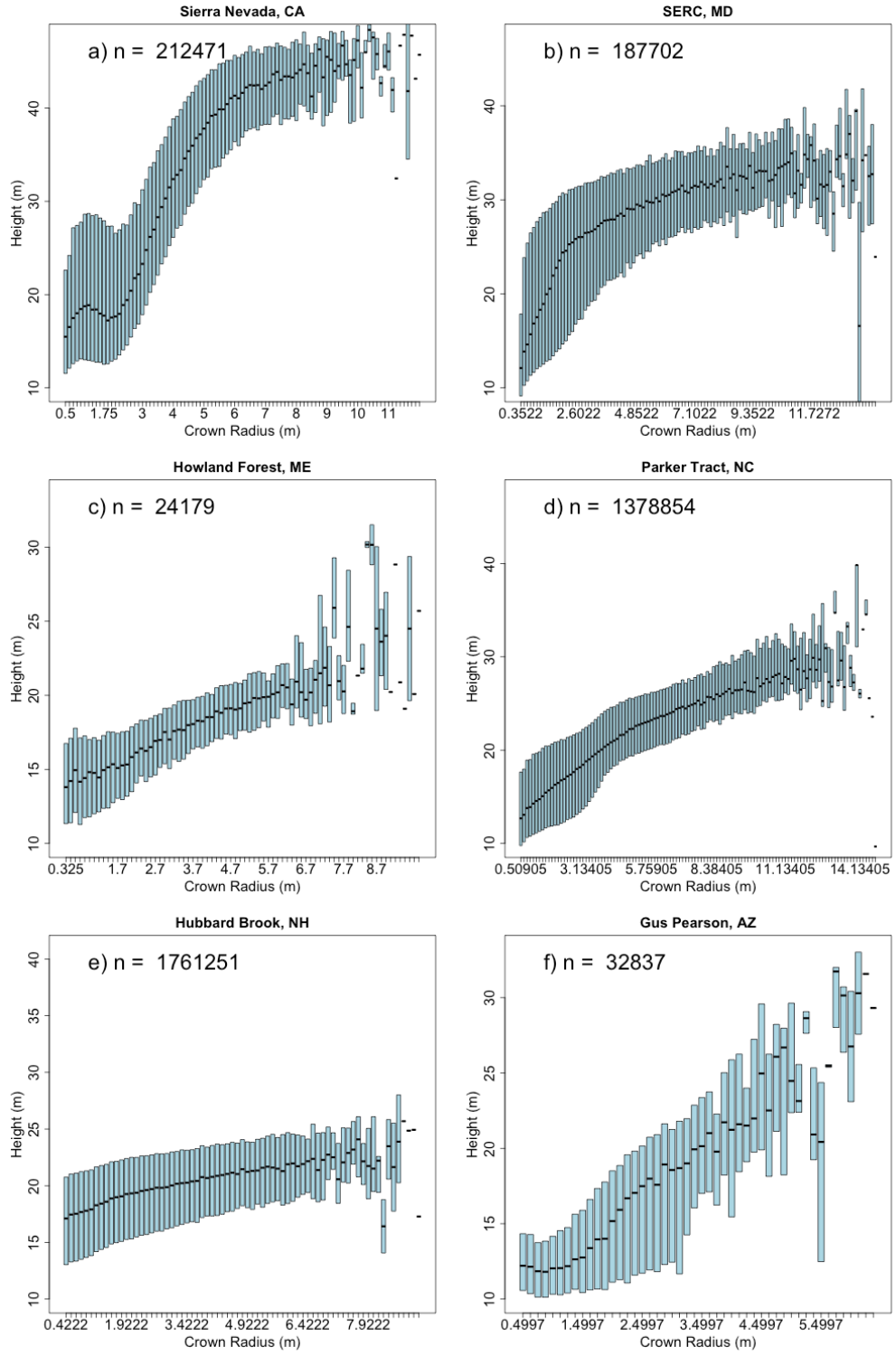

Figure 5-1. The relationships between crown radius and tree height at each study site. The number of delineated crowns at each site is displayed in the top left of each figure. The blue bars represent the 10th to 90th percentiles of heights in each crown radius bin, while the black bars represent the median tree height

in each bin, at a) Sierra Nevada, b) SERC, c) Howland, d) Parker Tract, e) Hubbard Brook and f) Gus Pearson, respectively.

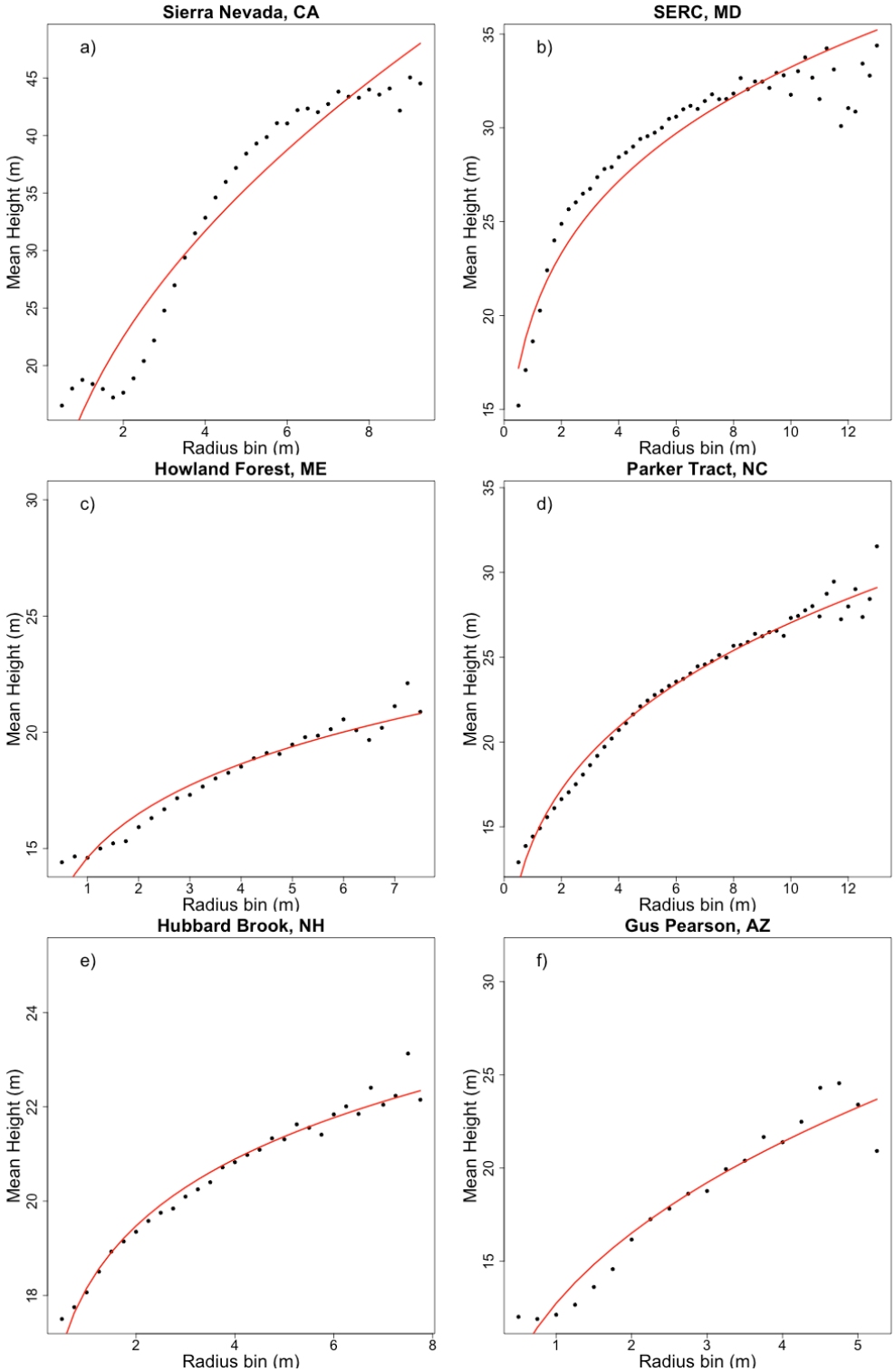

Figure 5-2. The black dots represent the median tree height in each 25 cm crown radius bin, roughly representative of the black bars in Figure 5-1. The red lines

are power law curves fit to each distribution. The parameters of these red curves are assumed to represent the true, or site-level allometry at each site.

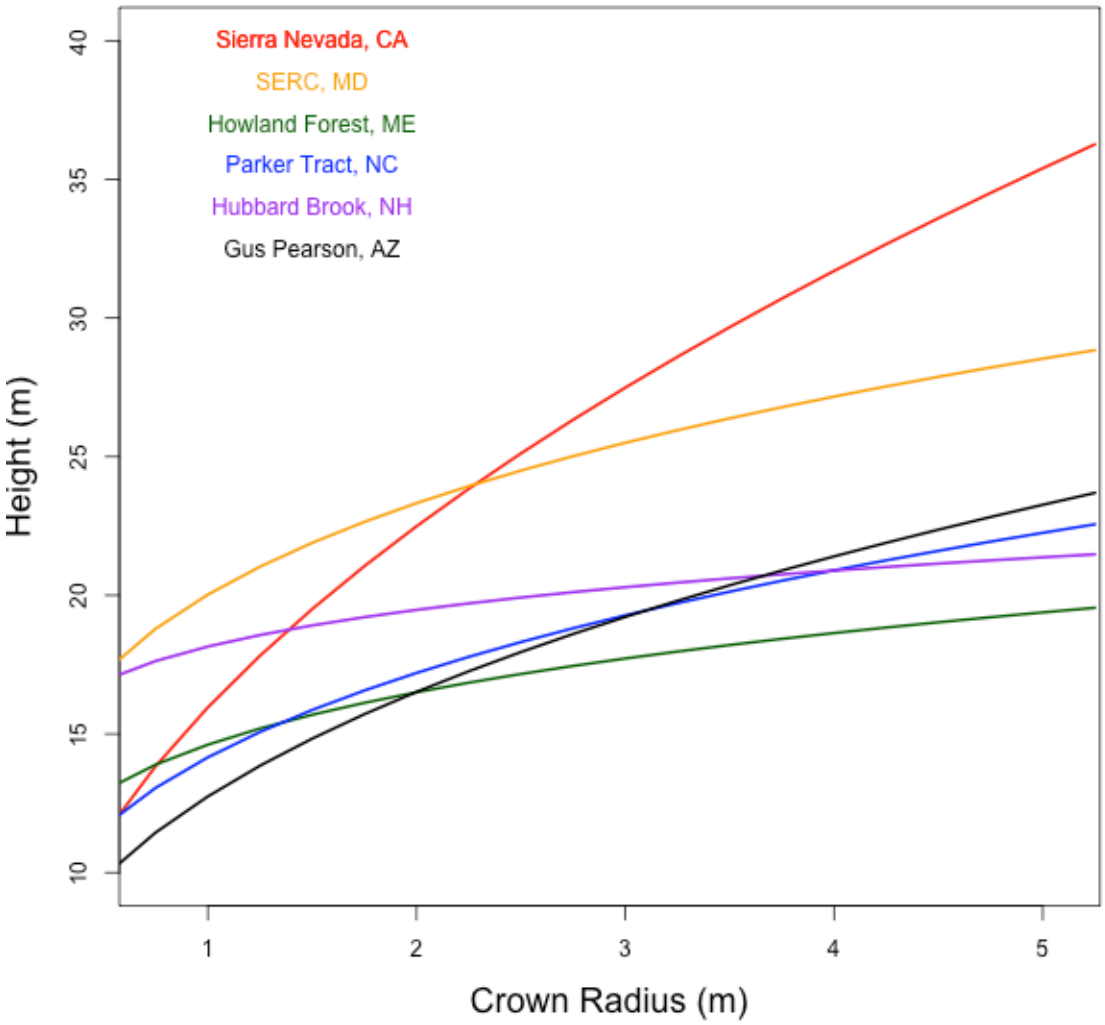

Figure 5-3. Combining the six allometric equations displayed in Figure 5-2, the range of allometric variability is seen across the six study sites. The color of each line corresponds to the color of the text representing each study area.

The effects of Sampling on Allometric Parameters

Random Sampling

The average scaling parameters for a given sample size are presented in Fig. 5-4 and Fig. 5-5, with vertical red bars representing site-level parameters. With our random

sampling approach, as sample size increases there is a consistent decrease in *a* (Fig. 5-4) a corresponding increase of *b* (Fig. 5-5). These trends are consistent across our study sites. Taken alone, an overestimation of *a* would yield an overestimation in height for a given crown radius, while an underestimation of *b* would yield an underestimation of height. To better interpret the relative importance of these two trends, we standardized the parameters with respect to the site-level parameters (Figs. 5-6 and 5-7). We see that *a* can be overestimated by up to 100% at very small sample sizes, while *b* is only underestimated by ~10%. Therefore we expect sample size to be more important for the fitting of the allometric scaling exponent, *a*, than the scalar, *b*.

It is apparent that even at a sample size of 2000, parameters do not match site-level fitted parameter values. The fitted parameters shown in Figs. 5-4 and 5-5 represent the average parameter over 500 random samples for each sample size. Therefore the probability that rare, large trees are included in the sample increases with sample size, and is reflected by the convergence toward site level values with increasing sample size. Although 2000 is a large sample when considering destructively sampling trees, it still only represents a small fraction of the trees at each site.

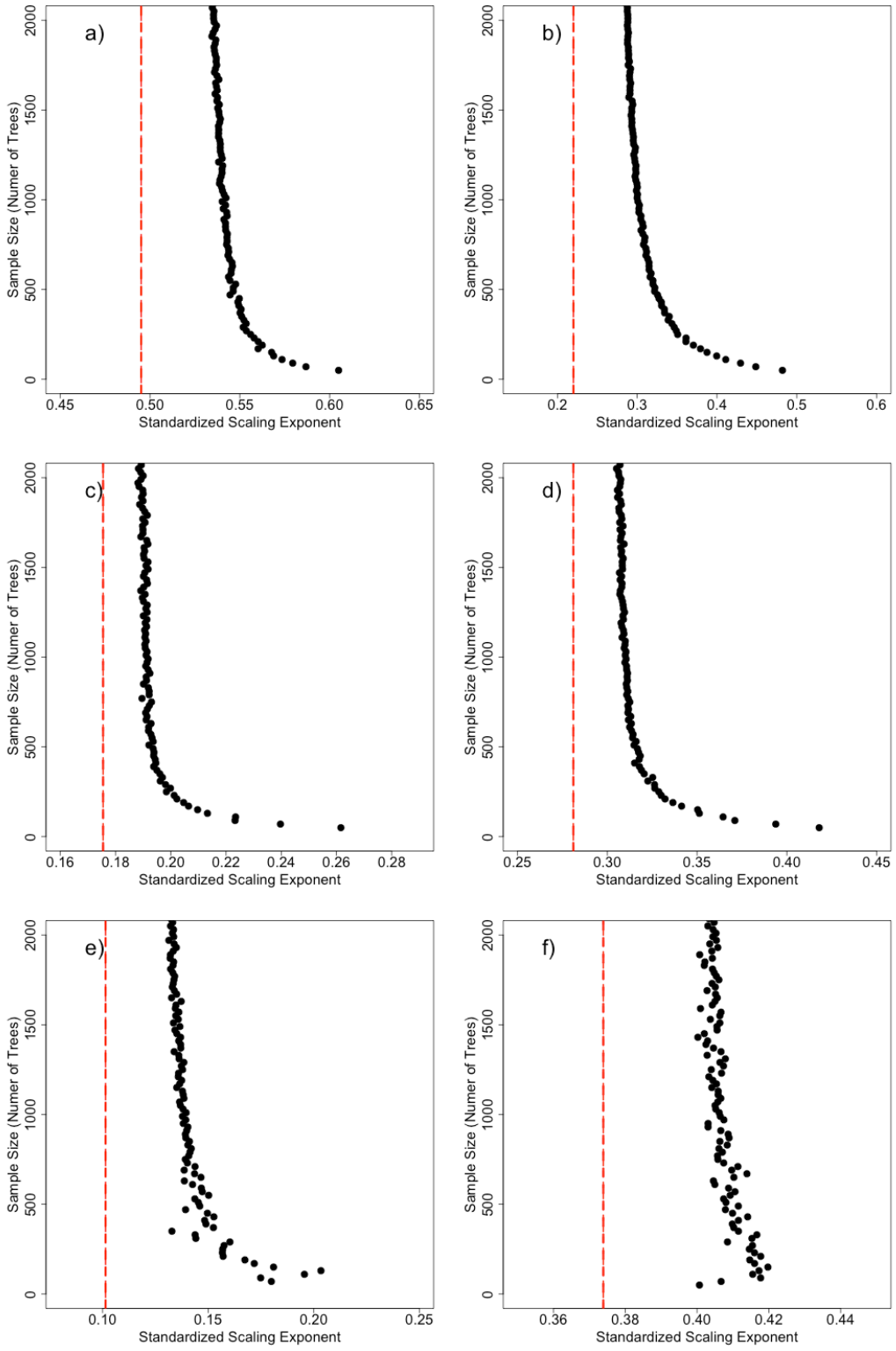

Figure 5-4. The average allometric power law exponent, *a*, for a given sample size at from the random sampling approach at a) Sierra Nevada, b) SERC, c) Howland, d) Parker Tract, e) Hubbard Brook, and f) Gus Pearson. In general,

we see that the exponent decreases as the sample size increases, approaching an value representing the true or site-level allometry.

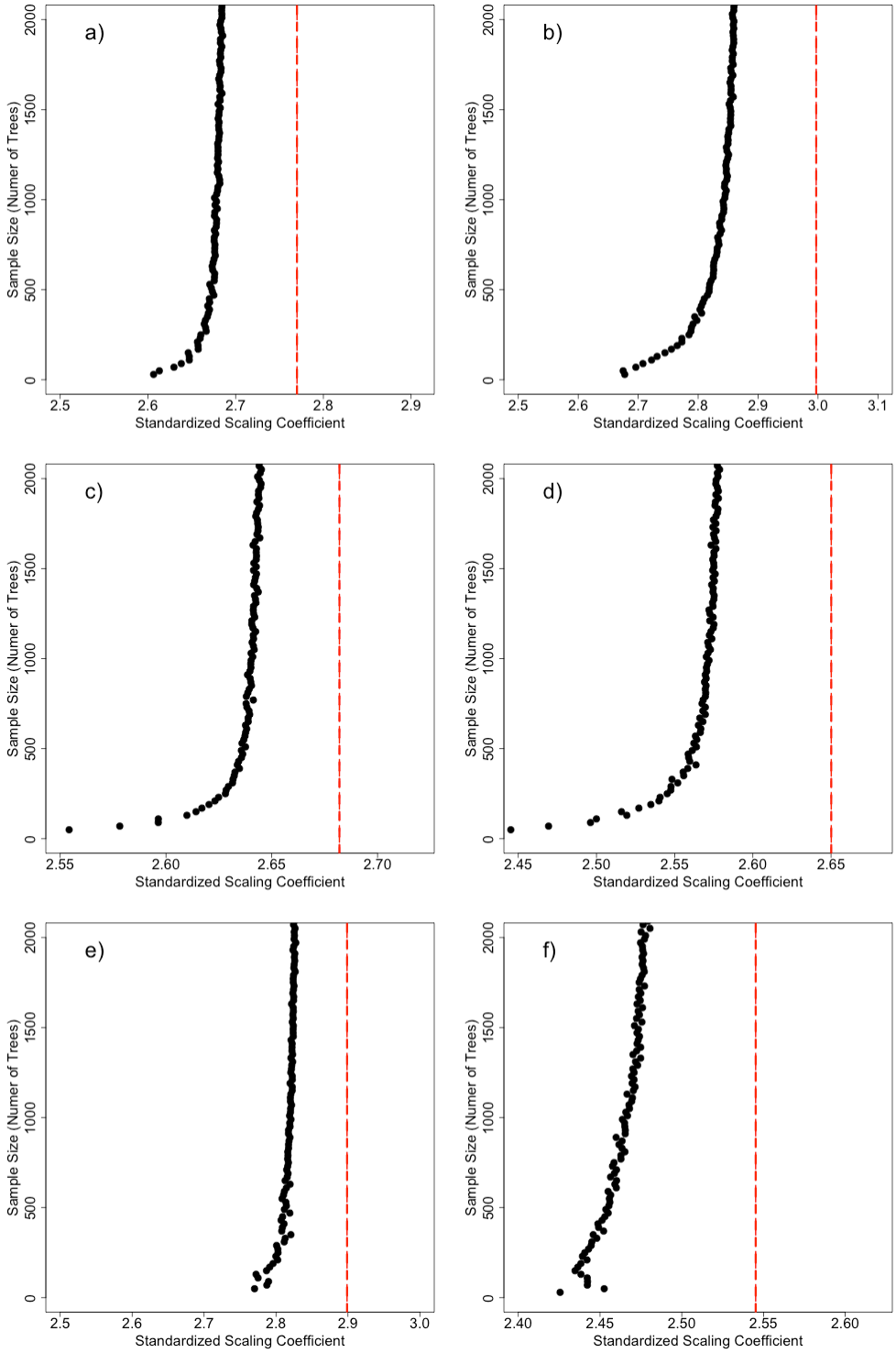

Figure 5-5. The average allometric power law scalar, *b*, for a given sample size at a) Sierra Nevada, b) SERC, c) Howland, d) Parker Tract, e) Hubbard Brook and f) Gus Pearson, using the random sampling approach. In general, we see that the

scalar increases as the sample size increases, approaching a value representing the true or site-level allometry. , at a) Sierra Nevada, b) SERC, c) Howland, d) Parker Tract, e) Hubbard Brook and f) Gus Pearson, respectively.

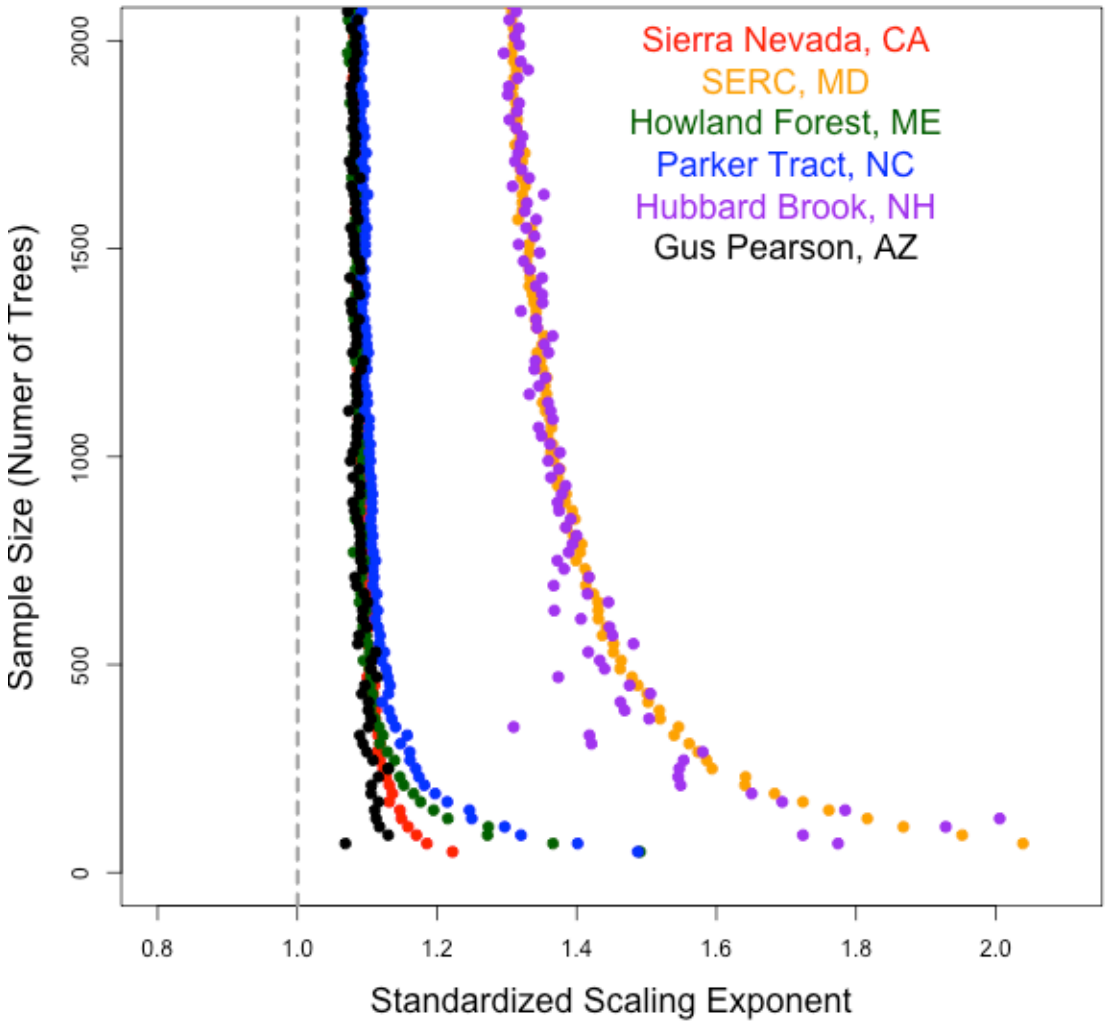

Figure 5-6. The pooled deviation from site-level allometry for the allometric exponent, a with the random sampling approach. A value of 1.2 of the standardized a represents an overestimation of the parameter by 20%.

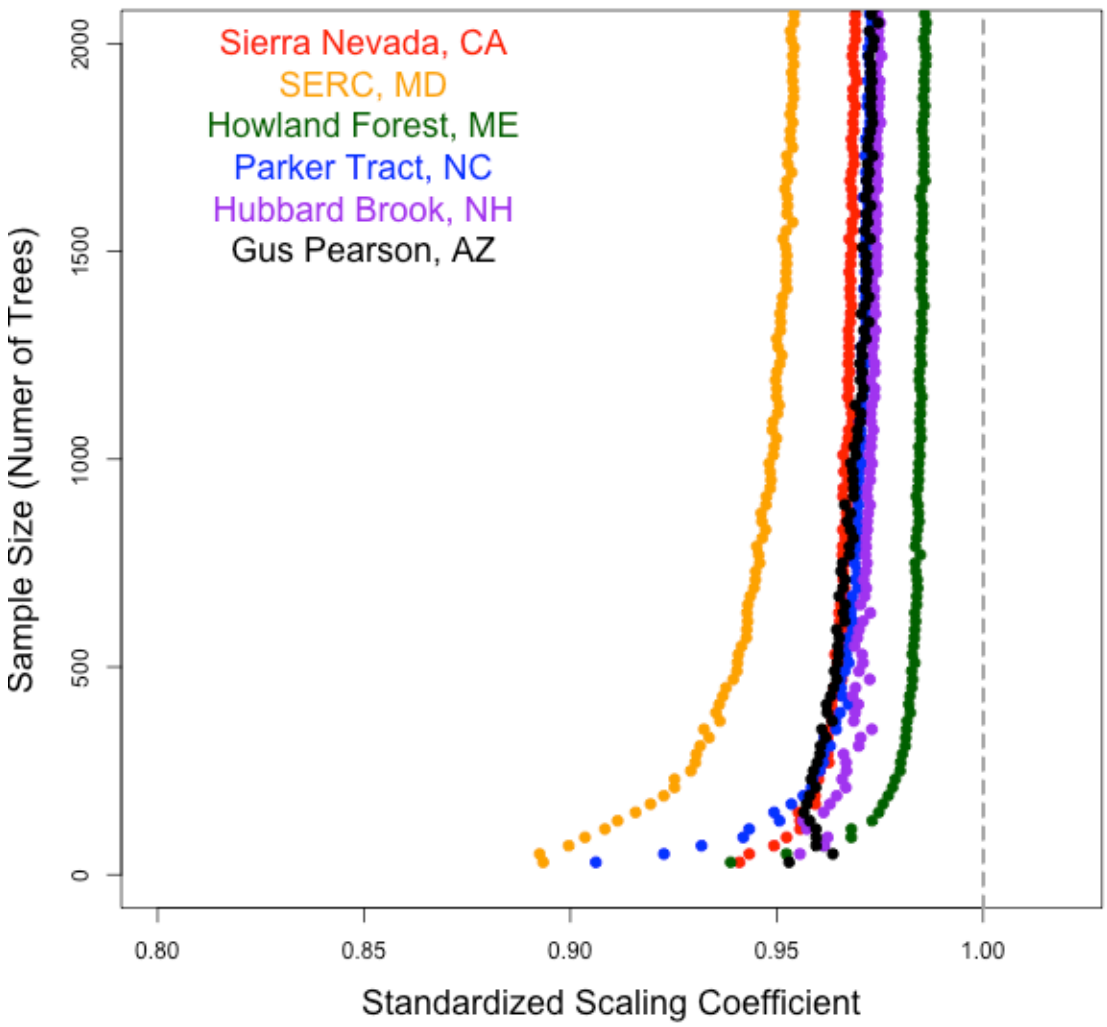

Figure 5-7. The pooled deviation from site-level allometry for the allometric scalar, *b* with the random sampling approach. A value of 0.95 of the standardized scaling parameter represents an underestimation of the parameter by 5%.

Stratified Sampling

For our more realistic sampling approach, our results are generally very similar to those found with random sampling, suggesting that our trend of overestimating *a,* and underestimating *b* at small sample sizes is not a function of sampling strategy.

However, the fitted parameters have different values using stratified sampling than random sampling (Fig. 5-8, 5-9). In most sites, parameters approach higher values of *a* and lower values of *b*. This represents more linear relationships (higher *a)* between height and crown radius, with shallower slopes (lower *b)*. Again, to analyze the relative importance of sample size on the two parameters, we pool these results with respect to site-level parameters (Figs. 5-10, 5-11). Deviations from site-level parameters are generally larger with stratified sampling than with random sampling.

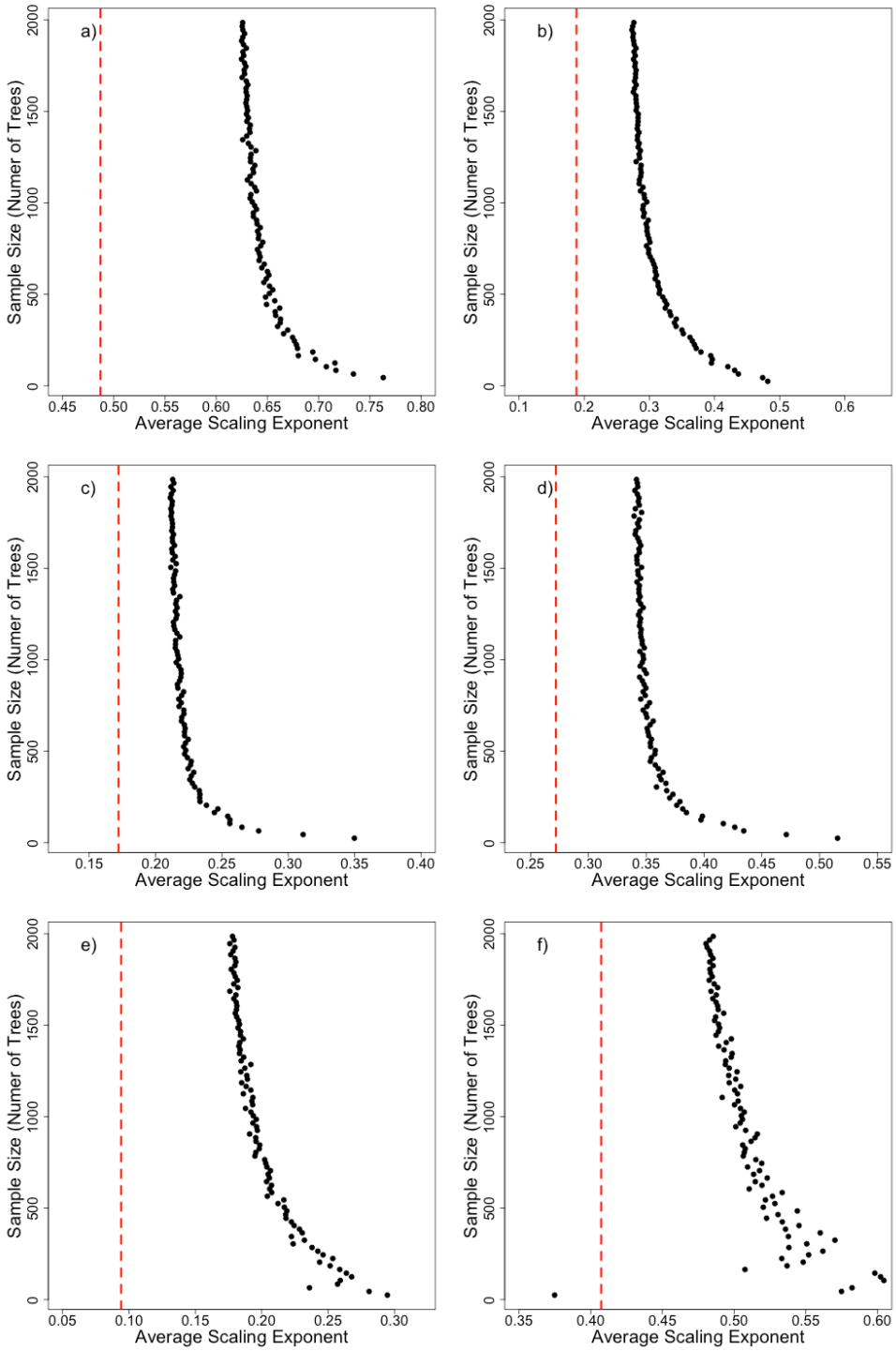

Figure 5-8. The average allometric power law exponent, *a*, for a given sample size at a) Sierra Nevada, b) SERC, c) Howland, d) Parker Tract, e) Hubbard Brook and f) Gus Pearson, using the stratified sampling approach. Red vertical lines represent site-level allometric parameters.

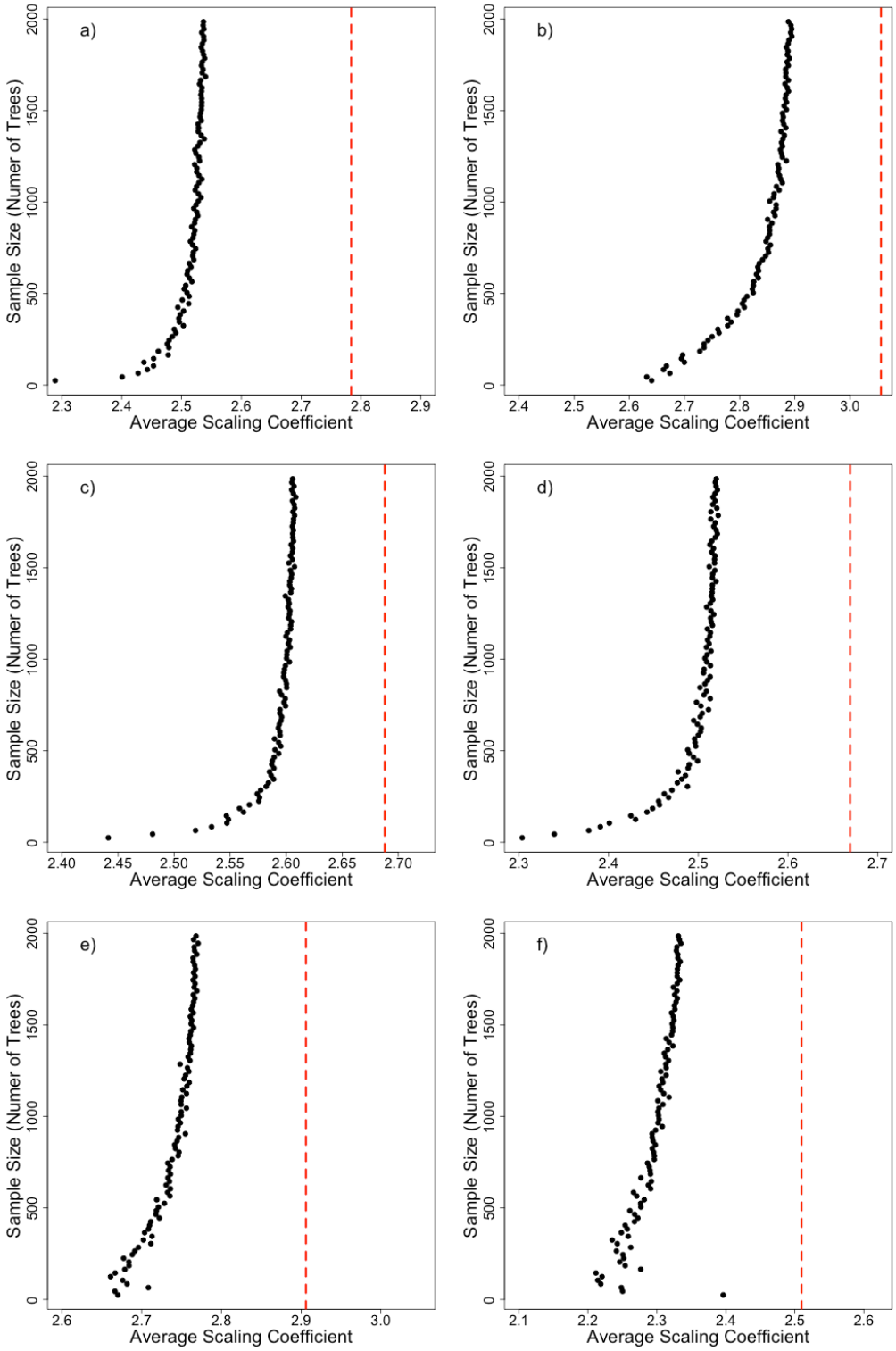

Figure 5-9. The average allometric power law scalar, *b*, for a given sample size at a) Sierra Nevada, b) SERC, c) Howland, d) Parker Tract, e) Hubbard Brook and f) Gus Pearson, from the stratified sampling approach. Vertical lines represent site-level allometric parameters.

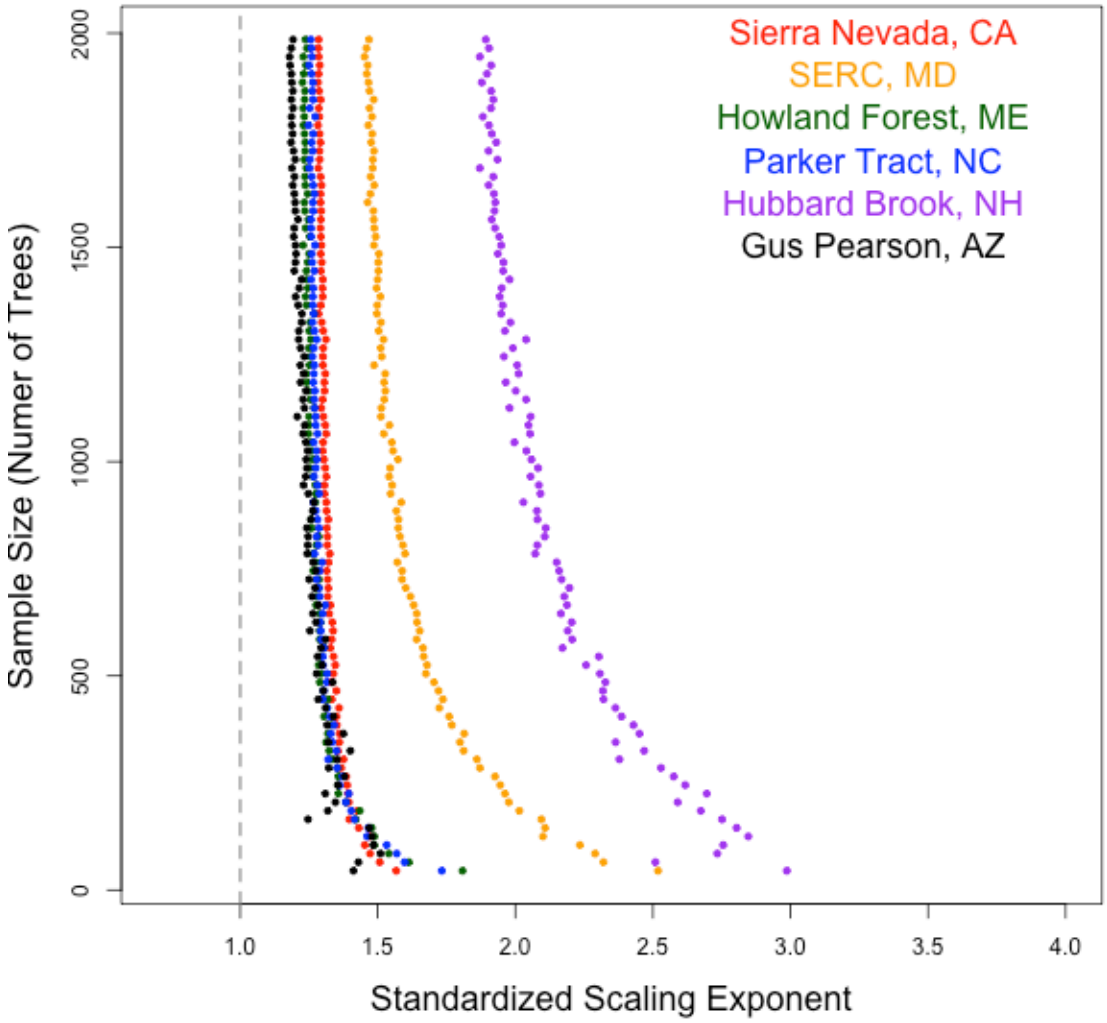

Figure 5-10. The pooled deviation from site-level allometry *a*, using the stratified sampling approach. A value of 1.2 of the standardized *a* represents an overestimation of the parameter by 20%.

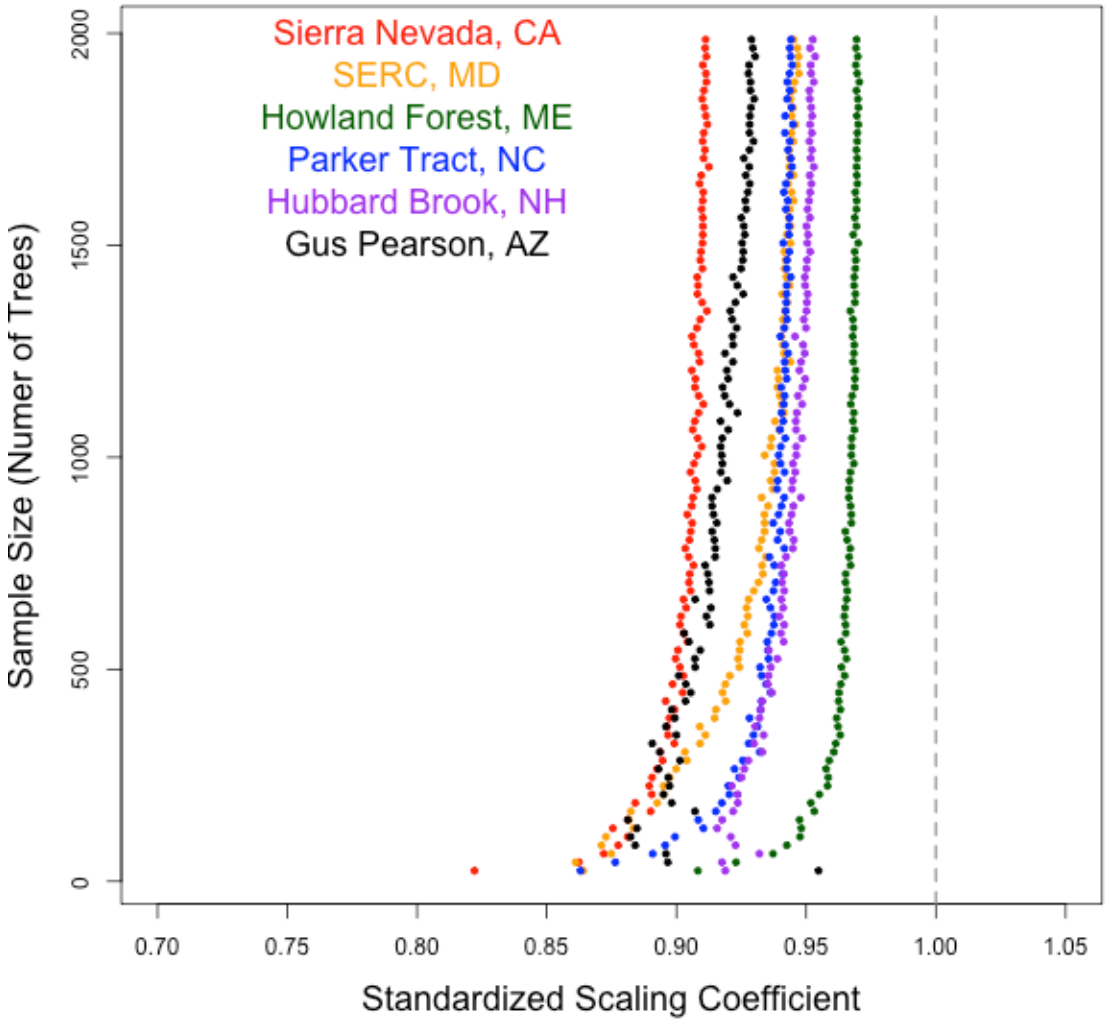

Figure 5-11. The pooled deviation from site-level allometry for the allometric scalar, *b*. A value of 0.95 of the standardized scaling parameter represents an underestimation of the *b* by 5%.

Carbon Implications

To address potential biomass implications, we use Equation 4 to estimate tree biomass as a function of crown radius and our allometric parameters, *a* and *b*. Summing these tree level estimates over the number of trees found in each study area, we estimate the deviation from site-level biomass as a function of sample size for

random sampling (Table 5-2) and stratified sampling (Table 5-3). To assign values of *a* and *b* for a given sample size, we fit a smoothing spline to the curves in Figs. 5-4, 5-5, 5-8 and 5-9 and extracted the parameter values corresponding to each selected sample size. Results vary considerably across our six study sites and between our two sampling strategies. However, we generally overestimate site-level biomass when using allometric equations developed from small sample sizes.

Table 5-2. Percentage deviation from site-level biomass estimation as a function of the sample size used to develop allometric equations, using random sampling. Values are presented as % under or overestimation.

Sample n	Sierra	SERC	Howland	Parker	Hubbard Brook	Gus Pearson
30	60	223	29	83	21	-4
50	44	162	18	47	12	-6
80	39	107	10	36	7	-7
100	36	88	8	25	5	-8
150	23	67	6	16	1	-7
200	26	53	3	13	0	-8
500	19	33	1	6	-2	-7

Table 5-3. Percentage deviation from site-level biomass estimation as a function of the sample size used to develop allometric equations, using stratified sampling. Values are presented as % under or overestimation.

Sample n	Sierra	SERC	Howland	Parker	Hubbard Brook	Gus Pearson
30	178	138	31	70	7	10
50	159	86	23	63	5	20
80	129	89	17	41	0	5
100	115	67	13	34	0	4
150	94	52	12	26	0	4
200	87	42	9	27	0	1
500	68	28	6	16	-3	-5

Discussion

Our analysis shows that the parameterization of allometric equations varies considerably as a function of sample size. Our results corroborate the findings of Chave et al. (2004) but illuminate that in some forests, the potential impact of using allometric models based on small sample sizes for biomass prediction extends well above 30% error, in some cases causing overestimations of more than double the presumed biomass, if our simulations are correct. This overestimate of biomass is due to the non-linear relationships between both crown radius and height, and crown radius and biomass. If we only sample smaller trees, we tend to fit a more linear relationship, which extended over the full tree size distribution of an area will overestimate the height and biomass of large individuals. It is therefore important to sample the full tree size distribution over which allometric equations will be applied.

There are three important trends visible in Tables 5-2 and 5-3. First, as sample size increases, errors in biomass estimation decrease. Importantly, in all sites but Gus Pearson, biomass is overestimated with small sample sizes, and this overestimation decreases as more trees are sampled. Secondly, stratified sampling typically yields lower overestimations than random sampling, presumably because more large trees are sampled in our stratified sampling scheme. Third, there is considerable variability in overestimations between sites, and this variability also decreases with increasing sample size.

Focusing on the results from stratified sampling, as these are likely more representative of real world forest mensuration, we see that at a sample size of 30, consistent with the average sampling from Jenkins et al., (2003), there is an overestimation of site level biomass ranging from 7% at Hubbard Brook to 178% at our Sierra Nevada site. The two largest overestimations, at SERC and Sierra Nevada, are likely because these are the sites with the largest trees, and biomass overestimation will increase with tree size. Therefore although parameters fits deviate more from site level values at Hubbard Brook than at the Sierra Nevada site, the higher proportion of large trees at the Sierra Nevada site yields larger site level overestimation of biomass.

There are several caveats to the work we have presented. First, our crown delineation algorithm is imperfect. It has been tested both in coniferous and deciduous forests (at the Sierra Nevada and SERC sites presented in our study) and performs better in coniferous forests. However, we found at SERC that errors in individual crown delineation were unbiased, and that ~71% of the dominant stems were correctly identified (Duncanson et al., 2014).

Our second major caveat involves the application of Metabolic Scaling Theory equations for translating between allometries. This is a highly contested theory, and although previous work has indicated that the theory is valid in resource and demographic steady state forests in the U.S., the forests in our study do not necessarily fit this description. In fact, the predicted MST exponent relating crown

radius and height is 0.66, which is higher than we found in any of our sites. We are confident in our assumption that crown radius scales linearly with height, as has been demonstrated at our Sierra Nevada and SERC sites through field measurement of crown radii, and is generally accepted in the literature (Pers. Comm. David Harding). The assertion that height will scale with biomass as in Equation 3 is uncertain, as limited data has been available to test this prediction. However, our goals were to determine the effect of sample size on parameterization, and the associated potential carbon implications. Applying MST predictions is the simplest way to translate between allometries and therefore our precise over or underestimates of biomass should not be directly used to correct for existing carbon estimates. Instead, these results should suggest care be taken when applying allometric equations that have been developed with small sample sizes.

These are not novel concerns. Researchers in this field have stressed the importance of developing allometric equations for different environments (Chave et al., 2004, Vieilledent et al., 2012) or the grouping of species into more theoretically appropriate groupings (Chovnacky, 2014). Further, we are not criticizing the work conducted by those who have developed generalized allometric relationships, as in Jenkins et al., (2003). These relationships are the best available in North America and as such are understandably widely applied. Unfortunately, given the observed allometric variability across the U.S. (Duncanson et al., submitted) and the compounding issue of small sample sizes, we believe that a new approach is required to accurately map forest aboveground biomass in the field.

We suggest that new sampling for allometries focus on volume estimates rather than biomass estimates, as in FIA, but that volume allometries are built over much larger sample sizes and a wider range of environmental conditions. The limiting factor here has always been the destructive sampling of trees. We believe that that may no longer be a requirement. Given recent advances in LiDAR technologies, particularly highly portable ground-based LiDAR (Strahler et al., 2008), highly precise estimates of individual tree volumes are increasingly available. These estimates do not require the destructive sampling of trees, and can be conducted in a systematic fashion in the field. As such, much higher sample sizes can be acquired, including samples of very large trees for which destructively sampling would be logistically impractical. In tandem with an increased understanding of the variability of wood densities (Chave et al., 2006, Muller-Landau et al., 2004), these individual tree volume estimates could be used to produce the sample sizes necessary to reduce biomass error at the individual tree level. With appropriate sampling and campaign design, a system could be developed to sample in situ tree volume across environmental gradients. Although this approach would require a commitment of considerable finances and personnel, we believe that this presents the best solution to outstanding problems in forest allometry.

Conclusions

We show here that allometric parameters are sensitive to sample size, and that parameters are systematically biased as a function of small sample sizes across six

forested sites in the United States. Our analysis on the carbon implications of these results suggest that we may be systematically overestimating field carbon stocks in North America through the application of allometric equations developed with excessively small samples sizes. This problem has been unavoidable in the past, and we have not previously been able to quantify the potential carbon implications of these small sample sizes in temperate systems. Through simulations, we predict that in six forest systems small sample sizes yield substantial (10-178%) potential overestimates of aboveground biomass. Although these values are based on theoretical allometric equations, and therefore may not represent precise biomass errors, the magnitude of these findings warrants a more thorough analysis of forest allometry. We believe that field estimates of aboveground biomass may be the limiting factor for reducing errors in remote sensing-based estimates of forest aboveground carbon and that a new approach to field biomass estimation is required. We have proposed a framework based on non-destructively sampling tree volumes with ground-based LiDAR. Building such a framework would take considerable effort, but quantifying carbon stocks on Earth is critical to the mitigation of climate change and therefore of great importance.

Chapter 6: Conclusions

Summary of Principal Findings

Chapter 2

In Chapter 2, we mapped the variability of forest structural allometry across the United States and modeled allometric parameters as a function of forest environment and life history. In this chapter we discovered that forest structural allometries vary significantly across space, and that different allometries have different spatial patterns. Approximately 40% of allometric variability could be explained as a function of environment and life history.

With respect to Metabolic Scaling Theory, our research shows that environment limits the applicability of theoretical predictions. However, allometric variability decreases with increasing forest height, and appears to asymptote at approximately theoretical predictions. The relationship between tree size distribution and forest height is particularly obvious, with both conifer and broadleaf dominated systems exhibiting the same trend and asymptote value. With respect to the relationship between DBH and tree height, conifers asymptote at a higher value indicating that they grow taller for a given DBH. This is logical, as lower wood densities would mean that the physical weight of trees would be lower at a given height, allowing conifers to grow taller with a reduced buckling constraint. However, this remains speculative and may also be the result of a higher proportion of conifers in mature forests in the western U.S.

Maximum forest height was the most important attribute for explaining allometric variability. As forests grow taller it is likely that trees allocate more of their biomass vertically to compete for light. Shorter, more open forests contain trees that grow broader for a given DBH. With respect to tree size distribution, shorter forests allocate more of their biomass to small trees, likely due to a lack of system maturity, which may allow a more stable tree size distribution including larger stems. As forests age, they undergo a self thinning type mechanism whereby small trees are out competed by their neighbors until a consistent tree demography is maintained. After about 35-40 meters in height, tree size distribution scaling becomes fairly consistent in the U.S. This does not mean that the same tree sizes will be found in all forests above 35 m, but that the same relative distribution with respect to size is maintained.

In approximately 10% of the FIA plots, there were so few trees in the smallest size classes that a power law no longer described tree size distributions with inclusion of small tree classes. To include these plots, a minimum size class was fit above which tree size distributions do, indeed, follow power law scaling. The exponents for tree size distribution allometry in these plots were more negative than other plots at the same height. This suggests that when there are fewer small trees than expected, there are either more medium sized trees or less large trees. This observation is important for understanding forest demography – there is something that is affecting tree size distributions in areas with fewer small trees that is not currently accounted for by MST. We speculate that this is caused by size dependent mortality, as many papers

have suggested that mortality rates increase with size (Muller-Landau et al., 2006, Coomes et al., 2003, Lines et al., 2010).

Metabolic Scaling Theory provides a simple set of scaling predictions that have been rejected by many forest ecologists. We argue that although allometric scaling is not universal, and does vary with environment, MST predictions are valid in forests that adhere to MST assumptions (optimized, fractal distribution networks, equal distribution of resources, no recruitment limitation, etc.). MST may therefore be of future use for constraining allometric relationships in forests systems, potentially serving as a set of prior predictions in Bayesian type models of forest allometry. This research is therefore important both for the theoretical ecology community and the practical forest management community as these findings may spur future research into the utility of MST predictions as theoretical constraints on empirically derived allometries.

Chapter 3

Chapter 3 contrasts with Chapter 2 in that it is the most technical paper in the dissertation and does not directly address science questions. Rather, it presents the development and validation of a LiDAR-based crown delineation algorithm capable of resolving individual tree structure across large areas and disparate forest types. The main findings in Chapter 3 relate to the validation of the algorithm, demonstrating that the algorithm performs best in open-conifer systems. However, it is still capable of accurately resolving dominant and co-dominant trees in closed-canopy broadleaf-dominated systems, as at SERC.

The validation procedure at SERC was novel, matching individual trees based on their crown dimensions and locations to trees measured in the field. It assumed a relationship between tree DBH and crown radius, and that there was minimal displacement in location from mapped stems to the center of their crowns. Considering allometric variability at SERC, issues with location accuracy in the field, and leaning trees, this validation was fairly conservative at it is likely that the reported accuracies were lower than reality.

This algorithm and its validation across systems contribute to the development of individual tree detection from LiDAR and high-resolution optical systems in general. This is a growing field in the LiDAR community, and many algorithms have been presented, although most of them focus on relatively small conifer trees, as seen in boreal forests. To our knowledge, no other algorithms have been applied to multiple temperate forest systems without local parameterization. We believe that other algorithms are likely more accurate in their sites of development but they typically depend on local calibration. These may be more useful for detailed, local ecological studies but will not be able to produce accurate estimates in other forests, or across wide study areas. Although this paper does not focus on science questions it was essential for addressing the questions in Chapters 4 and 5, and therefore is integral to this dissertation.

Chapter 4

Chapter 4 addressed the importance of spatial detail for biomass modeling in three forested ecosystems. Two novel approaches were tested in comparison to 'traditional' LiDAR-based biomass mapping. The first used the outputs from Chapter 3 to address the utility of individual crown information for biomass mapping. The second tested a novel allometric scaling based approach presented by Asner & Mascaro (2014) to use minimal input data for wide area mapping. The two approaches present the most extreme examples of data inputs to biomass models. We found that individual tree data only improves models when there is a large degree of spatial heterogeneity in biomass distributions. For fairly homogeneous sites, plot-aggregated LiDAR metrics, as typically used for biomass modeling, were equally capable of explaining variation in field-estimated biomass. In contrast, the scaling-based approach was only useful in one study site. It failed in the other two sites because basal area could not be accurately predicted from top of canopy height. This chapter contributes to the ongoing development of best practices for LiDAR-based biomass modeling and mapping.

Chapter 5

Chapter 5 focused on determining the sensitivity of empirical allometric equations to sample size. Using the individual tree structure derived from Chapter 3, six LiDAR study sites were used to assess both the sensitivity of allometric parameters to sample size, and the potential associated carbon implications. In all six study sites, the relationships between allometric parameters and sample size are similar, with the

allometric coefficient increasing, and the allometric exponent decreasing, as a function of sample size. At these six sites, power laws are good fits to the relationship between crown radius and tree height. In general, small trees are more likely to be selected for sampling than large trees. If a relationship is fit only to the smaller size classes in a given study area, the fit will tend to be more linear than a fit to the entire dataset. Applying a more linear relationship to larger trees yields overestimates of tree heights, and related overestimates of biomass. Therefore, at sites that exhibit power law scaling with relatively small exponents (very non linear), small sample sizes lead to the underestimation of biomass in larger stems.

The potential carbon implications for the parameterization at each site are also provided. Large deviations from site level parameters will not necessary yield a large difference in site-level AGB. For example, at Hubbard Brook, despite an over 50% increase in the scaling exponent with a sample size of 30, site-level biomass is only overestimated by approximately 7%, which is much lower than the overestimates at SERC where similar relationships between scaling exponents and sample size are exhibited. This suggests that small sample sizes capture the majority of biomass variability at Hubbard Brook, and that either large trees are rare, or underestimates in the scaling coefficient compensate for overestimates in the scaling exponent. SERC, Parker Tract and Sierra Nevada, conversely, show overestimations in site level AGB with random sampling by 70-178%. These precise quantities should not be used without appropriate caveats, as we made several simplifying assumptions to convert between CR:H allometries to CR:AGB allometries. However, the ultimate findings of

this chapter are that allometric parameters, and associated AGB estimates, are highly sensitive to sample size. In general, we believe that temperate biomass stocks in forests are overestimated, but the magnitude of that overestimation varies considerably between sites. We need to develop more robust allometries with much greater sample sizes in order to accurately map and monitor forest carbon.

Implications of Principal Findings

The goals of this research were to determine the generality of forest allometric scaling relationships and to increase our understanding of the limitations of empirically derived allometries. We have demonstrated that forest allometry varies considerably across space in the United States, partially as a function of environment, and that existing empirically-derived allometric equations are sensitive to sample size. Therefore future allometric equation development should consider both sample size and environment.

Theoretical constraints from MST appear valid in mature, steady-state forests. Therefore, the predictions of MST may serve as useful theoretical constraints on empirically-derived allometries. It should be noted, however, that the vast majority of forest plots in the U.S. deviated considerably from MST predictions, presumably because most forests in the U.S. violate one or more of assumptions underlying MST. System maturity, in particular, is violated in forests recovering from any type of disturbance. Additionally, this research only provided coarse resolution environmental variables for comparison, and a more mechanistic study would provide a richer understanding of the limitations of MST.

That being said, this research suggests that a single allometric equation will not describe forests in all environments. Allometric equations that have been developed without the inclusion of environment or disturbance should be reexamined in the light of this research and the maps presented here should be indicators of the applicability of existing allometries in a given environment. Additionally, this research should inform future sampling campaigns which can focus stratified samples within observed groupings of allometric parameters.

Future Research

Metabolic Scaling Theory

This research addressed two of the predictions of MST and tested them across the U.S. with respect to environment and life history. However, the conclusions with respect to the limitations of MST are fairly speculative. Using a mechanistic ecosystem model, such as the Ecosystem Demography model (ED, Hurtt et al., 2002), could greatly increase the mechanistic understanding of these limitations, particularly with respect to size-dependent mortality. Future research using ED could map ED's predictions of tree size distribution across the U.S. and compare these predictions with the observations from this dissertation. Further, if ED could allow changes to size dependent mortality rates, the sensitivity to size dependence morality could be specifically addressed.

Other expansions of this dissertation research with respect to MST include the testing of MST's prediction of canopy spacing. MST predicts that the spacing of trees within

a given size class will scale with the size of that class. This prediction has not garnered the attention of other MST predictions (such as those presented in this research), again because of limited datasets. However, the LiDAR datasets generated from the delineation algorithm are ideal for the testing of this prediction. The sensitivity of tree size distribution to spatial scale can also be tested with the LiDAR datasets, which will provide a much richer spatial understanding of MST that field-based datasets cannot easily capture.

Biomass Mapping

Chapter 4 of this dissertation directly tests two emerging avenues of biomass mapping, however the sample sizes are small and we only use three study sites. Further research into individual tree applications may be warranted in other study areas, particularly when large spatial heterogeneity in biomass is observed (for example in suburban areas). Scaling-based approaches also deserve more attention, largely because of the novelty and simplicity of the ideas presented by Asner & Mascaro (2014). Although we demonstrate that scaling-based approaches, in their current form, are generally inapplicable, it is possible that the general framework of the approaches could be maintained and they may become applicable using other LiDAR metrics rather than relying on canopy top height alone.

Allometric Equation Generation

In Chapter 5 we proposed the non-destructive sampling of thousands of trees using ground-based LiDAR. This is a conceptual proposal, the logistics of which remain unclear. However, the general idea is to increase the sample size used to develop

allometric equations, and conduct sampling across a range of environments. The logistics involved in destructively sampling a sufficient number of trees across wide ranges of environmental gradients is prohibitive. Therefore, ground-based LiDAR could be used to rapidly and systematically measure the volume of individual trees in field plots. In combination with wood density information, this volume-based sampling approach should enable an enormous increase in sample size, as necessary for accurate field-based AGB estimation. This should be conducted both within the U.S. and globally, and ideally individual tree data could be shared internationally through online tools that are already available (e.g. GlobAllomTree, Henry et al., 2013). Within the U.S., sampling should be conducted across areas exhibiting similar allometries. To conduct this sampling, a map is required that pools allometrically similar forests. Geographically Weighted Regression (GWR, Brunsdon et al., 1998) is one statistical approach that uses environment and location to predict spatial patterns. GWR could be used to produce maps that inform allometric sampling campaigns. In tandem with newly developed sampling techniques (described above), new, robust, and environmentally reasonable allometric equations can be developed for biomass estimation in forests.

Concluding Thoughts

Remote sensing science is unique. Throughout the history of scientific enquiry analyses have been limited by data availability, and statistics have been developed to overcome limitations involved with small sample sizes. With remote sensing, we have an abundance of airborne and spaceborne data, with technological

improvements allowing us to approach questions at sub meter spatial resolution, nanometer spectral resolution, and up to ~40 years of temporal resolution. New sensors are being launched every year, and new data are being collected every day, increasing this wealth of information about our natural planet – a wealth that is only beginning to be tapped. In a few short decades we have already learned so much about the natural cycles and anthropogenically-forced changes on our planet. We believe remote sensing will continue to enable an understanding of Planet Earth at spatial and temporal scales never before available.

This dissertation focuses on one small area of forest science, that of forest allometry, but demonstrates the potential of novel remote sensing datasets to address old research questions in new and powerful ways. That being said, with the plethora of data available it is tempting to focus entirely on empirical analyses, without incorporating a theoretical understanding of Earth science. Our analysis of MST was conducted largely as an attempt to merge the overtly empirical field of forest remote sensing with the data limited field of theoretical ecology. Data can be used to help develop theory, and theory in turn can inform the design of future science questions. For example, MST may serve as a set of theoretical constraints to empirical allometric analysis, while empirical data can help refine MST. Similar fusions are already in existence, for example between LiDAR and Ecosystem Modeling, as in the Ecosystem Demography model. We believe this marriage of theory and data is the best approach to improving our understanding of forest structure and function.

Bibliography

Abdi, H. (2010). Partial least squares regression and projection on latent structure regression (PLS Regression). *Wiley Interdisciplinary Reviews: Computational Statistics*, *2*,1, 97-106.

Agrawal, A., Nepstad, D., & Chhatre, A. (2011). Reducing emissions from deforestation and forest degradation. *Annual Review of Environment and Resources*, *36*, 373-396.

Anfodillo, T., Carrer, M., Simini, F., Popa, I., Banavar, J., & Maritan, A. (2012). An allometry-based approach for understanding forest structure, predicting tree-size distribution and assessing the degree of disturbance. *Proc. Roy. Soc.*, 280, 20122375.

Asner, G.P. (2009). Tropical forest carbon assessment: integrating satellite and airborne mapping approaches. *Environmental Research Letters*, 4, 3, 034009.

Asner, G.P. & Mascaro, J. (2014). Mapping tropical forest carbon: Calibrating plot estimates to a simple LiDAR metric. *Remote Sensing of Environment*, 140, 614-624.

Asner, G.P., Hughes, R.F., Mascaro, J., Uowolo, A.L., Knapp, D.E., Jacobson, J., Kennedy-Bowdoin, T., & Clark, J.K. (2011). High-resolution carbon mapping on the million-hectare Island of Hawaii. *Froniers in Ecology*, 9, 8, 434-439.

Baccini, A., Goetz, S.J., Walker, W.S., Laporte, N.T., Sun, M., Sulla-Menashe, D., Hackler, J., Beck, P.S.A., Dubayah, R., Friedl, M.A., Samanta, S., & Houghton, R.A. (2012). Estimated carbon dioxide emissions from tropical deforestation improved by carbon-density maps. *Nature Climate Change*, 2, 182-185.

Baccini, A., Laporte, N., Goetz, S., Sun, M. & Dong, H. (2008). A first map of tropical Africa's above-ground biomass derived from satellite imagery. *Environmental Research Letters*, 3, 4, 045011.

Bailey, J.D & Covington, W.W. (2002). Evaluating ponderosa pine regeneration rates following ecological restoration treatments in northern Arizona, USA. *Forest Ecology and Management*, 155: 271-278.

Bajrang, S., Misra, P., & Singh, B. 1996. Biomass, energy content and fuel-wood properties of Populus deltoides clones raised in North Indian plains. *Indian Journal of Forestry*. 18:278–284.

Bortolot, Z.J., & Wynne, R.H. (2005). Estimating forest biomass using small footprint data: An individual tree-based approach that incorporates training data. *ISPRS Journal of Photogrammetry and Remote Sensing*, 59, 6, 342-360.

Boudreau, J., Nelson, R. F., Margolis, H. A., Beaudoin, A., Guindon, L., & Kimes, D. S. (2008). Regional aboveground forest biomass using airborne and spaceborne LiDAR in Québec. *Remote Sensing of Environment*, *112*, 10, 3876-3890.

Breidenbach, J., Næsset, E., Lien, V., Gobakken, T., & Solberg, S. (2010). Prediction of species specific forest inventory attributes using a nonparametric semi-individual tree crown approach based on fused airborne laser scanning and multispectral data. *Remote Sensing of Environment*, *114*, 4, 911–924.

Breiman, L. (2001) Random forests. *Machine learning*, 45, 1, 5-32.

Brown, J., West, G. & Enquist, B. A. (1999). A general model for the structure and allometry of plant vascular systems. *Nature*, 400, 6745, 664-667.

Brunsdon, C., Fotheringham, S., & Charlton, M. (1998). Geographically weighted regression. *Journal of the Royal Statistical Society: Series D (The Statistician)*, *47*(3), 431-443.

Chave, J., Andalo, C., Brown, S., Cairns, M.A., Chambers, J.Q., Eamus, D., Fölster, H., Fromard, F., Higuchi, N., Kira, T., Lescure, J.-P., Nelson, B.W., Ogawa, H., Puig, H., Riera, B., & Yamakua, T. (2005). Tree allometry and improved estimation of carbon stocks and balance in tropical forests. *Oecologia*, 145, 87-99.

Chave, J., Condit, R., Aguilar, S., Hernandez, A., Lao, S., & Perez, R. (2004). Error propagation and scaling for tropical forest biomass estimates.*Philosophical Transactions of the Royal Society of London. Series B: Biological Sciences*, *359*, 1443, 409-420.

Chave, J., Muller-Landau, H. C., Baker, T. R., Easdale, T. A., Steege, H. T., & Webb, C. O. (2006). Regional and phylogenetic variation of wood density across 2456 neotropical tree species. *Ecological applications*, *16*, 6, 2356-2367.

Chen, Q., Gong, P., Baldocchi, D., & Tian, Y.Q. (2007). Estimating basal area and stem volume for individual trees from LiDAR data. *Photogrammetric Engineering and Remote Sensing*, *73*, 12, 1355-1365.

Chojnacky, D.C. 1988. Juniper, pinyon, oak and mesquite volume equations for Arizona. Res. Bull. INT-391. Ogden UT: U.S. Department of Agriculture, Forest Service, Intermountain Forest and Range Experiment Station.

Chojnacky, D.C., Heath, L.S. & Jenkins, J.C. (2014). Updated generalized biomass equations for North American tree species. *Forestry*, 87, 129-151.

Clark, A.I., & Schroeder, J. (1986). Weight, volume, and physical properties of major hardwood species in the southern Appalachian mountains. *USDA Forest Service Research Papers*, SE-153.

Clark, A.I., Phillips, D., & Frederick, D. (1985). Weight, volume, and physical properties of major hardwood species in the Gulf and Atlantic Coastal Plains. *USDA Forest Service Research Papers*. SE-250.

Clark, A.I., Phillips, D., & Frederick, D. (1986). Weight, volume, and physical properties of major hardwood species in the upland south. *USDA Forest Service Research Papers*, SE-257.

Clauset, A., Shalizi, C.R., & Newman, M.E. Power-Law Distributions in Empirical Data. *Siam Review*, **51**, 4, 661-703 (2009).

Cook, B.D., Corp, L.A., Nelson, R.F., Middleton, E.M., Morton, D.C., McCorkel, J.T., Masek, J.G., Ranson, K.J., Vuong, L., & Montesano, P.M. (2013). NASA Goddard's LiDAR, Hyperspectral and Thermal (G-LiHT) Airborne Imager. *Remote Sensing*, 5, 8, 4045-4066.

Coomes, D.A., Duncan, R.P., Allen, R.B., & Truscott, J. (2003). Disturbances prevent stem size-density distributions in natural forests from following scaling relationships. *Ecology Letters*, 6, 980-989.

Coomes, D.A., Jenkins, K.L., & Cole, L.E.S. (2007). Scaling of tree vascular transport systems along gradients of nutrient supply and altitude. *Biology Letters*, 3, 97-90.

Coops, N.C., Hilker, T., Wulder, M.A., St-nge, B., Newnham, G., Siggens, A., & Trofymow, J.A. (2007). Estimating canopy structure of Douglas-fir forest stands from discrete-return LiDAR. *Trees*: *Structure and Function*, 21, 3, 295-310.

Corbera, E., & Schroeder, H. (2011). Governing and implementing REDD+.*Environmental Science & Policy*, *14*(2), 89-99.

Curtis, R.O.; Bruce, D.; VanCoevering, C. (1968). Volume and taper tables for red alder. Res. Pap. PNW-RP-056. Portland, OR: U.S. Department of Agriculture, Forest Service, Pacifi c Northwest Forest and Range Experiment Station. 36 p.

Dietze, M.C., Wolosin, M.S. & Clark, J.S. (2008). Capturing diversity and interspecific variability in allometries: A hierarchical approach. *For. Ecol. and Mgmnt.*, 256, 1939-1948.

Domke, G.M., Woodall, C.W., Smith, J.E., Westfall, J.A., & McRoberts, R.E. (2012). Consequences of alternative tree-level biomass estimation procedures on U.S. forest carbon stock estimates. Forest Ecology and Management, 270, 108-116.

Drake, J.B., Dubayah, R.O., Knox, R.G., Clark, D.B., & Blair, J.B. (2002). Sensitivity of large-footprint LiDAR to canopy structure and biomass in a neotropical rainforest. *Remote Sensing of Environment*, 81, 378-392.

Dubayah, R. O., Sheldon, S. L., Clark, D. B., Hofton, M. A., Blair, J. B., Hurtt, G. C., & Chazdon, R. L. (2010). Estimation of tropical forest height and biomass dynamics using LiDAR remote sensing at La Selva, Costa Rica. *Journal of Geophysical Research: Biogeosciences (2005–2012)*, *115*(G2).

Dubayah, R.O., & Drake, J.B. (2000). LiDAR remote sensing for forestry. *Journal of Forestry*, 98, 44-46.

Duncanson, L. I., Cook, B. D., Hurtt, G. C., & Dubayah, R. O. (2014). An efficient, multi-layered crown delineation algorithm for mapping individual tree structure across multiple ecosystems. *Remote Sensing of Environment*.

Duncanson, L.I., Niemann, K.O., & Wulder, M.A. (2010). Integration of GLAS and Landsat TM data for aboveground biomass estimation. *Canadian Journal of Remote Sensing*, 36, 2, 129-141.

Enquist B.J. (2002). Universal scaling in tree and vascular plant allometry: toward a general quantitative theory linking plant form and function from cells to ecosystems. *Tree Physiology*, 22, 1045-1064.

Enquist B.J. & Bentley L.P. (2012). Land Plants: New Theoretical Directions and Empirical Prospects. In: *Metabolic Ecology: A Scaling Approach, First Edition* (ed. Richard M. Sibly JHB, Astrid Kodric-Brown). John Wiley & Sons, Ltd. pp. 164-187.

Enquist, B. J., West, G. B., & Brown, J. H. (2009). Extensions and evaluations of a general quantitative theory of forest structure and dynamics. *Proceedings of the National Academy of Sciences*, *106*(17), 7046-7051.

Enquist, B.J., & Niklas, K.J. (2001). Invariant scaling relations across tree-dominated communities. *Nature*, 410, 655-660.

Fatemi, F.R., Yanai, R.D., Hamburg, S.P., Vadeboncoeur, M.A., Arthur, M.A., Briggs, R.D., & Levine, C.R. (2011). Allometric equations for young northern hardwoods: the importance of age-specific equations for estimating aboveground biomass. *Canadian Journal of Forest Research*, 41, 4, 881-891.

Feldpausch, T.R., Banin, L., Phillips, Ol.L, Baker, T.R., Lewis, S.L., Quesada, C.A., Affum-Baffoe, K., Arets, E.J.M.M., Berry, N.J., Bird, M., Brondizio, E.S., de Camargo, P., Chave, J., Djagbletey, G., Domingues, T.F., Drescher, M., Fearnside, P.M., Franca, M.B., Fyllas, N.M., Lopez-Gonzalez, G., Hladik, A., Higuchi, N., Hunter, M.O., Iida, Y., Salim, K.A., Kassim, A.R., Keller, M., Kemp, J., King, D.A., Lovett, J.C., Marimon, B.S., Marimon-Junior, B.H., Lenza, E., Marshall, A.R., Metcalfe, D.J., Mitchard, E.T.A., Moran, E.F., Nelson, B.W., Nilus, R., Nogueira, E.M., Palace, M.,

Pitino, S., Peh, K.S.H., Raventos, M.T., Reitsma, J.M., Saiz, G., Schrodt, F., Sonke, B., Taedoumg, H.E., Tan, S., White, L., Woll, H., & Lloyd, J. Height-diameter allometry of tropical forest trees. *Biogeosciences*, **8,** 1081-1106 (2011).

Fellows, A.W., & Goulden, M.L. (2008). Has fire suppression increased the amount of carbon stored in western U.S. forests? *Geophysical Research Letters*, 35, L12404.

Ferraz, A., Bretar, F., Jacquemoud, S., Gonçalves, G., Pereira, L., Tomé, M., & Soares, P. (2012). 3-D mapping of a multi-layered Mediterranean forest using ALS data. *Remote Sensing of Environment, 121*, 210–223.

Ferster, C.J., Coops, N.C., & Trofymow, J.A. (2009). Aboveground large tree mass estimation in a coastal forest in British Columbia using plot-level metrics and individual tree detection from LiDAR.

Genuer, R., Poggi, J. M., & Tuleau-Malot, C. (2010). Variable selection using random forests. *Pattern Recognition Letters*, 31, 14*,* 2225-2236.

Gholz, H. L., Grier, C. C., Campbell, A. G., & Brown, A. T. (1979). *Equations for estimating biomass and leaf area of plants in the Pacific Northwest*. Corvallis: Forest Research Lab., Oregon State University, School of Forestry.

Gibbs, H K, Brown, S., Niles, J.O., & Foley, J.A. (2007). Monitoring and estimating tropical forest carbon stocks: making REDD a reality. *Environmental Research Letters*, 2, 045023.

Goetz, S.J., Baccini, A., Laporte, N., Johns, T., Walker, W.S., Kellndorfer, J.M., Houghton, R.A. & Sun, M. (2009). Mapping and monitoring carbon stocks with satellite observations: a comparison of methods. *Carbon Balance and Management*, doi:10.1186/1750-0680-1184-1182.

Goetz, SG & RO Dubayah. (2011). Advances in remote sensing technology and implications for monitoring, reporting and verifying forest carbon stocks and emissions. *Carbon Management*, 2, 231-244.

Gregorutti, B., Michel, B., & Saint-Pierre, P. (2013). Correlation and variable importance in random forests. *arXiv preprint arXiv:1310.5726*.

Henry, M., Bombelli, A., Trotta, C., Alessandrini, A., Birigazzi, L., Sola, G., ... & Saint-André, L. (2013). GlobAllomeTree: international platform for tree allometric equations to support volume, biomass and carbon assessment.*iForest-Biogeosciences and Forestry*, *6*(6), 326.

Hopkinson, C., Chasmer, L., & Hall, R. J. (2008). The uncertainty in conifer plantation growth prediction from multi-temporal LiDAR datasets. *Remote Sensing of Environment*, *112*(3), 1168-1180.

Houghton, R.A., Lawrence, K.T., Hackler, J.L., & Brown, S. (2001). The spatial distribution of forest biomass in the Brazilian Amazon: a comparison of estimates. *Global Change Biology*, 7, 7, 731-746.

Hudak, A. T., Strand, E. K., Vierling, L. A., Byrne, J. C., Eitel, J. U., Martinuzzi, S., & Falkowski, M. J. (2012). Quantifying aboveground forest carbon pools and fluxes from repeat LiDAR surveys. *Remote Sensing of Environment*, *123*, 25-40.

Hunsaker, C., Boroski, B., & Steger, G. (2002). Relationships between canopy cover and occurrence and productivity of California spottel owls, predicting species occurrences, issues of accuracy and scale. *Island Press*, Covelo, CA.

Hurtt, G. C., Pacala, S. W., Moorcroft, P. R., Caspersen, J., Shevliakova, E., Houghton, R. A., & Moore, B. I. I. I. (2002). Projecting the future of the US carbon sink. *Proceedings of the National Academy of Sciences*, *99*(3), 1389-1394.

Iida, Y., Poorter, L., Sterck, F.J., Kassim, A.R., Kubo, T., Potts, M.D., & Kohyama, T.S. (2012). Wood density explains architectural differentiation across 145 co-occurring tropical tree species. *Functional Ecology*. 26, 1, 274-282.

Jenkins, J. C., Chojnacky, D. C., Heath, L. S., & Birdsey, R. A. (2003). National-scale biomass estimators for United States tree species. *Forest Science*, *49*(1), 12-35.

Kaartinen, H., Hyyppä, J., Yu, X., Vastaranta, M., Hyyppä, H., Kukko, A., Holopainen, M., Heipke, C., Hirschmugl, M., Morsdorf, F., Naesset, E., Pitkanen, J., Popescu, S., Solberg, S., Wolf, B.M., & Wu, JC. (2012). An International Comparison of Individual Tree Detection and Extraction Using Airborne Laser Scanning. *Remote Sensing*, *4*, 4, 950–974.

Keeling, C. D., Bacastow, R. B., Bainbridge, A. E., Ekdahl, C. A., Guenther, P. R., Waterman, L. S., & Chin, J. F. (1976). Atmospheric carbon dioxide variations at Mauna Loa observatory, Hawaii. *Tellus*, *28*(6), 538-551.

Ker, M., & Van Raalte, G. (1981). Tree biomass equations for Abies balsamea and Picea glauca in northwestern New Brunswick. Can. J. For. Res. 11:13–17.

Kerkhoff, A.J., & Enquist, B.J. (2007). The implications of scaling approaches for understanding resilience and reorganization in ecosystems. *BioScience*, 57, 6, 489-499.

Ketterings, Q. M., Coe, R., van Noordwijk, M., Ambagau, Y., & Palm, C. A. (2001). Reducing uncertainty in the use of allometric biomass equations for predicting above-ground tree biomass in mixed secondary forests. *Forest Ecology and management*, *146*(1), 199-209.

Koch, B., Heyder, U., & Weinacker, H. (2003). Detection of individual tree crowns in airborne LiDAR data. *Photogrammetric Engineering & Remote Sensing, 72*, 4, 357-363.

Koch, G.W., Sillett, S.C., Jennings, G.M., & Davis, S.D. (2004). The limits to tree height. *Nature*, 428, 851-854.

Kwak, D., Lee, W., Lee, J., Biging, & G., Gong, P. (2007). Detection of individual trees and estimation of tree height using LiDAR data. *Journal of Forest Research, 12*, 6, 425-434.

Lai, J., Coomes, D.A., Du, X., Hsieh, C., Sun, I., Chao, W, Mi, X., Ren, H., Wang, X., Hao, Z., & Ma., K. (2013). A general combined model to describe tree-diameter distribution within subtropical and temperate forest communities. *Oikos*, 122, 1636-1642.

Lambert, M.C., Ung, C.H. and Raulier, F. 2005. Canadian national tree aboveground biomass equations. *Canadian Journal of Forest Resources*, 35, 1996-2018.

Le Toan, T., Quegan, S., Davison, M.W.J., Balzter, H., Paillou, P., Papathanassiou, K., Plummer, S., Rocca, F., Saatchi, S., Shugart, H., & Ulander, L. 2011. The BIOMASS mission: Mapping global forest biomass to better understand the terrestrial carbon cycle. *Remote Sensing of Environment*, 115, 2850-2860.

Leckie, D., Gougeon, F., Hill, D., Quinn, R., Armstrong, L., & Shreenan, R. (2003). Combine high-density LiDAR and multispectral imagery for individual tree crown analysis. *Canadian Journal of Remote Sensing*, *29*, 5, 633-649.

Lefsky, M A (2010) A global forest canopy height map from the Moderate Resolution Imaging Spectroradiometer and the Geoscience Laser Altimeter System. *Geophysical Research Letters* 37(15).

Lefsky, M.A., Cohen, W.B., Acker, S.A., Parker, G.G., Spies, T.A. & Harding, D. (1999a). LiDAR remote sensing of the canopy structure and biophysical properties of Douglas-fir western hemlock forests. *Remote Sensing of Environment*, 70, 339-361.

Lefsky, M.A., Cohen, W.B., Harding, D.J., Parker, G.G., Acker, S.A., & Gower, S.T. (2003). LiDAR remote sensing of above-ground biomass in three biomes. *Global Ecology and Biogeography*, 11, 5, 393-399.

Lefsky, M.A., Harding, D., Cohen, W.B., Parker, G., & Shugart, H.H. (1999b). Surface LiDAR remote sensing of basal area and biomass in deciduous forests of eastern Maryland, USA. *Remote Sensing of Environment*, 67, 83-98.

Lefsky, M.A., Harding, D.J., Keller, M., Cohen, W.B., Carabajal, C.C., Espirito-Santo, F.D., Hunter, M.O., de Oliveira, R., & de Camargo, P.B. (2005). Estimates of forest canopy height and aboveground biomass using ICESat. Geophysical Research Letters, 32, doi:10.1029/2005GL023971

Legendre, P. (1998). Model II Regression User's Guide, R edition. *R Vignette*.

Li, H., Lin, Y., Manikin, G., Parrish, D., & Shi, W. (2005). North American Regional Reanalysis. *American Meteorological Society.* 87, 3, 343-360.

Lim, K., Trietz, P., Wulder, M.A., St-Onge, B., & Flood, M. (2003). LiDAR remote sensing of forest structure. *Progress in Physical Geography*, 72, 88-106.

Lines, E.R., Coomes, D.A., & Purves, D.W. Influences of forest structure, climate and species composition on tree mortality across the Eastern U.S. *PLOS One*, **5**, 10, e14212 (2010).

Lines, E.R., Zavala, M.A., Purves, D.W., & Coomes, D.A. (2012). Predictable changes in aboveground allometry of trees along gradients of temperature, aridity and competition. *Global Ecology and Biogeography*, 21, 1017-1028.

MacLean, C.D.; Berger, J.M. 1976. Softwood tree volume equations for major California species. Res. Note PNW-266. Portland, OR: U.S. Department of Agriculture, Forest Service, Pacifi c Northwest Forest and Range Experiment Station. 33 p. 60-144

Maltamo, M., Mustonen, K., Hyyppa, J., Pitkanen, J., & Yu, X. (2004). The accuracy of estimating individual tree variables with airborne laser scanning in a boreal nature reserve. *Canadian Journal of Forest Research*, *34,* 9, 1791-1801.

Martin, J., Kloeppel, B., Schaefer, T., Kimbler, D., & McNulty, S. (1998). Aboveground biomass and nitrogen allocation of ten deciduous southern Appalachian tree species. *Canadian Journal of Forest Research*, 28, 1648-1659.

Mitchard, E. T. A., Saatchi, S. S., Lewis, S. L., Feldpausch, T. R., Gerard, F. F., Woodhouse, I. H., & Meir, P. (2011). Comment on'A first map of tropical Africa's above-ground biomass derived from satellite imagery'. *Environmental Research Letters*, *6*(4), 049001.

Mitchard, E. T., Saatchi, S. S., Baccini, A., Asner, G. P., Goetz, S. J., Harris, N., & Brown, S. (2013). Uncertainty in the spatial distribution of tropical forest biomass: a comparison of pan-tropical maps. *Carb Bal Manage*.

Monteith, D. (1979). Whole tree weight tables for New York State. University of New York College of Environmental Science and Forestry, Applied Forest Research Institute. *AFRI Research Repository*, No. 40.

Moorcroft, P. R., Hurtt, G. C., & Pacala, S. W. (2001). A method for scaling vegetation dynamics: the ecosystem demography model (ED). *Ecological monographs*, *71*(4), 557-586.

Muller-Landau, H.C., Condit, R.S., Chave, J., Thomas, S.C., Bohlman, S.A., Vunyavejchewin, S., Davies, S., Foster, R., Gunatilleke, S., Gunatilleke, N., Harms, K.E., Hart, T., Hubbel, S.P., Itoh, A., Kassim, A.R., LaFrankie, J.V., Lee, H.S., Losos, E., Makana, R.R., Ohkubo, T., Sukamar, R., Sun, I.F., Supardi, N., Ran, S., Thompson, J., Valencia, R., Munoz, G.V., Wills, C., Yamakura, T., Chuyong, G., Dattaraja, H.S., Esufali, S., Hall, P., Hernandex, C., Kenfack, D., Kiratiprayoon, S., Suresh, H.S. Thomas, D., Vallejo, M.I. & Ashton, P. (2006a). Testing metabolic ecology theory for allometric scaling of tree size, growth, and mortality in tropical forests. *Ecology Letters,* 9, 575-588.

Muller-Landau, H.C., Condit, R.S., Harms, K.E., Marks, C.O., Thomas, S.C., Bunyavajchewin, S., Chuyong, G., Co, L., Davies, S., Foster, R., Gunatilleke, S., Gunatilleke, N., Hart, T., Hubbell, S.P., Itoh, A., Rahman Kassim, A., Kenfack, D., LaFrankie, J., Lagunzad, D., Seng Lee, H., Losos, E., Makana, J.R., Ohkubo, T., Samper, C., Sukumar, R., Sun, I.F., Supardi, N., Tan, S., Thomas, D., Thompson, J., Valencia, R., Vallego, M.I., Munoz, G.V., Yamakura, T., Zimmerman, J.K., Dattaraja, H.S., Esufali, S., Hall, P., He, F. Hernandez, C., Kiratiprayoon, S., Suresh, H.S., Wills C., & Ashton, P. (2006b) Comparing tropical forest tree size distributions with the predictions of metabolic ecology and equilibrium models. *Ecology Letters*, 9: 589-602.

Muller‐Landau, H. C. (2004). Interspecific and inter‐site variation in wood specific gravity of tropical trees. *Biotropica*, *36*(1), 20-32.

Nabuurs, G.J., O. Masera, K. Andrasko, P. Benitez-Ponce, R. Boer, M. Dutschke, E. Elsiddig, J. Ford-Robertson, P. Frumhoff, T. Karjalainen, O. Krankina, W.A. Kurz, M. Matsumoto, W. Oyhantcabal, N.H. Ravindranath, M.J. Sanz Sanchez, X. Zhang, 2007: Forestry. In Climate Change 2007: Mitigation. Contribution of Working Group III to the Fourth Assessment Report of the Intergovernmental Panel on Climate Change [B. Metz, O.R. Davidson, P.R. Bosch, R. Dave, L.A. Meyer (eds)], Cambridge University Press, Cambridge, United Kingdom and New York, NY, USA.

Næsset, E. (1997). Determination of mean tree height of forest stands using airborne laser scanner data, *ISPRS Journal of Photogrammetry and Remote Sensing*, 52, 2, 49-56.

Næsset, E. (2004). Accuracy of forest inventory using airborne laser scanning: evaluating the first nordic full-scale operational project, *Scandinavian Journal of Forest Research*, 19, 6, 554-557.

Naidu, S., Delucia, E., & Thomas, R. (1998). Estimating weights of loblolly pine trees and their components in natural stands and plantations in central Mississippi. *Mississippi Agricultural and Forest Explorations Station Technical Bulletin*, 73.

Ni-Meister, W., Lee, S.Y., Strahler, A.H., Woodcock, C.E., Schaaf, C., Yao, T.A., Ranson, K.J., Sun, G.Q., & Blair, J.B. (2010). Assessing general relationships between aboveground biomass and vegetation structure parameters for improved carbon estimate from LiDAR remote sensing. Journal of Geophysical Research-Biogeosciences, 115.

Niklas, K.J., Midgley, J.J., & Rand, R.H. (2003). Tree size frequency distributions, plant density, age and community disturbance. *Ecology Letters*, 6, 405-411.

Pan, Y., Birdsey, R.A., Fang, J., Houghton, R., Kauppi, P.E., Kurz, W.A., Phillips. O.L., Shvidenko, A., Lewis, S.L., Canadell, J.G., Ciais, P., Jackson, R.B., Pacla, S.W., McGuire, A.D., Piao, S., Rautianien, A., Sitch, S., & Hayes, D. (2011). A large and persistent carbon sink in the World's Forests. *Science*, 333, 6045, 988-993.

Pastor, J., Aber, J.C., & Melilo, J.M. (1984). Biomass prediction using generalized allometric regressions for some northeast tree species. *Forest Ecology and Management*, 7, 4, 265-274.

Persson, A., Holmgren, J., & Soderman, U. (2002). Detecting and measuring individual trees using an airborne laser scanner. *Photogrammetric Engineering and Remote Sensing, 68*, 9, 925-932.

Pflugmacher, D., Cohen, W., Kennedy, R., & Lefsky, M. (2008). Regional Applicability of Forest Height and Aboveground Biomass Models for the Geoscience Laser Altimeter System. Forest Science, 54, 647-657

Phillips, D. (1981). Predicted total-tre biomass of understory hard-woods. *USDA Forest Service Research Papers,* SE-223.

Popescu, S. & Wynne, R. (2004). Seeing the trees in the forest: using LiDAR and multispectral data fusion with local filtering and variable window size for estimating tree height. *Photogrammetric Engineering and Remote Sensing*, 70, 5, 589-604.

Popescu, S., (2007). Estimating biomass of individual pine trees using airborne LiDAR. *Biomass and Bioenergy*, *31*, 9, 646-655.

Popescu, S., Wynne, & R., Nelson, R. (2003). Measuring individual tree crown diameter with LiDAR and assessing its influence on estimating forest volume and biomass. *Canadian Journal of Remote Sensing. 29*, 5, 564-577.

Popescu, S.C., & Zhao, K. (2008). A voxel-based LiDAR method for estimating crown base height for deciduous and pine trees. *Remote Sensing of Environment.* 112, 3, 767-781.

Price C., Enquist B. & Savage V. (2007). A general model for allometric covariation in botanical form and function. *Proc. Nat. Acad. of Sci.*, 104, 13204-13209.

Rahman, M. & Gorte, B. (2009). Tree crown delineation from high resolution airborne LiDAR based on densities of high points. *Laserscanning09, XXXVIII*, Paris, France, 123-128.

Reams, G. A., Smith, W. D., Hansen, M. H., Bechtold, W. A., Roesch, F. A., & Moisen, G. G. (2005). The forest inventory and analysis sampling framework. *The enhanced forest inventory and analysis program—national sampling design and estimation procedures*, 11-26.

Reitberger, J., Schnörr, C.I., Krzystek, P., & Stilla, U. (2009). 3D segmentation of single trees exploiting full waveform LIDAR data. *ISPRS Journal of Photogrammetry and Remote Sensing*, 64, 6, 561-574.

Saatchi, S.S., Harris, N.L., Brown, S., Lefsky, M., Mitchard, E.T.A., Salas, W., Zutta, B.R., Buermann, W., Lewis, S.L., Hagen, S., Petrova, S., White, L., Wilman, M., & More, A. (2011). Benchmark map of forest carbon stocks in tropical regions across three continents. *PNAS*, 108, 24, 9899-9904.

Shinozaki, K., Yoda, K., Hozumi, K., & Kira, T. (1964). A quantitative analysis of plant form-the pipe model theory: I. Basic analyses. *日本生□学会□*, *14*(3), 97-105.

Siccama, T.G., Hamburg, S.P., Arthr, M.A., Yanai, R.D., Bormann, F., & Likens, G.E. (1994). Corrections to allometric equations and plant tissue chemistry for Hubbard Brook Experimental Forest. *Ecology*, 75, 246-248.

SIGEO, (2013), Smithsonian Institution Global Earth Observatories. Available online at: http://www.sigeo.si.edu/

Simard, M., Pinto, N., Fisher, J. B., & Baccini, A. (2011). Mapping forest canopy height globally with spaceborne LiDAR. *Journal of Geophysical Research: Biogeosciences (2005–2012)*, *116*(G4).

Strahler, A. H., Jupp, D. L., Woodcock, C. E., Schaaf, C. B., Yao, T., Zhao, F., ... & Boykin-Morris, W. (2008). Retrieval of forest structural parameters using a ground-based LiDAR instrument (Echidna®). *Canadian Journal of Remote Sensing*, *34*(sup2), S426-S440.

Suarez, J.C. (2013). The use of small footprint airborne LiDAR for estimation of individual tree parameters in Sitka spruce stands. *Challenges and opportunities for the world's forests in the 21st century.* 81, T. Fenning, Ed. Spring, 2013.

Swatantran, A., Dubayah, R., Roberts, D., Hofton, M., & Blair, J.B. (2011). Mapping biomass and stress in the Sierra Nevada using LiDAR and hyperspectral data fusion. *Remote Sensing of Environment*, *115*, 11, 2917-2930.

Thomas, R. Q., Hurtt, G. C., Dubayah, R., & Schilz, M. H. (2008). Using LiDAR data and a height-structured ecosystem model to estimate forest carbon stocks and fluxes over mountainous terrain. *Canadian Journal of Remote Sensing*,*34*(sup2), S351-S363.

Ung, C-H., Bernier, P., and Guo, X.J. (2008). Canadian national biomass equations: new parameter estimates that include British Columbia data. *Canadian Journal of Forest Research*, 38, 1123-1132.

Van Aardt, J.A., Wynne, R.H., & Oderwald, R.G. (2006). Forest volume and biomass estimation using small-footprint LiDAR-distributional parameters on a per-segment basis. *Forest Science*, 52, 6, 2006.

Van Breugel, M., Ransijn, J., Craven, D., Bongers, F., & Hall, J. S. (2011). Estimating carbon stock in secondary forests: decisions and uncertainties associated with allometric biomass models. *For. Ecol. and Mgmnt.*, 262**,** 8, 1648-1657.

Vastaranta, M., Holopainen, M., Yu, X., Haapanen, R., Melkas, T., Hyyppa, J., & Hyyppa H. (2011). Individual tree detection and area-based approach in retrieval of forest inventory characteristics from low-pulse airborne laser scanning data. Photogrammetric Journal of Finland, 22, 2, 1-13.

Vieilledent, G., Vaudry, R., Andriamanohisoa, S. F., Rakotonarivo, O. S., Randrianasolo, H. Z., Razafindrabe, H. N., ... & Rasamoelina, M. (2012). A universal approach to estimate biomass and carbon stock in tropical forests using generic allome

West, G. B., Brown, J. H., & Enquist, B. J. (1999). A general model for the structure and allometry of plant vascular systems. *Nature*, *400*(6745), 664-667.

White, E.P., Enquist, B.J., & Green, J.L. (2008). On estimating the exponent of power-law frequency distributions. *Ecology*, 89, 905-912.

Williams, R.A., & McClenahen, J.R. (1984). Biomass prediction equations for seedlings, sprouts, and saplings of ten central hardwood species. *Forest Science*, 30, 523-527.

Woodall C., Heath, L. S., Domke, G. M., & Nichols, M. C. (2011). Methods and equations for estimating aboveground volume, biomass, and carbon for trees in the US forest inventory, 2010.

Wulder, M., Niemann, K.O., & Goodenough, D.G. (2000). Local maximum filtering for the extraction of tree locations and basal area from high spatial resolution imagery. *Remote Sensing of Environment*, *73*, 1, 103-114.

Wulder, M.A., & Seeman, D. (2003). Forest inventory height update through the integration of LiDAR data with segmented Landsat imagery. *Canadian Journal of Remote Sensing*, 29, 5, 536-543.

Wulder, M.A., Bater, C.W., Coops, N.C., Hilker, T., & White, J.C. (2008). The role of LiDAR in sustainable forest management. *The Forestry Chronicle*, 84, 6, 808-826.

Wulder, M.A., White, J.C., Nelson, R.F., Naesset, E., Orka, H.O., Coops, N.C., Hilker, T., Bater, C.W., & Gobakken, T. (2012). LiDAR sampling for large-area forest characterization: A review. *Remote Sensing of Environment*. *121*, 1, 196-209.

Zhao, F., Guo, Q., & Kelly, M. (2012). Allometric equation choice impacts LiDAR-based forest biomass estimates: A case study from the Sierra National Forest, CA. *Agricultural and Forest Meteorology*, 165, 64-72.

Zolkos, S.G., Goetz, S.J., & Dubayah, R. (2013). A meta-analysis of terrestrial aboveground biomass estimation using LiDAR remote sensing. *Remote Sensing of Environment*, 128, 289-298.